

**MODIFICATION OF LINEAR LOW DENSITY POLYETHYLENE FOR
IMPROVED PHOTO AND BIODEGRADATION**

*Thesis submitted to the
Cochin University of Science and Technology
in partial fulfilment of the requirements
for the award of the degree of
Doctor of Philosophy
under the
Faculty of Technology*

By

Vidya Francis



**Department of Polymer Science and Rubber Technology
Cochin University of Science and Technology
Kochi- 682 022, Kerala, India
<http://psrt.cusat.ac.in>**

November 2012

Modification of Linear Low Density Polyethylene for Improved Photo and Biodegradation

Ph. D Thesis under the Faculty of Technology

Author

Vidya Francis

Department of Polymer Science and Rubber Technology
Cochin University of Science and Technology
Cochin- 682 022, Kerala, India
E-mail: vidyakf@gmail.com

Guide:

Dr. Eby Thomas Thachil

Professor
Department of Polymer Science and Rubber Technology
Cochin University of Science and Technology
Cochin- 682 022, Kerala, India
E-mail: ethachil@cusat.ac.in

November, 2012



Department of Polymer Science and Rubber Technology
Cochin University of Science and Technology
Kochi - 682 022, Kerala, India
<http://psrt.cusat.ac.in>

Dr. Eby Thomas Thachil
B.Sc. Eng., M.Tech., Ph.D
Professor

Phone: 0484-2575723 (Off)
0484-2331426 (Res)
Email: ethachil@cusat.ac.in

Certificate

This is to certify that the thesis entitled “**Modification of Linear Low Density Polyethylene for Improved Photo and Biodegradation**” which is being submitted by **Ms. Vidya Francis** in partial fulfilment of the requirements for the award of the degree of Doctor of Philosophy, to the Cochin University of Science and Technology, Kochi-22 is a record of the bonafide research work carried out by her under my supervision and guidance, in the Department of Polymer Science and Rubber Technology, Kochi-682 022, and no part of the work reported in the thesis has been presented for the award of any degree from any other institution.

Kochi
12-11-12

Dr. Eby Thomas Thachil
(Supervising Teacher)

Declaration

I hereby declare that the work presented in this thesis entitled **“Modification of Linear Low Density Polyethylene for Improved Photo and Biodegradation”** is based on the original research work carried out by me under the guidance and supervision of Dr. Eby Thomas Thachil, Professor, Department of Polymer Science and Rubber Technology, Cochin University of Science and Technology, Kochi-682 022 and no part of the work reported in this thesis has been presented for the award of any degree from any other institution.

Kochi-22
12-11-12

Vidya Francis

Dedicated to

My Parents, Teachers, Husband Georfy

&

Son John Georfy

Acknowledgement

I express my hearty thanks and indebtedness to Dr. Eby Thomas Thachil, Professor, Department of Polymer Science and Rubber technology, Cochin University of Science and Technology, my research guide, for his inspiring guidance, encouragement and invaluable suggestions which paved way for the completion of my work.

I am extremely grateful to Dr. Sunil K. Narayanankutty Head of the Department and Dr. Thomas Kurian, former Head of the Department for providing all facilities during my research work.

With pleasure, I thank all other faculty members Dr. K.E George, Dr. Rani Joseph, Dr. Philip Kurian and Smt. Jayalatha of the Department for their wholehearted co-operation throughout the course of this work.

I extend my gratitude to Dr. Sarita G Bhat, Professor, Department of Biotechnology, Cochin University of Science and Technology, for her support, and encouragement.

Let me thank Mr. Raghul Subin S, Research Scholar, Department of Biotechnology, Cochin University of Science and Technology, for his support and co-operation at various stages of this work.

I am indebted to my teachers Dr.P.V Sreenivasan, Dr.K.P Unnikrishnan, Dr.A Benny Cherian, Dr.Lopez Mathew, Dr. Mary Alexander, Dr.Mary Kurian, Dr. Philomina Mathew, Dr.Sheelakumari Issac and Dr.Jyothi Mariam John, Department of Chemistry, Union Christian College for their encouragement, help and moral support.

I am extremely thankful to Dr. Beena T Abraham ,Dr. Parameswaran P.S, Dr.Bhuvanasewari M.G, Dr.Sinto Joseph and Dr.Suma K.K, for their selfless co-operation.

I am grateful to my co-researchers, Mr. Jenish Paul, Mrs. Anna Dilfi K,F, Ms.Vidya G, Mrs.Resmi V.C, Mrs.Renju V.S, Ms.Saisy K Esthappan, Mrs.Nisha Nandakumar, Mrs.Nimmi K.P, Mrs. Sona Narayanan, Mr.Abhilash G, Mr.Bipinpal P.K, Mr.Sreejesh P.R, Mrs. Dennyamol P.V, Mrs. Prameladevi M.S, Mrs. Jabin, Mrs. Preetha K Nair, Mrs. Sobha, Mrs. Newly, Mrs. July Chandra , Mrs.Neena George, Mrs.Tresa Sunitha George, Mrs. Shadiya M. A, Ms.Aiswarya E.P, and Ms.Asha Krishnan of the Department of Polymer Science and Rubber Technology for their whole-hearted co-operation and for making my course of study a delightful experience.

I am especially indebted to Mr.Ajilesh B Nair for his support in many ways throughout my research period.

I also extend my sincere thanks to the members of the non-teaching staff of the Department of Polymer Science and Rubber technology, CUSAT for their support at different stages of my research work.

At this moment I remember with love and thanks, the inspiration, love and prayers of my parents and brothers. Finally I thank my husband Georfy and my loving son John for the understanding, patience and love they have shown at all times.

*Above all, I pray and thank **God Almighty** who enlightens me with wisdom and courage for all the success in my life, without which all the efforts will be in vain.*

Vidya Francis

Preface

Polyolefins are one of the most popular class of synthetic polymers, especially due to their useful combinations of properties, good availability and low price. The case of linear low-density polyethylene (LLDPE) is especially significant as it is widely used for packaging and other applications. This synthetic polymer is normally not biodegradable until it is degraded into low molecular mass fragments that can be assimilated by microorganisms.

The present study aims to enhance the rate of photo and biodegradation of polyethylene by (i) adding biodegradable components and (ii) suitable combinations of pro-oxidants. The effect of metallic photo initiators like TiO_2 and cobalt stearate and different combinations of these pro-oxidants with vegetable oil on the photo and biodegradation of linear low-density poly(ethylene)-poly(vinyl alcohol) (LLDPE/PVA) blended films is the subject of this study. Photo degradation leads to physical embrittlement of the blends and leaves a porous and mechanically weakened plastic. This will accelerate the final degradation of the polymer by diffusion of oxygen, moisture, and enzymes into the porous polymer matrix. Mechanical, thermal, spectroscopic and morphological studies were done to estimate the extent of degradation.

The results of the investigations are presented in eight different chapters, as follows:

Chapter 1 is a literature survey and general introduction to polyolefins and biodegradable polymers including the mechanism and methods of biodegradation and photodegradation. Areas of application of biodegradable and photodegradable polymers and their characterization techniques are also

discussed. Finally the scope and objectives of the research project are also presented.

Chapter 2 is a report of the study to improve the biodegradability of LLDPE by blending it with a biodegradable component namely PVA. LLDPE was blended with poly (vinyl alcohol) in a torque rheometer and mechanical, thermal, spectroscopic and biodegradation properties were investigated. The biodegradability of LLDPE/PVA blends was studied (i) in culture medium containing *Vibrio sp.* and (ii) in garden soil environment. The degraded samples were characterized by different techniques.

Chapter 3 describes a rapid hydrothermal synthetic method to produce phase pure, monodisperse anatase particles with small grain size and high specific surface area at low temperature.

Chapter 4 deals with the performance of titanium dioxide and vegetable oil on the degradation behaviour of LLDPE/PVA blends. The outdoor weathering performance of nanoanatase and two crystalline forms of TiO₂ (rutile and anatase) in the absence as well as presence of vegetable oil was examined. This was followed by (i) biodegradation and (ii) soil degradation. The extent of degradation was monitored by mechanical property measurements, thermal studies, weight loss measurements, spectroscopic studies, melt flow index and morphological studies.

Chapter 5 gives an account of the effect of nano and commercial forms of TiO₂ and/or vegetable oil on the UV degradability of the blends. This was evaluated by exposing the test specimens to low pressure mercury vapor discharge lamp (TUV 30W, $\lambda = 253.7\text{nm}$) in air atmosphere. The samples

were retrieved after 600 hours of UV exposure and then subjected to (i) biodegradation and (ii) soil degradation studies by using *Vibrio sp.*

Chapter 6 discusses the effect of a metallic photoinitiator, cobalt stearate and different combinations of cobalt stearate and vegetable oil on the degradation undergone during outdoor exposure and subsequent biodegradation of LLDPE/PVA blend films.

In Chapter 7 studies on the UV degradation of LLDPE/PVA films containing varying amounts of cobalt stearate in the absence as well as presence of vegetable oil are described. Subsequently, partial biodegradation of the UV-degraded samples was done with the help of *Vibrio sp.* bacteria isolated from marine benthic environment.

Chapter 8 is a summary of the entire work. All the important conclusions and observations are highlighted here.

.....❧.....

Abstract

LLDPE was blended with poly (vinyl alcohol) and mechanical, thermal, spectroscopic properties and biodegradability were investigated. The biodegradability of LLDPE/PVA blends has been studied in two environments, viz. (1) a culture medium containing *Vibrio sp.* and (2) a soil environment over a period of 15 weeks. Nanoanatase having photo catalytic activity was synthesized by hydrothermal method using titanium-iso-propoxide. The synthesized TiO₂ was characterized by X-Ray diffraction (XRD), BET studies, FTIR studies and scanning electron microscopy (SEM). The crystallite size of titania was calculated to be $\approx 6\text{nm}$ from the XRD results and the surface area was found to be about $310\text{m}^2/\text{g}$ by BET method. SEM shows that nanoanatase particles prepared by this method are spherical in shape. Linear low density polyethylene films containing polyvinyl alcohol and a pro-oxidant (TiO₂ or cobalt stearate with or without vegetable oil) were prepared. The films were then subjected to natural weathering and UV exposure followed by biodegradation in culture medium as well as in soil environment. The degradation was monitored by mechanical property measurements, thermal studies, rate of weight loss, FTIR and SEM studies. Higher weight loss, texture change and greater increments in carbonyl index values were observed in samples containing cobalt stearate and vegetable oil. The present study demonstrates that the combination of LLDPE/PVA blends with (i) nanoanatase/vegetable oil and (ii) cobalt stearate/vegetable oil leads to extensive photodegradation. These samples show substantial degradation when subsequent exposure to *Vibrio sp.* is made. Thus a combined photodegradation and biodegradation process is a promising step towards obtaining a biodegradable grade of LLDPE.

.....✉.....

Contents

Chapter-1

Introduction and Literature Survey	01 - 57
1.1 Plastics	01
1.2 Types of Plastics	03
1.2.1 Thermoplastics	03
1.2.2 Thermosetting plastics	05
1.3 Polyolefins.....	06
1.3.1 Polyethylene	06
1.3.2 Polypropylene.....	09
1.3.3 Polybutelene.....	10
1.3.4 Polyisobutelene	10
1.4 Polymer degradation	11
1.4.1 Photo-oxidative degradation	12
1.4.2 Thermal degradation	13
1.4.3 Ozone-induced degradation	13
1.4.4 Mechano-chemical degradation	14
1.4.5 Catalytic degradation	15
1.4.6 Biodegradation.....	16
1.5 Factors affecting polymer degradation.....	16
1.5.1 Chemical composition	16
1.5.2 Molecular weight	17
1.5.3 Hydrophobic character.....	17
1.5.4 Size of the molecules	17
1.5.5 Introduction of functionality	17
1.5.6 Additives.....	18
1.5.7 Environmental conditions	18
1.6 Biodegradable polymers	19
1.6.1 Biodegradable polymers from renewable resources	19
1.6.2 Biodegradable polymers from petroleum derived products ---	23
1.7 PVA based biodegradable polymer blends	25
1.7.1 PVA- structure and manufacture	25
1.7.2 Toxicity of PVA	28
1.7.3 Biodegradability of PVA	28
1.8 Biodegradability of polyethylene	29
1.9 Mechanism and methods of biodegradation	31
1.9.1 Mechanism of biodegradation	31
1.9.2 Methods of biodegradation.....	32
1.10 Photodegradability of polyethylene	33
1.11 Mechanism and methods of Photodegradation	34

1.11.1	Mechanism of photodegradation	34
1.11.2	Methods for photodegradation	37
1.12	Biodegradation of photodegradable polyolefins	38
1.13	Characterisation of degraded polymers	39
1.13.1	Mechanical properties	39
1.13.2	Physical properties	39
1.13.3	Gel permeation chromatography	40
1.13.4	Fourier transform infrared spectroscopy	40
1.13.5	Differential scanning calorimetry	41
1.14	Application of biodegradable and photodegradable polymers	41
1.15	Scope and objectives of the present work	43
1.16	References	44

Chapter-2

Preparation, Property Evaluation and Biodegradation of Linear Low Density Polyethylene/Polyvinyl Alcohol

Blends		59 - 87
2.1	Introduction	59
2.2	Experimental	61
2.2.1	Materials	61
2.2.2	Blend preparation	61
2.2.3	Molding	63
2.2.4	Mechanical properties	63
2.2.5	Water absorption studies	64
2.2.6	Degradation studies	65
2.2.6.1	Biodegradation in culture	65
2.2.6.1.1	Screening of microorganisms for PVA degradation	65
2.2.6.1.2	Medium for biodegradation studies	66
2.2.6.1.3	Preparation of consortia for biodegradation studies	66
2.2.6.1.4	Preparation of inoculum and shake flask culture	66
2.2.6.2	Biodegradation in soil environment	67
2.2.7	Spectroscopic studies	67
2.2.8	Thermogravimetric analysis	68
2.2.9	Differential scanning calorimetry	68
2.2.10	Scanning electron microscopy	69
2.3	Results and Discussion	69
2.3.1	Mechanical properties	69
2.3.2	Water absorption studies	72
2.3.3	Biodegradation studies	74
2.3.3.1	Culture medium	74
2.3.3.2	Soil environment	75
2.3.4	FTIR analysis	77
2.3.5	Thermogravimetric analysis	78

2.3.6	Crystallinity studies -----	80
2.3.7	Surface morphological studies-----	83
2.4	Conclusions -----	84
2.5	References-----	85

Chapter-3

Hydrothermal Synthesis of nano- TiO₂ Photocatalyst and its Characterization 89 - 104

3.1	Introduction -----	89
3.2	Experimental -----	90
3.2.1	Chemicals -----	90
3.2.2	Experimental set up -----	90
3.2.3	Preparation of nano-TiO ₂ photocatalyst by hydrothermal method -----	91
3.2.4	Characterization of nanotitania -----	93
3.2.4.1	X-Ray diffraction -----	93
3.2.4.2	Bulk density -----	93
3.2.4.3	BET studies -----	94
3.2.4.4	Fourier transform infrared spectroscopy-----	94
3.2.4.5	Scanning electron microscopy -----	94
3.3	Results and Discussion -----	94
3.3.1	X-Ray diffraction -----	94
3.3.2	Bulk density -----	99
3.3.3	BET studies -----	100
3.3.4	Infrared spectroscopy -----	100
3.3.5	Scanning electron microscopy -----	101
3.4	Conclusions -----	103
3.5	References-----	103

Chapter-4

Effect of TiO₂ on the Weathering and Biodegradation of LLDPE/PVA Blends Containing Vegetable Oil 105 - 142

4.1	Introduction -----	105
4.2	Experimental -----	106
4.2.1	Materials -----	106
4.2.2	Sample preparation-----	107
4.2.3	Degradation studies -----	109
4.2.3.1	Natural weathering -----	109
4.2.3.2	Degradation studies in culture medium and in garden soil---	109
4.2.4	Evaluation of extent of degradation-----	109
4.3	Results and Discussion -----	110
4.3.1	Effect of glycerol and vegetable oil -----	110

4.3.2	Effect of TiO ₂ -----	113
4.3.3	Outdoor weathering studies and degradation by microorganisms -----	115
4.3.4	Spectroscopic studies -----	123
4.3.5	Thermal studies -----	130
4.3.6	Percentage weight loss -----	131
4.3.7	Morphological studies -----	132
4.4	Conclusions -----	139
4.5	References -----	140

Chapter-5

Effect of Pro-oxidant Activity of TiO₂ on the UV and Biodegradation of LLDPE/PVA Blends 143 - 169

5.1	Introduction -----	143
5.2	Experimental -----	144
5.2.1	Materials and sample preparation -----	144
5.2.2	Photo-degradation procedure -----	144
5.2.3	Evaluation of extent of degradation -----	145
5.3	Results and discussion -----	145
5.3.1	UV degradation studies and degradation by microorganisms -----	145
5.3.2	Spectroscopic studies -----	152
5.3.3	Thermal studies -----	158
5.3.4	Percentage weight loss -----	160
5.3.5	Morphological studies -----	160
5.4	Conclusions -----	167
5.5	References -----	168

Chapter - 6

Effect of Cobalt Stearate as Pro-oxidant on Weathering and Biodegradation of LLDPE/PVA Blends..... 171 - 192

6.1	Introduction -----	171
6.2	Experimental -----	172
6.2.1	Materials -----	172
6.2.2	Materials and sample preparation -----	173
6.2.3	Degradation studies -----	173
6.2.3.1	Natural weathering -----	173
6.2.3.2	Biodegradation -----	173
6.2.4	Evaluation of extent of degradation -----	174
6.3	Results and discussion -----	174
6.3.1	Degradation by natural weathering -----	174
6.3.2	Degradation by microorganisms -----	181

6.3.3	Differential scanning calorimetry studies -----	185
6.3.4	Morphological characterization -----	187
6.4	Conclusions -----	190
6.5	References-----	191

Chapter -7

Effect of Pro-oxidant Activity of Cobalt Stearate on the UV and Biodegradation of LLDPE/PVA Blends..... 193 - 208

7.1	Introduction -----	193
7.2	Experimental -----	194
7.2.1	Materials and specimen preparation -----	194
7.2.2	Degradation studies -----	194
7.2.3	Evaluation of extent of degradation-----	194
7.3	Results and Discussion-----	194
7.3.1	Degradation by UV irradiation -----	194
7.3.2	Degradation by microorganisms-----	200
7.3.3	Thermal studies -----	202
7.3.4	Morphological characterization -----	204
7.4	Conclusions -----	206
7.5	References-----	207

Chapter-8

Summary and Conclusions 209 - 211

Abbreviations

Publications

Conferences Papers

INTRODUCTION AND LITERATURE SURVEY

<i>Contents</i>	1.1	<i>Plastics</i>
	1.2	<i>Types of plastics</i>
	1.3	<i>Polyolefins</i>
	1.4	<i>Polymer degradation</i>
	1.5	<i>Factors affecting polymer degradation</i>
	1.6	<i>Biodegradable polymers</i>
	1.7	<i>PVA based biodegradable polymer blends</i>
	1.8	<i>Biodegradability of polyethylene</i>
	1.9	<i>Mechanism and methods of biodegradation</i>
	1.10	<i>Photodegradability of polyethylene</i>
	1.11	<i>Mechanism and methods of photodegradation</i>
	1.12	<i>Biodegradation of photodegradable polyolefins</i>
	1.13	<i>Characterization of degraded polymers</i>
	1.14	<i>Application of biodegradable and photodegradable plastics</i>
	1.15	<i>Scope and objectives of the present work</i>
	1.16	<i>References</i>

1.1 Plastics

The word “plastic” comes from the Greek word “plastikos” meaning “to form”. In more technical terms, a plastic is a material that can be heated and molded so that it keeps its molded shape after it cools. Petrochemical based plastics such as polyolefin, polyesters and polyamides have been increasingly used as packaging materials because of their availability in large quantities at low cost and favorable functional characteristics such as good tensile and tear strength, good barrier properties to oxygen and aroma compounds and heat sealability [1].

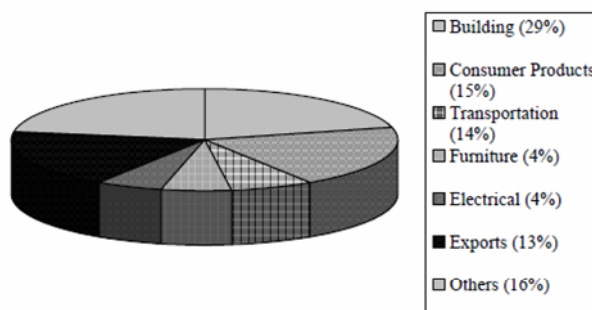


Fig. 1.1 Major uses of plastics [1]

The physicochemical behavior of plastics gives rise to unique pollution problems. Firstly, the major groups of hydrocarbon polymers, the polyolefins, are lighter than water and unlike glass and metals they do not disintegrate and end up at the bottom of the sea. They are therefore carried by wind and waves over large distances and for long periods of time. They are highly visible when finally grounded on coastlines remote from their origin [2] and this biodegradation-resistant debris tends to accumulate from year to year [3]. Some of it, because of its persistence, causes the deaths of sea mammals, birds and fish due to ingestion and entanglement [4].

The accumulation of plastics in the environment is a matter of great concern. It leads to long-term environmental, economic and waste management problems. Degradation of waste plastics by various means and subsequent assimilation into the environment is one of the options to deal with such problems [5,6]. A wide variety of synthetic polymers absorb solar ultraviolet (UV) radiation and undergo photolytic, photo-oxidative, and thermo-oxidative reactions that result in the degradation of these materials [7,8]. The propensity of plastic products to undergo solar UV radiation induced degradation/ ozone-induced degradation can be increased by addition of some additives [9,10]. Besides these degradation phenomena, biodegradation

offers another most efficient and attractive route to environmental waste management. The mechanisms involved in biodegradation are complex due to the interaction of different oxidative processes caused by the oxygen present in the air, by microorganisms or by a combination of the two [11].

1.2 Types of plastics

Plastics are, in general, classified into two groups i.e. thermoplastics and thermosets[12]. This classification is based on their behavior when exposed to heat. Thermoplastics melt or soften and attain a plastic stage on heating. On cooling they solidify but can be softened or remelted on further heating. Thermosets, on the other hand, tend to char on continued heating although an initial softening may be noticed. Hence reshaping of a thermoset material is impossible.

1.2.1 Thermoplastics

Thermoplastics are linear chain macromolecules where the atoms and molecules are joined end-to-end into a series of long, carbon chains. The bi-functionality necessary to form a linear macromolecule from unsaturated monomers can be achieved by opening the double bond and reaction proceeds by a free radical mechanism. Such type of polymerization is known as addition polymerization [13,14]. Thermoplastic polymers are normally produced in one step and then made into products in a subsequent shaping process at high temperature. When cooled significantly below their softening point they again become rigid and usable as a formed article. This type of polymer can be readily recycled because each time it is reheated it can again be reshaped or formed into a new article. Some common thermoplastics and their properties are shown in Table-1.1[15].

Table 1.1 List of common thermoplastics and their properties

Polymer	Density kg/m ³	Tensile strength N/mm ²	Young's modulus GPa	Properties	Applications and uses
PE	950	20-30	0.7	Insulator, chemical resistant	Packaging, bags, bottles, domestic appliances
PVC	1330	48	3.4	Stiff, hard, tough, light	Cables, hoses, sheet, fabric
PP	900	27	1.3	Tough, light, chemical resistant, will scratch, quite soft	Containers, pots, plastic seats, ropes, nets.
PMMA	1190	74	3.0	Stiff, durable, insulator, machines well, polishes well, scratches easily	Car light covers, baths, shower trays, basins. Can be line bent/vacuum formed/injection moulded with ease
PS	1050	48	3.4	Light, stiff, transparent, brittle, waterproof/resistant	Toys, electrical product cases, boxes, packaging, vacuum formings
PTFE	2100	13	0.3	excellent dielectric properties, chemical inertness	used as a thread seal tape, as feet for computer mice, in industrial air filtration applications
Nylon	1160	60	2.4	Tough, hard, light, self lubricating, chemical resistant, machines well, extrudable, injects well	Bearings, gears, rope, hinges and catches, engineering applications
Cellulose acetate	1300	40	1.4	Tough, stiff, hard, transparent, light, heat resistant	Tool handles, pen bodies, frames for glasses. Can be injection moulded
PET	1370	55-75	2.8	Lightweight, impact-resistant, a good gas barrier, good alcohol and solvent barrier	plastic bottles, food packaging, thermal insulation
Polycarbonate	1200	55-75	2.0-2.4	Hard, strong, transparent, high refractive index	Spectacle lenses
PEEK	1320	90-100	3.6	excellent mechanical, thermal and chemical resistance, resistant to attack by both organic and aqueous environments	used to fabricate bearings, piston parts, pumps, HPLC columns, compressor plate valves, and cable insulation.
PVA	1190	40-90	2.3	excellent film forming, emulsifying and adhesive properties, resistant to oil, grease and solvents	Textile sizing agent, Paper coatings, release line, Used in eye drops and hard contact lens solution as a lubricant

1.2.2 Thermosetting plastics

Thermoset plastics are formed by step-growth polymerization under suitable conditions allowing bi-functional molecules to condense intermolecularly with the liberation of small by-products such as H₂O, HCl etc. at each reaction step [14]. The thermosetting polymers are normally produced and shaped in the same step. Upon heating, thermosetting polymers will become soft, but cannot be shaped or formed to any great extent, and will definitely not flow. Some common thermosetting plastics and their properties are shown in Table-1.2 [15].

Table 1.2 List of common thermosetting plastics and their properties

Polymer	Density kg/m ³	Tensile strength N/mm ²	Young's modulus GPa	Properties	Applications and uses
Urea formaldehyde (cellulose filled)	1500	38-90	7-10	Strong, insulator, brittle, hard, stiff	Electrical fittings, handles and knobs
Epoxy resin (glass filled)	1600-2000	68-200	20	Good insulator, brittle chemical resistant	Adhesives bonding fibers, encapsulation
Melamine formaldehyde (fabric filled)	1800-2000	60-90	7	Hard, strong, heat resistant	Adhesives bonding fibers, encapsulation
Phenol formaldehyde (mica filled)	1600-1900	38-50	17-35	Good electrical properties	used in the high speed bearing market, binding agent in normal (organic) brake pads, brake shoes and clutch disks
Polyimide	1430	75-90	3.2	thermal stability, good chemical resistance, excellent mechanical properties	Used in the electronics industry for flexible cables, as an insulating film on magnet wire and for medical tubing.
Polyamide-imide	1340	152	4.5	high temperature and chemical resistance	Ideal candidates for membrane based gas separations

1.3 Polyolefins

The polyolefins are saturated hydrocarbon polymers based on ethylene, propylene and higher α -olefins or combinations of these monomers. Besides polyethylene and polypropylene, which are the most important representatives of polyolefins, also polybut-1-ene, polyisobutylene and poly-(4-methylpent-1-ene) are interesting and prospective materials [16].

1.3.1 Polyethylene

Polyethylene (PE) is a thermoplastic polymer consisting of long chains produced by combination of the monomer molecules viz. ethylene. Depending on the mode of polymerization, three basic types of polyethylene are frequently used: linear high-density polyethylene (HDPE), branched low-density polyethylene (LDPE), and linear low-density polyethylene (LLDPE) (Fig. 1.2) [17].

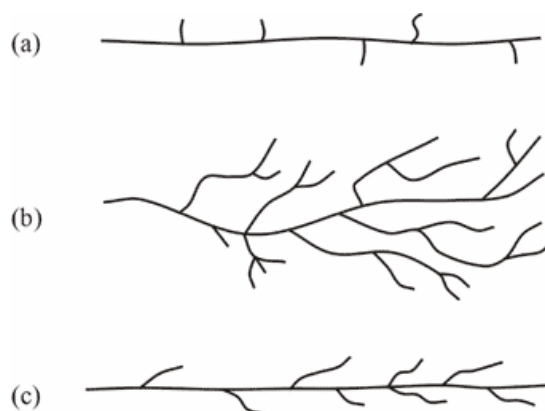


Fig. 1.2 Structure of polyethylene: a) HDPE b) LDPE c) LLDPE [18]

HDPE- HDPE has a low degree of branching and thus greater intermolecular forces and tensile strength. It can be produced by chromium/silica catalysts, Ziegler-Natta catalysts or metallocene catalysts. HDPE is used

in products such as appliances, milk jugs, detergent bottles, margarine tubs, garbage containers, toys and water pipes and in packaging.

LDPE- LDPE has a high degree of short and long chain branching. It has, therefore, less strong intermolecular forces as the instantaneous-dipole induced-dipole attraction is less. LDPE is created by free radical polymerization. It is used for both rigid containers and plastic film applications such as plastic bags and film wrap.

LLDPE- LLDPE is a substantially linear polymer with significant numbers of short branches, commonly made by copolymerization of ethylene with short-chain alpha-olefins. It has higher tensile strength and also higher impact and puncture resistance than LDPE. LLDPE is used in packaging, particularly films for bags and sheets. While other applications are available, LLDPE is preferred for film applications due to its toughness, flexibility and relative transparency.

Polyethylene molecule consists of long chain of carbon atoms, with two hydrogen atoms attached to each carbon. Commercially, it is produced from ethylene (Fig. 1.3).

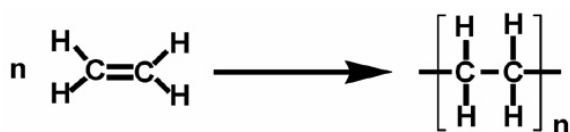


Fig.1. 3 Polymerization of ethylene [19]

Table 1.3 Five distinct routes of PE preparation

Preparation method	Temperature (°C)	Pressure (MPa)	Catayst	Grade
High-Pressure Process	80-300	100-300	benzoyle peroxide, azodi-isobutyronitrile or oxygen	LDPE
Ziegler Process	70-150	< 1	alkyls of groups I-III metals with halides and other derivatives of transition metals in groups IV-VIII of the periodic table	LDPE and HDPE
Phillips Process	130-160	1.4-3.5	metal oxide	HDPE
Standard Oil Company (Indiana) Process	230-270	4.0-8.0	transition metal oxide (Molybdenum oxide) in combination with a promoter (sodium or calcium as metals or hydrides).	HDPE
Gas phase process	≤ 100	0.7-2.1	transition metal	LLDPE

PE has near-zero moisture absorption, excellent chemical resistance and electrical insulating properties and can be easily processed. In the bulk condition it is opaque due to crystallization but thin films may be transparent [20]. Mechanical properties strongly depend on the molecular weight and on the degree of branching of the polymer. These properties are also dependent on the rate of testing, the temperature of test etc.

Polyethylene is the polymer which is most often seen in daily life. HDPEs major use is in blow-moulded bottles, drums, automotive gasoline tanks; injection-moulded crates, trash and garbage containers and extruded pipe products. LDPE/LLDPEs find major applications in plastic bags, films, cable insulations and bottles [17].

1.3.2 Polypropylene

The worldwide consumption of PP occupies third place among commodity plastics, after LDPE and PVC but before HDPE and PS [21]. As early as 1869 propylene was polymerized by Berthelot by reaction with concentrated sulphuric acid. Its industrial importance resulted from the discovery of crystalline high molecular weight polypropylene in 1955 by Natta from organo-metallic catalysts based on titanium and aluminium (Fig. 1.4).

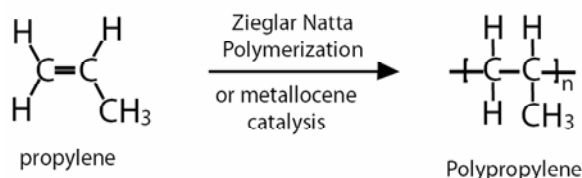


Fig. 1.4 Polymerization of propylene [22]

Mechanical properties of PP are strongly dependent on its crystallinity. Increasing crystallinity enhances stiffness, yield stress, and flexural strength; however, toughness and impact strength decrease [23]. PP indicates some similar properties to polyethylene, particularly swelling and solution behaviour, and electrical properties.

Since PP is resistant to fatigue, most plastic living hinges are made from this material. It is often used for blow moulded bottles and automotive parts,

injection-moulded closures, toys and housewares. It can be also extruded into fibres and filaments for production of carpets, rugs, and cordage [20].

1.3.3 Polybut-1-ene

Polybut-1-ene (PB) is the youngest member of the polyolefin family (1965) being linear in structure (Fig.1.5) [24]. The monomer butylene is obtained from the petrochemical industry [24]. PB is produced by Ziegler-Natta system and the commercial material have very high molecular weight of 770000 to 3000000, that is about ten times higher than that of the normal LDPE [20].

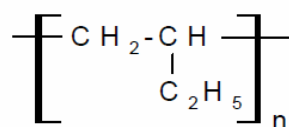


Fig. 1.5 Polybut-1-ene

It has a melting point and stiffness intermediate between PE and PP, but it is less resistant to aliphatic hydrocarbons than PE and PP. Because it has very high molecular weight, the polymer has a very high resistance to creep. One advantage of this is that the wall thicknesses of PB pipes may be much less than for corresponding PE and PP pipes [20].

The main interest of PB is in its use as a piping material. The principal application is for small-bore cold and hot water piping (up to 95°C) for domestic plumbing [20].

1.3.4 Polyisobutylene

In chronological terms polyisobutylene (PIB) was the first of the polyolefins. Low polymers were prepared as early as 1873. PIB is made from the monomer isobutylene by cationic vinyl polymerization (Fig. 1.6).

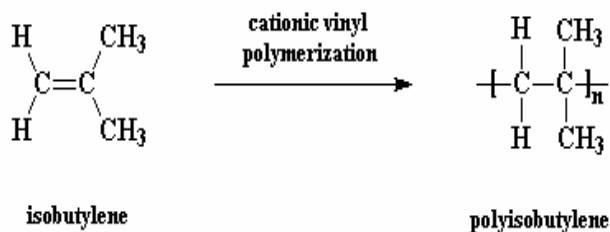


Fig. 1.6 Polymerization of PIB

The homopolymer finds uses as an adhesive component, as a base for chewing gum, in tank linings, as a motor oil additive to provide suitable viscosity characteristics and to improve the environmental stress-cracking resistance of polyethylene. It has been incorporated in quantities of up to 30% in HDPE to improve the impact strength of heavy duty sacks [17].

1.4 Polymer degradation

Thermal, environmental and UV exposure of polymers generally leads to their degradation and deterioration [25-27]. Changes in polymer properties due to chemical, physical or biological reactions resulting in bond scission and subsequent chemical transformation are categorized as polymer degradation [28]. Degradation reflects changes in material properties such as mechanical, optical or electrical characteristics manifest as crazing, cracking, erosion, discoloration and phase separation [29]. “A plastic designed to undergo a significant change in its chemical structure under specific environmental conditions resulting in a loss of some properties that may vary as measured by standard test methods appropriate to the plastic and the application in a period of time that determines its classification is called a degradable plastic” (ASTM D 883-93)[24].

Depending upon the nature of the causing agents, polymer degradations have been classified as photo-oxidative degradation, thermal degradation, ozone-induced degradation, mechanochemical degradation, catalytic degradation and biodegradation [30].

1.4.1 Photo-oxidative degradation

A degradable plastic in which the degradation results from the action of natural daylight is called a photodegradable plastic (ASTM D 883-93) [23]. The photo-induced degradation process can be initiated either by the absorption of the photon by the polymer chain itself or by some of the additives incorporated in the product. The degraded sites act as stress concentrators and crack will occur when the material is subjected to stress [31]. Thus, they diminish the tensile strength and ultimately cause the mechanical failure of the material. The above effects will result in change in tensile properties [32, 33]. In the case of photoactive-pigments like TiO₂, ZnO or CdS, formation of an electron-hole pair on the pigment surface in the presence of oxygen and water can produce reactive species which can eventually cause oxidation of the polymer [34]. The direct effect of radiation on plastic is usually limited to the surface region, due to light absorption by the pigment or the degraded material itself.

Most of the synthetic polymers are susceptible to degradation initiated by UV and visible light. Normally the near-UV radiations (290-400 nm) in the sunlight determine the lifetime of polymeric materials in outdoor applications [35-37]. Polymer degradation occurs mainly at the polar groups, where photo-irradiation generates ester, aldehyde and formate end groups [38]. UV radiations have sufficient energy to cleave C-C bond [39]. Photo-degradation

changes the physical and optical properties of the plastic. The most damaging effects are the visual effect (yellowing), the loss of mechanical properties of the polymers, the changes in molecular weight and the molecular weight distribution [40-45]. PE and PP films when exposed to solar UV radiation readily lose their extensibility, mechanical integrity and strength along with decrease in their average molecular weight [46-50].

1.4.2 Thermal degradation

Under normal conditions, photochemical and thermal degradations are similar and are classified as oxidative degradation. The main difference between the two is the sequence of initiation steps leading to auto-oxidation cycle. Another major difference is that thermal reactions occur throughout the bulk of the polymer sample whereas photochemical reactions occur only on the surface [51]. Thermal degradation of polymers occurs through random chain degradation initiated by thermal radiation and UV light [52]. A large number of addition polymers depolymerize at elevated temperatures for example PE has been decomposed into long olefinic fragments and actually producing little monomer [53]. Thermal degradation above 200⁰C leads to chain scission and largely depends on factors like unsaturation sites, head-to-head units, etc. [46]. Polyolefins are known to be sensitive to thermal oxidation, due to the impurities generated during their manufacture at high temperatures [47].

1.4.3 Ozone-induced degradation

Atmospheric ozone usually causes the degradation of polymers under conditions that may be considered as normal; when other oxidative aging processes are very slow and the polymer retains its properties for a rather

longer time [48-50]. The presence of ozone in the air, even in very small concentrations, markedly accelerates the aging of polymeric materials [54]. This process in saturated polymers is accompanied by the intensive formation of oxygen-containing compounds, by a change in the molecular weight and by impairment of the mechanical and electrical properties of the specimens [55]. Exposure of polymers to ozone results in the rapid and consistent formation of a variety of carbonyl and unsaturated carbonyl products based on aliphatic esters, ketones, and lactones. This is followed by a more gradual formation of ether, hydroxyl and terminal vinyl groups with time and concentration [56]. These reactions of ozone with polymers occur with main chains containing C=C bonds, aromatic rings or saturated hydrocarbon links. The reaction proceeds through unstable intermediates such as the bipolar ion or peroxy radicals which can isomerize, degrade or cause decomposition of macromolecules [57].

In PVA, the chain scission is based on the ozone oxidation of the alcoholic groups of PVA with formation of ketone groups which in turn are the source of a keto-enol tautomerism which leads to random chain scission by further ozone attack. The analysis with FTIR spectra indicates that the final product is a PVA oligomer with numerous ketone groups along the main oligomer backbone and with carboxylic end groups [58]. Exposure to ozone gas causes change in the mechanical properties of LLDPE, oriented PP and biaxially oriented nylon [59].

1.4.4 Mechano-chemical degradation

Mechano-chemical degradation of polymers involves the degradation of polymer under mechanical stress and by strong ultrasonic irradiations [60].

The mechano-degradation of polymers in melts occurs by means of free radical processes. Mechanically generated radicals are believed to result from the cleavage of the main backbone segments of polymer chains in the stressed amorphous regions connecting crystallites [61]. Gel permeation chromatographic (GPC) studies of the degradation of LDPE and HDPE under high shear conditions have indicated that most of the changes in molecular weight distribution and long-chain branching have occurred from thermal or thermo-oxidative degradation. On the other hand, the orientation of solid PP under high shear conditions (high draw rates and relatively low temperatures) has produced oxidation products directly as a result of the shear process [62]. Ultrasound is responsible for the breakage of macromolecular C-C bonds and termination reactions of mechano-radicals occur as disproportionation and combination reactions. These reactions are suppressed in the presence of radical scavengers [63].

1.4.5 Catalytic degradation

Catalytic transformation of waste polymers into hydrocarbons with higher commercial value is a field of great interest. Polyolefins are thermally or catalytically degraded into gases and oils. Garforth et al. [64] have investigated catalytic degradation of polyolefins using TGA as a potential method for screening catalysts and have found that the presence of catalyst led to decrease in the apparent activation energy. For polymer degradation, different types of catalysts have been reported in the literature which include Pt-Co and Pt-Mo supported over SiO₂ [65], zeolite catalysts and non-zeolite catalysts [66], transition metal catalysts (Cr, Ni, Mo, Co, Fe) supported on Al₂O₃, SiO₂ etc. [67], zeolite [68] and zirconium hydride [69].

1.4.6 Biodegradation

Biodegradation or biotic degradation is chemical degradation of polymers brought about by the action of naturally occurring microorganisms such as bacteria, fungi and algae [70-72]. As biodegradation proceeds it produces CO₂ and/or CH₄ and H₂O. If oxygen is present aerobic degradation takes place and CO₂ is produced. If there is no oxygen available, the biotic degradation is anaerobic and CH₄ is produced instead of CO₂. Under some circumstances both gases are produced.

Mineralization is defined as the conversion of biodegradable materials or biomass to gases (like CO₂, CH₄ and nitrogen compounds), water, salts and minerals and residual biomass. Complete mineralization represents the rendering of all chemical elements into natural biogeochemical cycles [70,73].

1.5 Factors affecting polymer degradation

Degradation of plastics is affected by various factors discussed in the following sections.

1.5.1 Chemical composition

Chemical composition of the polymers plays a very important role in their degradation. Presence of solely long carbon chains in the thermoplastic polyolefins makes these polymers non-susceptible to degradation by microorganisms. By the incorporation of heterogroups such as oxygen in the polymer chains, polymeric substances are made labile for thermal degradation and biodegradation [74]. Linear saturated polyolefins are resistant to oxidative degradation. Presence of unsaturation in the polymer chain makes them susceptible to oxidation, for example natural rubber is more susceptible to

degradation than PE [75]. Amorphous regions in the polymer have been reported to be more labile to thermal oxidation compared to crystalline areas because of their high permeability to molecular oxygen [76].

1.5.2 Molecular weight

Increase in molecular weight of the plastic decreases the rate of plastic degradation [77]. It has been reported that some microorganisms utilize polyolefins with low molecular weight faster compared to high molecular weight polyolefins [78,79]. Linear polyolefins with molecular weight lower than about 620 support microbial growth [80].

1.5.3 Hydrophobic character

Petrochemical-based plastic materials are not easily degraded in the environment because of their hydrophobic character and three-dimensional structure [78]. Hydrophobicity of PE interferes with the formation of a microbial bio-film, thus limiting the extent of biodegradation [81].

1.5.4 Size of the molecules

Chain length of the molecules in the polymers affects their mechanical degradation, thermal degradation and biodegradation. These degradations increase as the size of the molecule decreases [74].

1.5.5 Introduction of functionality

Introduction of carbonyl groups in polyolefins makes these polymers susceptible to photodegradation. As the number of chromophores increases the rate of photodegradation increases. This is because of the possibility of absorbing more photons and initiating the reactions leading to degradation. The carbonyl chromophore absorbs near-UV radiation and form radicals by the Norrish Type I,

II and H-abstraction processes for photochemical degradation. Chromophores other than carbonyl group C=O such as metal-metal bonds, if incorporated into polymer backbone, also induce photodegradability. In such a case, metal-metal bond cleaves homolytically on irradiation [82].

1.5.6 Additives

Metals act as good pro-oxidants in polyolefins making polymers susceptible to thermo-oxidative degradation. Upon activation by heat in the presence of oxygen, pro-oxidants produce free radicals on the PE chain which undergo oxidation and change the physical properties of the polymer [83]. In addition, the pro-oxidant catalyzes the chain scission reactions in the polymer. This leads to low molecular weight oxidation products containing functional groups like -COOH, -OH and C=O [84]. Traces of transition metals accelerate thermal oxidative processes of polyolefins by inducing hydroperoxide decomposition [85]. For example, TiO₂ delustrant makes the polyamides susceptible to heat- and light induced oxidation [39]. Oxidation of plastic (polyolefin) is influenced by the amount of pro-oxidant additives, chemical structure, morphology of plastic sample and the surface area [86]. The use of pro-oxidant additives can make the polyolefins thermoxo-biodegradable by making the polymer hydrophilic and also catalyzing the breakdown of high molecular weight polyolefin to lower molecular weight products [87]. Susceptibility of PE to biodegradation is enhanced by blending with starch or certain polyesters and biodegradation depends upon the type of polymer and the blend composition [88].

1.5.7 Environmental conditions

Biodegradation of polymer depends upon environmental conditions such as moisture, temperature, oxygen, and suitable population of microorganisms

[83]. In warm climates when the relative humidity is higher about 70%, the rate of polymer degradation by the microorganisms increases [76]. Temperature of the material and the presence of moisture show a considerable synergistic effect on the photodegradation of the polymeric materials [89]. Weathering is a degradation process and as such is temperature dependent, i.e. it will occur more rapidly at higher temperatures. Humidity also affects the degradation processes; most weathering processes are considerably slower in hot dry climates than in hot wet climates.

1.6 Biodegradable polymers

ASTM definition of a biodegradable plastic is “a plastic designed to undergo a significant change in its chemical structure under specific environmental conditions resulting in a loss of some properties in which the degradation results from the action of naturally occurring micro-organisms such as bacteria, fungi and algae”(ASTM D 883)[24].

1.6.1 Biodegradable polymers from renewable resources

The materials that make up renewable resources are agricultural products and those based on biosynthesis.

(i) Agriculture based

(a) Cellulose

Cellulose is a linear condensation polymer consisting of anhydroglucose units joined together by β -1,4-glycosidic bonds [90]. Cellulose is readily biodegradable and is mineralized by many micro-organisms due to the activity of the cellulose enzyme complex which catalyses the hydrolysis and/or oxidation of cellulose resulting in the formation of cellobiose, glucose and

finally mineralization [90]. Several enzymes have been shown to act synergistically in the breakdown of cellulose with endocellulases attacking the amorphous regions and cellulases causing random chain scission [91,92].

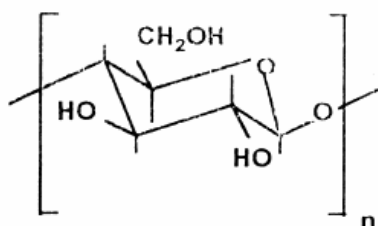


Fig. 1.7 Cellulose

(b) Starch

Starch can be considered as a condensation polymer of glucose consisting of two types, amylose, a linear chain molecule of α -1,4-linked D-glucose and amylopectin a branched polymer of α -1,4-linked D-glucose with a 1,6-linked D-glucose unit. Due to its function as food storage, starch is readily biodegraded through enzyme catalyzed hydrolysis by a number enzyme [93]. Various processing techniques have been developed resulting in reducing or eliminating amylopectin crystallinity and amylose complexation [94].

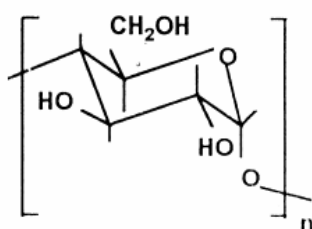


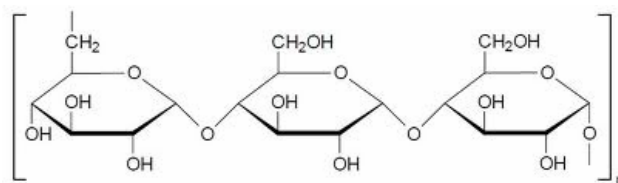
Fig. 1.8 Starch

(ii) Biosynthesis based**(a) Polyhydroxy alkananoates (Bacterial polyesters)****Fig. 1.9 Structures of PHA and PHB**

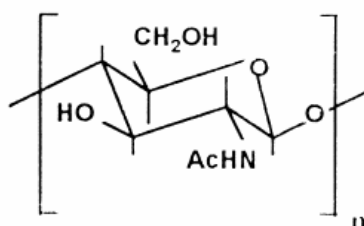
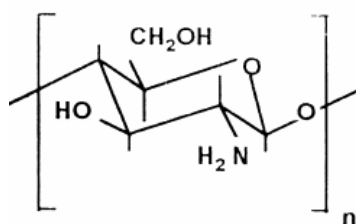
Polyhydroxyalkanoates (PHA) are polymers produced as intracellular storage materials by a variety of bacteria grown under physiologically stressed conditions. Poly- β -hydroxybutyrate-co- β -hydroxyvalerate (PHBV) is a semicrystalline aliphatic polyester that was first produced commercially by Imperial Chemical Industries from the bacteria *Alcaligenes eutrophus*. The effect of crystallinity on the enzymatic degradation of PHBV shows a dramatic decrease in the degradation rate with increasing crystallinity [95].

(b) Pullulan

Pullulan, a biodegradable polysaccharide first described in 1959 [96], is a water-soluble extracellular neutral glucose synthesized by the fungus *Aureobasidium Pullulans*, more commonly referred to as *Pullularia Pullulans*. The structure of pullulan has been proposed to consist of predominantly maltotriose units linked via α -1,6-glycosidic bonds [97]. Pullulan can be solution cast from aqueous media, although it has been difficult to process by conventional melt processing techniques [98]. Pullulan, like starch begins to degrade thermally at approximately at 250⁰C, then carbonizes and generates neither extreme heat nor toxic gas [98,99].

**Fig. 1.10 Pullulan****(c) Chitin and chitosan**

Chitin is a naturally occurring polysaccharide derived primarily from the exoskeleton of shellfish and is described as β -1,4-linked 2-acetamido-2-deoxy-D-glucose. Chitin is also found in insects and filamentous fungi [100]. Chitin has been shown to be readily biodegraded by microorganisms producing chitinases and lysozyme and is subsequently mineralized [101,102].

**Fig. 1.11 Chitin****Fig 1.12 Chitosan**

Chitosan is deacetylated chitin. This polymer is produced commercially from the base catalyzed deacetylation of shellfish waste. Chitosan has also been found to exist naturally, being synthesized by zygomycete fungi as part of their cell wall. Chitosan has been shown to be biodegraded by chitosanases [101,102].

(d) Polylactic acid

Polylactic acid (PLA) is a thermoplastic, aliphatic polyester that can be synthesized from biologically produced lactic acid. Currently, the major production of polylactic acid is from the ring opening polymerization of lactide [103,104]. This material has been used extensively in the medical field for sutures, staples and the like and as such is very expensive. Recently, it has been found to be biodegradable in a compost environment [103,105].

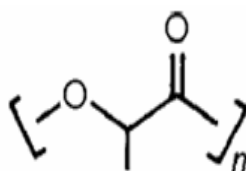


Fig. 1.13 Polylactic acid

1.6.2 Biodegradable polymers from petroleum derived products

(a) Polycaprolactone

Poly- ϵ -caprolactone (PCL) is a semicrystalline, thermoplastic, linear aliphatic polyester synthesized by the ring opening polymerization of ϵ -caprolactone. PCL is readily degraded and mineralized by a variety of micro-organisms [105]. The degradation mechanism proposed is hydrolysis of the

polymer to 6-hydroxy caproic acid, which can then undergo further degradation in the citric acid cycle [105].

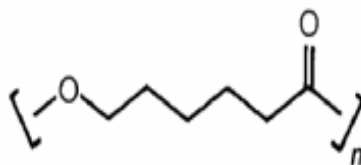


Fig. 1.14 Polycaprolactone

(b) Polyvinyl alcohol

Polyvinyl alcohol (PVA) obtained by the hydrolysis of polyvinyl acetate is the only synthetic carbon chain polymer accepted as fully biodegradable. The properties depend on the molecular weight and degree of hydrolysis. The common commercial grades of PVA include water soluble PVA which contains a degree of hydrolysis of 88% and water insoluble PVA with a degree of hydrolysis >98%. PVA has been found to be biodegradable and mineralized in various environments, although most of the work has been conducted on water soluble PVA [106]. Being water soluble and biodegradable PVA is used to make water soluble and biodegradable carriers, paper coatings, in eye drops and hard contact lens solution as a lubricant.

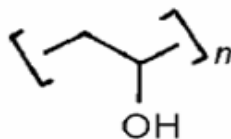


Fig. 1.15 Polyvinyl alcohol

1.7 PVA based biodegradable polymer blends

Water soluble and/or biodegradable plastics are now available based on thermoplastic starch, polyvinyl alcohol, aliphatic and aliphatic/aromatic copolyesters, polylactic acid and blends of these polymers [107]. Extensive advances in PVA formulating and processing technology over the past decade enable these polymers to be melt-processed as thermoplastics without undergoing thermal or shear degradation. Prior to this, PVA was useable only in the form of aqueous solutions or solution-cast films [108]. PVA product types are now available with controllable water-dissolution temperatures ranging from 5-80°C. These can be employed for production of film, sheet, fibers, foams, tubing, profile extrusions and moldings by using processes including film blowing, sheet casting, thermoforming, extrusion, coextrusion and injection and blowmolding.

Combination of these PVA-based materials with recently developed engineered thermoplastic and water-soluble starches now enables economical water-soluble blends to be produced which retain many of the high performance characteristics of PVA.

1.7.1 PVA-structure and manufacture

Unlike most vinyl polymers, PVA is not prepared by polymerization of the corresponding monomer. The monomer, vinyl alcohol, almost exclusively exists as the tautomeric form, acetaldehyde. Consequently, it is manufactured by hydrolyzing polyvinyl acetate, generally in methanolic sodium hydroxide [109] as shown in Fig. 1.16

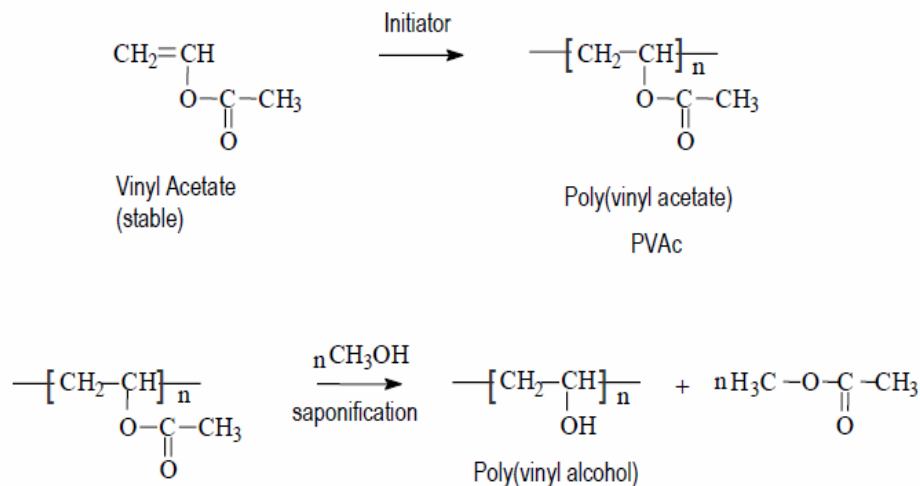


Fig.1.16 Synthesis of polyvinyl alcohol from polyvinyl acetate

The properties of the PVA obtained, such as molecular weight distribution and degree of branching, depend upon the structure of the polyvinyl acetate precursor which itself depends on the polymerization method used to make it. Unlike PVC, PVA properties are largely controlled by hydrogen bonding, resulting from the high hydroxyl group content and its ability to crystallize. Depending on the degree of hydrolysis, i.e. the proportion of unhydrolyzed acetate groups remaining materials with different property combinations may be obtained, varying from partially to fully hydrolyzed, with differing hydrogen bonding abilities and propensities towards crystallization.

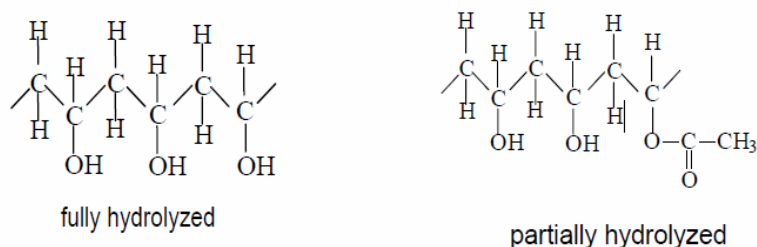


Fig 1.17 Partially and fully hydrolysed forms of PVA

Most commercially-available PVA polymer grades are atactic, and the degree of crystallinity attainable in practical PVA formulations depends on various factors such as the production processes used to make the precursor polyvinyl acetate and convert it to PVA, the degree of hydrolysis, the molecular weight, the water content and the contents and types of plasticizer or other constituents incorporated [110]. Consequently, physical properties such as strength, water solubility, gas permeability, and thermal characteristics can be manipulated by varying these factors. Examples of the range of standard materials and some typical applications are shown in Table 1.4 [107].

Table 1.4 Standard Formulated PVA Grades.(Available from Adept Polymers Ltd. under the name of Depart)[107].

Grade	Description	Typical Applications
C-5	Cold water soluble (low viscosity)	Injection & rotational molding
C-10	Cold water soluble at 10°C	Bags (bait bags, detergent sachets); film (chemical packaging, cling film); injection & blow molding
C-25	Cold water soluble at 25°C	Bags (cement additives); film (embroidery & weld dam); injection and blow molding
W-40	Warm water soluble at 40°C	Bags (dry detergent packing) & film
W-50	Warm water soluble at 50°C	Infected laundry bags: injection and blow molding
W-60 W-63	Warm water soluble at 60-65°C	Infected laundry and compostable bags
H-70	Hot water soluble at 70°C (low viscosity)	Injection molding
H-80	Hot water soluble at 80°C	Bags (nuclear waste), film (auto tape, curing tape)

Table 1.5 shows some typical film properties compared with some other common polymers [108].

Table 1.5 Typical properties of PVA films compared with traditional film materials*. (* Film thickness 25 microns.)

Property	PVA	Cellophane	PVC	LLDPE
Clarity (light transmitted): %	60-66	58-66	48-58	54-58
Gloss (light reflected): %	81	60	80	22
Tear strength (Elmendorf): g	260-3000	20-40	390-780	290-980
Tensile strength: MPa	40-90	55-131	20-76	17-19
Elongation at break: %	110-400	-	5-250	50-600

1.7.2 Toxicity of PVA

PVA polymers are non-toxic and formulated products can maintain this nontoxicity by selection of non-toxic plasticizers and other formulating components. PVA-based materials have been approved as indirect food additives, for food contact, and for drug delivery purposes and tablet coatings by the US FDA and the EU [111].

1.7.3 Biodegradability of PVA

PVA is inherently biodegradable. Biodegradation has been observed by at least 20 different genera of bacteria and several yeasts and molds which occur in activated sludge, compost, facultative ponds, landfills, anaerobic digesters and septic systems and in natural soil and aquatic environments. The degradation mechanism is unusual since it occurs randomly along the PVA

polymer chain unlike many other polymers which primarily degrade from the chain ends. Several mechanisms participate, involving oxidation of hydroxyl groups to ketone groups and then formation of acetic acid, alcohols and ketones which are further metabolized to carbon dioxide and water [112-115].

PVA is completely degraded and utilized by a bacterial strain, *Pseudomonas O-3*, as a sole source of carbon and energy. However, PVA-degrading microorganisms are not ubiquitous within the environment. Almost all of the degrading strains belong to the genus *Pseudomonas* although some do belong to other genera [116]. Generally the carbon-carbon linkage of PVA is degraded either by the enzymes dehydrogenase or oxidase, which is further degraded by the action of hydrolase or aldolase to form simple compounds. Sturm (aquatic) biodegradation tests (ISO FDIS 14852) show that PVA-based formulations degrade in the presence of activated sewage sludge at a similar rate to cellulose [108,117].

1.8 Biodegradability of polyethylene

PE is a stable polymer, and consists of long chains of ethylene monomers. PE cannot be easily degraded with microorganisms. However, it was reported that lower molecular weight PE oligomers (MW = 600-800) were partially degraded by *Acinetobacter sp.* 351 upon dispersion, while high molecular weight PE could not be degraded [118]. Biodegradability of PE can also be improved by blending it with biodegradable additives, photo-initiators or copolymerization [119-121].

Environmental degradation of PE proceeds by synergistic action of photo-and thermo-oxidative degradation and biological activity. When PE is subjected to thermo- and photo-oxidization, various products such as alkanes,

alkenes, ketones, aldehydes, alcohols, carboxylic acid, keto-acids, dicarboxylic acids, lactones and esters are released. Blending of PE with additives generally enhances auto-oxidation, reduces the molecular weight of the polymer and then makes it easier for microorganisms to degrade the low molecular weight materials. It is worthy to note that despite all these attempts to enhance the biodegradation of PE blends, the biodegradability due to microbial activity on the PE part of the blends is still very low. *Phanerochaete chrysosporium* has also been found to degrade starch blended LDPE in soil [122].

High molecular weight polyethylene is also degraded by lignin-degrading fungi under nitrogen-limited or carbon-limited conditions, and by manganese peroxidase. Fungi like *Mucor rouxii* NRRL 1835 and *Aspergillus flavus* and several strains of *Streptomyces* are capable of degrading polyethylene containing 6% starch. Degradation was monitored from the changes in the mechanical properties like tensile strength and elongation [123]. No microorganism or bacterium has been found so far that could degrade PE without additives [124].

Modification of backbone through copolymerization and through anchoring monosaccharide with polyolefin or blending with nutrients and biodegradable fillers makes the plastic degradable [125-128]. These micronutrients help the growth of specific microorganisms thus inducing biodegradability and through the incorporation of polar functional groups which can serve as points of microbial attack [129,130]. Biodegradation of PE occurs through two mechanisms: hydro-biodegradation and oxo-biodegradation [131]. These two mechanisms work successfully on the modified PE (by additive starch) making the material hydrophilic. Chiellini et al. [132] have reported the oxidative degradation of PE film containing pro-oxidant additives. Some

strains of bacteria such as *Pseudomonas aeruginosa*, *Pseudomonas fluorescens* and fungi *Penicillium simplicissimum* have been reported as the most commonly used organisms for the plastic degradation [133,134].

1.9 Mechanism and methods of biodegradation

1.9.1 Mechanism of biodegradation

Biodegradation of polymers occurs through four different mechanisms: solubilization, charge formation followed by dissolution, hydrolysis and enzyme-catalyzed degradation [135,136].

(a) Solubilization.

The hydration results from disruption of secondary and tertiary structure stabilized by van der Waals forces and hydrogen bonds. During and after hydration, the polymer chains may become water soluble and/or the polymer backbone may be cleaved by enzyme-catalyzed hydrolysis to result in loss of polymer strength [137].

(b) Ionization.

Some polymers show water insolubility initially but become solubilized by ionization or protonation of a pendent group. Polyacids become soluble at high pH and become hydrophilic [138]. Cellulose acetate phthalate becomes water soluble at a pH > 6, while poly(vinyl acetate phthalate) is ionized at a lower pH [139].

(c) Hydrolysis

Hydrolysis of the polymer backbone is most desirable since it produces low molecular weight by-products. Natural polymers undergo degradation by

hydrolysis whereas synthetic polymers are water insoluble. For hydrolysis to occur, the polymer has to contain hydrolytically unstable bonds, which should be reasonably hydrophilic for the access of water.

(d) Microbial degradations

Microbial degradation results from the action of naturally occurring microorganisms such as bacteria, fungi, algae, etc [140]. Addition of natural polymers to thermoplastics is one of the approaches to enhance biodegradability [141].

1.9.2 Methods for biodegradation

(a) Soil burial method

Soil burial method is one of the frequently used methods for the determination of biodegradability of plastics [142,143]. In this method, biodegradation test is performed under natural or laboratory conditions. Samples with definite weight and dimension are buried to a specific depth in the soil for different time intervals.

(b) Pure culture method

In pure culture method, pre-weighed disinfected films are aseptically added to sterilized culture medium and films in culture medium are incubated with shaking for 24 h before inoculation to ensure asepsis. The presence of microbes can be confirmed by using a microscope [144].

(c) Compost method

In this method, a definite weight of the dry plastic is subjected to the mixture of definite amount of mature compost and then incubated at 58⁰C with

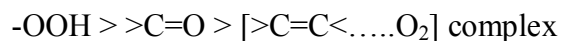
moisture content maintained at 65%. Biodegradation is measured based on the amount of material carbon converted to gaseous CO₂ [145].

1.10 Photodegradability of polyethylene

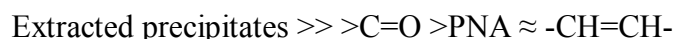
In the absence of oxygen, pure polyethylene is a relatively stable material under ultraviolet radiation. After long exposure to UV light of short wavelength (254 nm) in a vacuum or in a nitrogen atmosphere, chain scission and hydrogen abstraction occur. Also crosslinking and evolution of hydrogen are observed [146].

Degradation of PE is influenced by a great extent of its crystallinity. It has long been known that branched polyethylene oxidizes faster than linear polyethylene, and it has been discovered that its oxidation rate is roughly proportional to the amount of amorphous fraction present. This suggests that the oxidation of semicrystalline polyethylene is restricted to its amorphous region. It was subsequently discovered that the crystalline region absorbs practically no gas which implies that oxygen is simply not available in the crystalline region. Based upon these facts, polyethylene of low crystallinity has a high rate of carbonyl formation and a low concentration of radicals [28].

During extensive studies of photo-degradation and photo-oxidation of polyolefins in the past decade, the initiation mechanism has been discussed in connection with various chromophoric species such as carbonyl groups, hydroperoxides, metallic impurities, polynuclear aromatics (PNA), oxygen-polymer charge transfer complexes, and so on. For the photo-oxidation of low-density polyethylene (LDPE) the following order of importance of the chromophoric impurities is given by Scott [147]:



The author also concluded the following order of effect of the impurities on the photodegradation of HDPE [148].

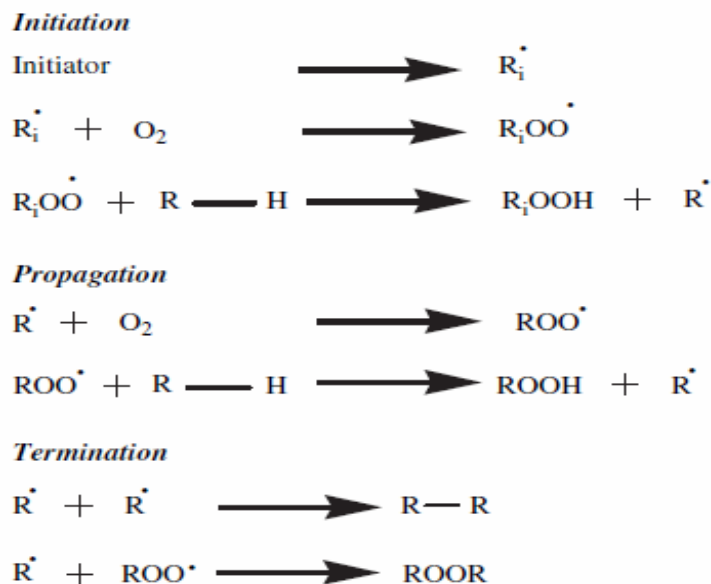


Carbonyl species have long been considered the main chromophores for the photodegradation of polyolefins.

1.11 Mechanism and methods of photodegradation

1.11.1 Mechanism of photodegradation

In photooxidative degradation, initially (Scheme 1.1) short-lived singlet state is transformed to long-lived triplet state [149]. Excited triplet states may cleave the polymer chains and form radical pairs (Norrish Type I reaction) or form pairs of saturated and unsaturated chain ends by hydrogen transfer (Norrish Type II reaction) [150]. The polymer radicals thus formed may add molecular oxygen (in triplet ground state) to peroxy radicals. These, in turn, abstract hydrogen and form hydroperoxide groups which absorb UV light or become excited by energy transfer. The weak O-O bonds break and pairs of alkoxy and hydroxyl radicals are formed which may react in various ways, e.g. by hydrogen abstraction, chain scission, rearrangement, etc. and accelerate photodegradation [151]. Double bonds may add excited oxygen molecules in singlet state. In photo-oxidative degradation, the mechanism involves an auto-oxidation cycle comprising of various steps shown in scheme 1.1



Scheme 1.1 Photo-oxidative degradation

(a) Initiation

Different initiation steps under varied conditions have been noticed in different polymers.

- (i) **Photosensitized cleavage.** Photosensitizers are highly photosensitive, readily get excited on exposure to light and are generally employed to bring about effective homolysis of the polymeric chains which otherwise do not undergo sufficient photo-excitation at the frequency of light available to the system.
- (ii) **Catalyst residues as source of generation of radicals.** Some metal salts and their oxidation products when added to the polymers act as catalysts to generate free radicals [152]. Polymerization catalysts such as transition metals (Ti) may remain in polyolefins at 2-100 ppm, depending on workup and catalyst efficiency. These residues have been

implicated in both photo- and thermal stability problems. For example, TiO₂ is a well-known photosensitizer for polyamide and polyolefin degradation and absorbs at 480 nm. Photosensitization involves the formation of highly reactive species including atomic oxygen, ·OH, ·OOH and O₂. The primary process involves the promotion of the Ti electron to the conduction band of the semiconductor to form an electron-positive hole pair. The relative proportions of the reactive species depend on the presence of water. No TiO₂ sensitization will be observed unless both oxygen and water are present [39].

(iii) Incorporation of carbonyl groups. Carbonyl groups formed by mild oxidation of polymer during synthesis or processing act as chromophores and become source of the initiation radicals. Carbonyl chromophore absorbs near-UV radiations and subsequently forms radicals following Norrish Type I, Norrish Type II and H-atom abstraction processes [153].

(iv) Introduction of peroxides and site of unsaturation The peroxides or C=C sites become source of initiation radicals [151]. The near UV component of sunlight (280-390 nm) is energetic enough to cleave C-C bond and C-heteroatom bonds provided that light of the appropriate wavelength is absorbed. In the case of unsaturated polymers, light generated singlet oxygen ¹O₂ reacts with an unsaturated site by way of an “ene” reaction and starts chain oxidation [39].

(b) Propagation reaction

The propagating reactions of auto-oxidation cycle are common to all carbon backbone polymers. These reactions lead to generation of hydroperoxide species and are not directly led to backbone cleavage but are

the key intermediates to further reactions as shown in Scheme 1.1. Hydroperoxide species generated in propagating step lead to backbone degradation through cleavage of hydroperoxide O-O bond followed by β -scission. The scission process generates two chain ends that are free to restructure, and can often lead to increase in crystallinity as oxidative degradation proceeds [39, 51].

(c) Termination reactions

This occurs naturally by combining free radicals or assisted by using stabilizers in the plastic. Peroxide radicals eventually terminate by reaction with other radicals to give dialkyl peroxides, carbonyl species or alcohols [39].

1.11.2 Methods for photodegradation

(a) Natural weathering

Outdoor exposure can be performed on samples mounted on testing racks, oriented under standard conditions to expose the material to the full radiation spectrum besides the temperature and humidity of that location [29]. In order to observe the aging of the material, it is characterized with respect to mechanical properties (elongation at break, tensile properties or impact strength) and visible characteristics, such as crack formation, chalking, and changes in color [154]. The alterations in the polymeric materials on exposure can be characterized by FTIR spectroscopy and ultra violet/visible (UV/vis) spectroscopy [155,156].

(b) Artificial weathering/laboratory test

Pure laboratory testing involves using environmental chambers and artificial light sources to approximately replicate outdoor conditions but with a

greatly reduced test time under highly controlled conditions. Laboratory testing can quickly assess the relative stability of plastics but has the major disadvantage that the quicker the test the lower is the correlation to real behavior in the field [157].

1.12 Biodegradation of photodegradable polyolefins

About 80% of all plastic packing materials consist of polyolefins [158]. With the increase in the amount of plastic packaging, the plastic litter problem has become threatening. Litter is a highly visible national concern. This situation can be improved if polyolefin packaging materials are made both photodegradable and biodegradable.

Polyolefin films have been used as agricultural mulch films to retain moisture, increase the soil temperature and inhibit weeds. It is necessary to remove these films from the fields after use. This kind of work is expensive and unattractive. When photodegradable polyolefins are used for mulch films, the situation becomes more favorable. The action of sunlight during the growing season causes the embrittlement of the film [159]. Once the film is broken up, the minute pieces may be ploughed into the soil. Even further degradation of the film pieces to CO₂ and H₂O is expected if microbial assimilation of the polymers is possible and thus there will be no harmful effects on plants.

Generally, polyolefins are not easily biodegraded. It is commonly considered that the high molecular weight of polyolefins is one of the major factors inhibiting their biodegradation [160-162].

The attack on polymeric materials by micro-organism is due to the action of an enzyme produced by the living organism. Because of its hydrophobic nature, the common polyolefin is not easily penetrated by enzymes. The introduction of hydrophilic groups into polyolefins therefore makes it easy for enzyme to penetrate into the polymer molecule. From this point of view it is understandable that the photodegraded polyolefin which already has hydrophilic groups is ready to undergo microbial assimilation. Photodegraded polyolefins of low molecular weight (c.2000) containing carbonyl groups were reported to be biodegradable when in contact with soil. From a measurement of the net oxygen uptake by fungi the complete biodegradation of these samples was estimated to occur in about 4 years [163,164].

1.13 Characterization of degraded polymers

The methods available to measure the deterioration of a photo-oxidised or weathered polymer are many and varied. Their validity obviously depends on the nature of the material and the mode of deterioration.

1.13.1 Mechanical properties

Tensile strength, elongation and modulus measurements have generally been the basic assessment techniques for weathering trials [165,166].

1.13.2 Physical properties

Dimensional changes and changes in weight can prove simple means of following deterioration. Exposure can often affect the appearance of a polymer. Loss of gloss is often one of the first indications of such deterioration (ISO 4582). As degradation proceeds, surface flaws can develop which apart

from serving as stress centers for mechanical failure, tend to reduce the transparency of clear polymers.

1.13.3 Gel permeation chromatography

GPC analysis has to a great extent replaced solution viscosity measurements. The broadening of molecular weight distribution occurs after exposure indicating that branching as well as scission processes are involved. This is confirmed by an increase in the ratio M_z/M_w with exposure time.

1.13.4 Fourier transform infrared spectroscopy

IR spectroscopy is one of the most popular techniques for studying the chemical changes brought about by polymer degradation. It has been used for both qualitative and quantitative characterization of degradation products [167-171]. The chemical changes resulting from polymer ageing involve the formation of various functional groups at rates that are strongly dependent on the chemical structure of the polymer. The main chemical species detectable by infrared spectroscopy are hydroxyl and carbonyl groups [172]. The formation of these groups generally leads to visible changes in the infrared spectrum, with carbonylated products and hydroxyl and hydroperoxy compounds appearing in the regions of $1850-1550\text{ cm}^{-1}$ and $3700-3200\text{ cm}^{-1}$ respectively [168,173]. Associated hydroperoxides and hydrogen-bonded hydroxyl groups are known to give rise to a band around 3400 cm^{-1} in the infrared spectrum [172-174] with free hydroperoxides appearing at around 3560 cm^{-1} [174].

The absorption bands of the degradation products often overlap to form complex absorption bands, which complicates their identification. From the

hydroxyl and carbonyl groups, degradation products such as peroxides, alcohols, carboxylic acids, ketones, aldehydes, esters and γ -lactones can be identified by means of derivatisation reactions [168,175]. This method usually involves the treatment of oxidised samples with a reactive gas that can selectively convert degradation products. This leads to the disappearance of some bands in the infrared spectrum and the appearance of some new bands of the derived products.

FTIR has also been useful in determining changes in unsaturation of PE during degradation [172,176]. The unsaturated groups typically detected, include vinylidene end groups (characteristic bands at 889 and 1684 cm^{-1}) terminal vinyl groups appearing at 910 cm^{-1} and trans-vinylenes at 965 cm^{-1} . The extent of degradation within the polymer samples is often determined on the basis of their carbonyl index [169,177-179]. Changes in the carbonyl index of different polymer materials as a function of degradation time or temperature are a convenient way for comparing the degradation behavior of different polymer systems.

1.13.5 Differential scanning calorimetry

Differential scanning calorimetry is another technique often used to obtain information on the degradation behavior of polymers [180-182]. Changes in the peak temperatures and shape of melt endotherms as well as the overall percentage crystallinity, can supply information on the susceptibility of different crystalline phases or arrangements to degradation.

1.14 Application of biodegradable and photodegradable plastics

Biodegradable polymers are now being considered as an alternative to the existing largely nonbiodegradable petrochemical-based polymers

[183,184]. New applications based on synthetic polyester-based biodegradable polymers have been commercialized, especially in the packaging industry, paper coating and garbage bags. These polyesters are made using modified polyethylene polymerization processes and as blends.

Fully biodegradable synthetic polymers are commercially available since 1990. Among these biopolymers, PLA was extensively studied in medical implants, suture, and drug delivery systems since 1980s due to its biodegradability. PLA has been attractive for disposable and biodegradable plastic substitutes due to its better mechanical properties. Starch may offer a substitute for petroleum-based plastics. Starch is a renewable, degradable carbohydrate biopolymer that can be purified from various sources by environmentally sound processes. It is a relatively low-cost polymer available from agricultural surplus with potential thermoplasticity.. Another widely available carbohydrate material is cellulose, which is biodegradable, but cannot be thermally processed because it decomposes before melting. High molecular weight of starch provides better stability and physical strength but decreases the moldability [184,185].

Photodegradable plastics are a meaningful approach for beverage can loops which will rapidly photodegrade and reduce the prospects of injury and death to various creatures. Their use in agricultural mulches is a practical means of improving the cultivation of various plants. However, long-term considerations need to be explored further to determine whether the accumulation of polyethylene residues in soil over many years is ecologically sound [186].

1.15 Scope and objectives of the present work

Polyethylene is a thermoplastic widely used for packaging applications because of its high tensile strength, elongation at break, good barrier properties against waterborne organisms, lower cost, higher energy effectiveness, light weight and good water resistance. However, polyethylenes are normally not degradable because of their hydrophobicity, high molecular weight, absence of polar groups, relative impermeability to oxygen, chemical inertness etc.

Biodegradable plastics are an innovative means of solving the plastic disposal problem from the standpoint of development of new materials. Incorporation of pro-oxidant additives represents a promising step in solving the problem of environmental contamination by polyethylene films. Pro-oxidants accelerate photo oxidation and consequent polymer chain cleavage apparently rendering the product more susceptible to biodegradation.

Transition metals like Co, Mn, Fe especially in the form of carboxylates, have been employed to initiate degradation in polyethylene films [187]. White pigments like oxides of titanium and zinc are also used to induce degradation in polyolefins.

When pro-oxidants are introduced into the polymer matrix degradation proceeds faster than under normal conditions. The use of pro-oxidant additives can make the polyolefins themoxo-biodegradable by making the polymer hydrophilic and also catalyzing the breakdown of high molecular weight polyolefin to lower molecular weight products. Weathering produces cracks and grooves on the surface of the materials and when these materials are subjected to biodegradation studies microorganisms can easily attack the polymer matrix.

The **objectives of the present work** are spelt out below

- To develop LLDPE/PVA blends in the laboratory and do their characterization.
- To subject these blends to weathering in the presence of pro-oxidants namely TiO₂ (both rutile and anatase grades) and cobalt stearate in combination with vegetable oil and evaluate the changes.
- To subject these blends to UV irradiation again in the presence of pro-oxidants and evaluate the changes.
- To conduct biodegradation studies on the degraded samples from the above experiments in culture medium and in garden soil and to evaluate the changes.
- To develop a process for preparing nano-TiO₂ for pro-oxidant usage and do the characterization.
- To make a comparative study of these processes to decide upon the best way to achieve maximum degradability.

1.16 References

- [1] R. N. Tharanathan; *Trends in Food Science & Technology* **2003**,14,71.
- [2] G. Scott; *Int.J.Envirion.Studies* **1975**,3,35.
- [3] G. Scott; *Int.J.Envirion.Studies* **1975**, 7,131.
- [4] R. S. Shomura, Godfrey M.L; (eds). *Proccedings of second International conference on Marine Debris, US Dept.of Commerce.1990.*

- [5] A. Karaduman ; *J. Energy Sources* **2002**, 24,667.
- [6] G. J. L. Griffin; *Chemistry and technology of biodegradable polymers*, Glasgow, Blackie **1994**.
- [7] F. Gugumus; *Polym. Degrad.Stab.* **1993**,39,117.
- [8] A. L. Andrady; *Adv. Polym. Sci.* **1997**,128,49.
- [9] F .Cataldo; *Polym. Degrad. Stab.* **2001**, 72, 287.
- [10] A.L Andrady, H.S Hamid, A.Torikai; *J. Photochem.Photobiol. Sci.* **2003**, 2,68.
- [11] J. E Glass, G. S wift; *In: ACS Symp Ser, vol. 433. Washington, DC: Am.Chem.Soc.***1989**, 9.
- [12] M. Alauddin, I. A. Choudkury, M. A. Baradie, M. S. J. Hashmi; *J. Mater. Process. Technol.* **1995**, 54, 40.
- [13] F. A. Bovey, F. H. Winslow; *Macromolecules-an introduction to polymer science. Academic Press Inc (London) Ltd* **1979**, 423.
- [14] P. Ghosh; *Polymer science and technology of plastics and rubbers. New Delhi: Tata McGraw-Hill Publishing Company Ltd;* **1990**,175.
- [15] Wikipedia – The free encyclopedia-**2012**.
- [16] J. Mleziva; *Polymery- struktura vlastnosti a použití: Sobotáles Praha*, ISBN: 80-901570-4-1, **1993**.
- [17] Kutz, Myer; *Handbook of Materials Selection: John Wiley & Sons*, ISBN: 0-471-35924-6, **2002**.
- [18] DostupnénaWWW17.5.**2006**:<http://www.ims.tut.fi/kuva_vmv/b_06_10.gif>
- [19] Dostupné na WWW 17.5.**2006**: < www.chemistry.wustl.edu>

- [20] J. Brydson; *Plastics Materials (7th Edition)*, Elsevier, ISBN:0-7506-4132-0, **1999**.
- [21] Gobi International: *Polypropylene – The International Market 2003* [online]. Available on www.gobi.co.uk/pdfs/polypropylene.pdf. London (United Kingdom): Gobi International, **2003**.
- [22] J. Výchopnová; *Crystallization behaviour of nucleated PP*, Master thesis, Zlín, **2004**.
- [23] L. Vasek; Photodegradation of polyolefins, Bachelor Thesis, **2006**.
- [24] A. Ram; *Fundamentals of Polymer Engineering*, New York, Plenum Press, ISBN 0-306-45726-1, **1997**.
- [25] ASTM D883-93, Vol.8.01, West Conshohoken, PA, **2000**, 176.
- [26] A. L. Andradý, in J.E Mark; ed., *Physical Properties of Polymers Handbook*, American Institute of Physics, Woodbury, New York, **1996**, Chapter 40, 547.
- [27] K. Daves, L.C. Glover; in J.E Mark,ed., *Physical Properties of Polymers Handbook*, American Institute of Physics, Woodbury, New York, **1996**, Chapter 41, 557.
- [28] J. Pospisil, Z. Horak, Z. Krulis, S.Nespurek; *Macromol Symp* **1998**, 35,247.
- [29] <<http://www.Cabot-Corp.com/Plastics>>.
- [30] N. Grassie, Scott G; *Polymer degradation and stabilization*. New York, NY: Cambridge University Press; **1985**.
- [31] M. Raab, L. Kotulak, J. Kolarik, J. Pospisil; *J.Appl. Polym.Sci.* **1982**, 27, 2457.

- [32] P. G. Komitov; *Polym.Degrad.Stabil.* **1988**, 24, 313.
- [33] R. Giesse, M.A. De Paoli; *Polym. Degrad. Stabil.* **1988**, 21, 181
- [34] R. P. Singh, J. Lacoste, R. Arnaud, J. Lemaire; *Polym. Degrad. Stabil.* **1988**, 20, 49.
- [35] B. Ranby; *J. Anal. Appl. Pyrolysis.* **1989**,15, 237.
- [36] J. P. T. Jensen, J.Kops; *J. Polym. Sci. Polym. Chem. Ed.* **2003**,18,2737.
- [37] G. E. Sheldrick, O.Vogl; *J. Polym. Eng. Sci.* **2004**,16,65.
- [38] Y. Nagai, D. Nakamura, T. Miyake, H. Ueno, N. Matsumoto, A. Kaji; *Polym. Degrad. Stab.* **2005**,88,251.
- [39] H. F Mark, N.M Bikales, C.G Overberger, Menges G; *Encyclopedia of polymer science and engineering.* 2nd ed., vol. 4. New York: Wiley Interscience Publication; **1986**, 630.
- [40] J. W. Martin, J.W Chin, T.Nguyen; *Prog. Organic Coatings* **2003**,47,292.
- [41] J. Czerny; *J. Appl. Polym. Sci.* **2003**, 16, 2623.
- [42] M. Abadal, R. Cermak, M. Raab, V. Verney, S. Commereuc, F. Fraisse; *Polym. Degrad. Stab.* **2006**, 91, 459.
- [43] S. H. Hamid, W. Pritchard; *J. Appl. Polym. Sci.* **1991**,43, 651.
- [44] A. Marek, L. Kapralkova, P. Schimdt, J. Pflieger, J. Humlicek, J. Pospisil; *Polym. Degrad. Stab.* **2006**, 91, 444.
- [45] A. Torikai; Wavelength sensitivity of the photodegradation of polymers. In: S. H. Hamid, editor. *Handbook of polymer degradation.* 2nd ed. New York: Marcel Dekker; **2000**, 573.
- [46] X. Ramis, A. Cadenato, J.M. Salla, J.M. Morancho, A. Valles, L. Contat; *Polym. Degrad. Stab.* **2004**, 86, 483.

- [47] F. Khabbaz, A.C Albertsson, S. Karlsson; Polym. Degrad. Stab. **1999**, 63, 127.
- [48] F. Cataldo, G. Ricci, V. Crescenzi; Polym. Degrad. Stab. **2000**, 67, 421.
- [49] F. Cataldo; Polym. Degrad. Stab. **1998**, 60, 223.
- [50] F.Cataldo; Polym. Degrad. Stab. **1998**, 60, 233.
- [51] D. R. Tayler; J. Macromol. Sci. Part C- Polym. Rev. **2004**, 44, 351.
- [52] D. O. H. Teare, N. Emmison, C. Tonthat, R. H Bradley; Langmuir **2000**, 16, 2818.
- [53] E. P Goodings, G. Kamerbeek, H. Kroes, W. Grolle; Soc. Chem. Ind. (London) Monograph **1961**, 13, 357.
- [54] A. A. Kefeli, S. D. Razumovskii, G. Y Zaikov; Polym. Sci. USSR **1971**, 13, 904.
- [55] A. L. Andrady, S. H Hamid, X. Hu, A. Torikai; J. Photochem. Photobiol. B Biol. **1998**, 46, 96.
- [56] N. S Allen, M. Edge, D. Mourelatou, A. Wilkinson, C. M Liauw, M.D Parellada; Polym. Degrad. Stab. **2003**, 79, 297.
- [57] R. N. Ghosh, B.C Ray; J. Polym. Mater. **2004**, 21, 425.
- [58] F. Cataldo, G. Angelini; Polym. Degrad. Stab. **2006**, 91, 2793.
- [59] B. F. Ozen, J.D Floros, P.E Nelson; (73D-19) 2001 IFT annual meeting, New Orleans, Louisiana, **2001**.
- [60] J. Li, S. Guo, X. Li; Polym. Degrad. Stab. **2006**, 89, 6.
- [61] G. M. Bristow, W. F. Watson. In: Batman L; editor. The chemistry and physics of rubber like substances. London: McLaren, **1963**.

- [62] Y. Li, J. Li, S. Guo, H. Li; Mechanochemical degradation kinetics of highdensity polyethylene melt and its mechanism in the presence of ultrasonic irradiation. *Ultrason Sonochem* **2005**, 12, 183.
- [63] G. Schmidt-Naake, M. Drache, M. Weber; *Macromol. Chem. Phys.* **2002**, 203, 2232.
- [64] A. Garforth, S. Fiddy, Y. H. Lin, A. Ghanbari-Siakhali, P. N. Sharratt, J. Dwyer; *Thermochim. Acta.* **1997**, 294, 65.
- [65] K. Gimouhopoulos, D. Doulia, A. Vlyssides, D. Georgiou; *Waste. Manag. Res.* **2000**, 18, 352.
- [66] Y. H. Lin, H. Y. Yen; *Polym. Degrad. Stab.* **2006**, 89, 101.
- [67] P. T Williams, R. Bagri; *Int. J. Energy Res.* **2003**, 28, 31.
- [68] K. Jong-Ryeol, V. Jong-Ho, P. Dae-Won¹, L. Mi-Hye; *React. Kinet. Catal. Lett.* **2004**, 81, 73.
- [69] W. Kaminsky, F. Hartmann; *Angew. Chem. Int. Ed.* **2000**, 39, 331.
- [70] E. S. Stevens; *Green plastics: an introduction to the new science of biodegradable plastics.* Princeton University Press. **2002**.
- [71] M. Weiland, A. Dacro, C. David; *Polym. Degrad. Stab.* **1995**, 48, 275.
- [72] Environmental and Plastic Industry Council, *Biodegradable Polymers, Technical Review.* **2000**.
- [73] S. Bonhomme, A. Cuer, A.M. Delort, J. Lemaire, M. Sancelme, G. Scott; *Polym. Degrad. Stab.* **2003**, 81, 441.
- [74] V. R. Gowariker, N. V. Viswanathan, J. Sreedhar; *Polymer science.* NewDelhi, India: New Age International (P) Limited Publishers, **2000**, 263.

- [75] B. Seymour Raymond; Additives for polymers, Introduction to polymer chemistry. New York, McGraw-Hill Book Company, **1971**, 268.
- [76] F. A. Bovey, F. H. Winslow; Macromolecules-an introduction to polymer science, Academic Press Inc (London) Ltd, **1979**, 423.
- [77] M. N. Kim, K. H. Kim; J. Environ. Biol. **1997**, 15, 195.
- [78] K. Yamada-Onodera, H. Mukumoto, Y. Katsuyaya, A. Saiganji, Y. Tani; Polym. Degrad. Stab. **2001**, 72, 323.
- [79] P. M. Santos, J. M Blatiny, I. D. Bartolo, Savein; J. Appl. Environ. Microbiol. **2000**, 66, 1305.
- [80] J. R. Haines, M. Alexander; Appl. Microbiol. **1974**, 28, 1084.
- [81] D. Hadad, S. Geresh, A.Sivan; J. Appl. Microbiol. **2005**, 98, 1093.
- [82] T. J. Meyer, J. V. Caspar; Chem. Rev. Washington, DC, United States, **1985**, 85, 187.
- [83] Y. Orhan, J. Hrenovic, H. Buyukgungor; Acta. Chim. Slov. **2004**, 51, 579.
- [84] I. Jakubowicz; Polym. Degrad. Stab. **2003**, 80, 39.
- [85] Y. Zheng, E. K. Yanful, A. S. Bassi; Crit. Rev. Biotechnol. **2005**, 25, 243.
- [86] P. Agamuthu, P. N. Faizura; Waste. Manag. Res. **2005**, 23, 95.
- [87] J. W. Summers; J. Vinyl. Technol. **1983**, 5, 43.
- [88] B. Erlandsson, S. Karlsson, A. C. Albertsson; Polym. Degrad. Stab. **1997**, 55, 237.
- [89] A. L. Andrady, H. S Hamid, A. Torikai; J. Photochem. Photobiol. Sci. **2003**, 2, 68.

- [90] P. Finch, J.C. Robert, in T.P Novell, S.H Zeronian; eds., cellulose chemistry and its applications, Ellis Horwood, West Sussex, England, **1985**, 312.
- [91] G. Halliwell, M.Griffin; *Biochem. J.* **1973**, 128,1183.
- [92] L. E. R Berghem, L.G Peterson; *Eur. J. Biochem*, **1973**, 37,21
- [93] J. J. Marshall; ed., *Mechanism of Saccharide Polymerization and Depolymerization*, Academic, New York, **1980**, 55.
- [94] R. Shogren, B. Jasberg; *J. Environ. Polym. Degrad.* **1994**, 2, 99.
- [95] M. Parikh, R.A Gross, S.P McCarthy; *Polym. Mat. Sci. Eng.***1992**, 66,408,
- [96] H. Bender, J. Lehmann, K. Wallenfels; *Biochem. Biophys. Acta* **1959**, 36, 309.
- [97] S. Yuen; *Process. Biochem.* **1974**, 7, 22.
- [98] H. Matsunaga, K. Tsuji, T. Saito; U.S Patent 4,045,388, Aug.30, **1977**.
- [99] J. N. Boyer, R.S. Wolfe; *Biological. Bull.* **1993**, 165, 505.
- [100] S. Arcidiacono, D.L. Kaplan; *Biotechnol. Bioeng.* **1992**, 39, 281,
- [101] D. L. Kaplan, J. M. Mayer, S. J. Lombardi, B. Wiley, S. Arcidiacono; *Polym. Preprints Am. Chem. Soc. Div. Polym. Chem.* **1990**, 63, 732.
- [102] J. M. Mayer, M. Greenberger, D. H. Ball, D. L. Kaplan; *Polym. Mat. Sci. Eng.* **1992**, 63,732.
- [103] E. S. Lipinsky, R. G. Sinclair; *Chem. Eng. Prog.* **1986**, 82, 26,
- [104] D. H. Lewis; in M. Chasin, R. Langer; eds. *Biodegradable polymers as drug delivery systems, drugs and the pharmaceutical sciences*, Marcel Dekker, New York, **1990**, 45, 1.

- [105] L. J. E. Potts; in Encyclopedia of Chemical Technology, 2nd ed., Suppl. Volume, Wiley Interscience, New York, **1984**, 626.
- [106] U.Witt, R.J.Mueller, W. D. Deckwer; J. Environ. Polym. Degrad. **1997**, 81.
- [107] G. J. Whitchurch, T.A.Cooper; Stanelco plc, Adept, Polymer, Ltd, Manchester, UK, Paper Abstract #19B GPEC **2006**.
- [108] T. A. Cooper, P.E. Harrison, T.M. Wilkes; “Recent Advances in Thermoplastically-Processable Polyvinyl Alcohol-based Materials”, Society of Plastics Engineers Global Plastics Environmental Conference, Detroit, MI, 14 February **2002**, 369.
- [109] K. Noro; “Hydrolysis of Polyvinyl Acetate to Polyvinyl Alcohol”, Chapter 4, and “Manufacturing and Engineering Aspects of the Commercial Production of Polyvinyl Alcohol”, Chapter 5, in C.A. Finch (Ed.), “Polyvinyl Alcohol”, Wiley, **1973**.
- [110] A. G. Hoechst, Frankfurt; 6. Mowiol® Polyvinyl Alcohol", Technical Brochure, **1991**.
- [111] V. O. Sheftel; “Indirect Food Additives and Polymers”, Lewis Publishers, 2000, 1167 et seq. **1973**.
- [112] K. Sakai, N. Hamada, Y. Watanabe; Agric. Biol. Chem. 50, **1986**, 989 and 49, **1985**, 817; **1901-2**.
- [113] T. Suzuki; J.Appl.Polym. Sci. Appl.Polym. Symp. **1979**, 35, 431; T. Suzuki, Y. Ishihara et al; Agric. Biol. Chem. **1973**, 37, 747.
- [114] Y. Watanabe; Arch. Biochem. Biophysics, **1976**, 174, 575.
- [115] T. Suzuki et al; Agr. Biol. Chem. **1973**, 37, 747.
- [116] E. Chiellini, A.Corti, S. D’Antone, R. Solaro; Progr. Polym. Sci, **2003**, 28, 963.

- [117] E. Chiellini, A. Corti, R. Solaro; *Polym. Degrad. and Stabi.* **1999**, 64, 305.
- [118] A. Tsuchii, T. Suzuki, S. Fukuoka; *Rep. Ferment. Res. Inst.* **1980**, 55, 35.
- [119] D. Bikiaris, C. Panayiotou; *J. Appl. Polym. Sci.* **1998**, 70, 1503.
- [120] G. J. L. Griffin; *J. Polym. Sci. Polym. Symp.* **2007**, 57, 281.
- [121] M. Hakkarainen, A.C. Albertsson; *Adv. Polym. Sci.* **2004**, 169, 177.
- [122] Y. Orhan, H. Buyukgungor; *Int. Biodeterior. Biodegrad.* **2000**, 45, 49.
- [123] H. A. El-Shafei, N.H. El-Nasser, A.L. Abd Kansoh, A.M Ali; *Polym. Degrad. Stab.* **1998**, 62, 361.
- [124] S. Karlsson, O. Ljungquist, A.C. Albertsson; *Polym. Degrad. Stab.* **1998**, 21, 237.
- [125] P. Galgali, A. J. Varma, U. S. Puntambekar, D. V. Gokhale; *Chem. Commun.* **2002**, 2884.
- [126] M. Ratajska, S. Boryniec; *Polym. Adv. Technol.* **1999**, 10, 625.
- [127] D. Zuchowska, D. Hlavata, R. Steller, W. Adamiah, W. Meissner; *Polym. Degrad. Stab.* **1999**, 64, 339.
- [128] R. A. De Graaf, L. P. B. M. Janssen; *Polym. Eng. Sci.* **2000**, 40, 2086.
- [129] S. Kiathemjornwong, M. Sonsuk, S. Wiltagapichet, P. Prasassarakich, P. C. Vejjanukroh; *Polym. Degrad. Stab.* **1999**, 66, 323.
- [130] E. M. Nakamura, L. Cordi, G. S. G. Almeida, N. Duran, L.H.I. Mei; *J. Mater. Process. Technol.* **2005**, 162, 236.
- [131] S. Bonhomme, A. Cuer, A. M. Delort, J. Lemaire, M. Sancelme, C. Scott; *Polym. Degrad. Stab.* **2003**, 81, 441.

- [132] E. Chiellini, A. Corti, S. D'Antone, R. Baciù; *Polym. Degrad. Stab.* **2006**, 91, 2739.
- [133] R. S. Norman, R. Frontera-Suau, P. J. Morris; *Appl Environ Microbiol* **2002**, 68, 5096.
- [134] R. M. Tadros, H. Nouredini, D. C. Timm; *J. Appl. Polym. Sci.* **1999**, 74, 3513.
- [135] D. K. Gilding; Biodegradable polymers. In: Williams DF, editor. *Biocompatibility of clinic implant materials*, vol. II. Boca Raton, FL: CRC Press, chapter 9, **1981**.
- [136] R. L. Kronenthal; Biodegradable polymers in medicine and surgery. In: Kronenthal RL, Oser Z, Martin E; editors. *Polymers in medicine and surgery*. New York, NY: Plenum Press, **1975**, 119.
- [137] T. Ishigaki, Y. Kawagoshi, M. I. M. Fujita; *World J. Microbiol. Biotechnol.* **1999**, 15, 321.
- [138] W. G. Chambliss; *J. Pharm. Technol.* **1983**, 7, 124.
- [139] A. R. Gennaro; editor. *Pharmaceutical sciences*. 17th ed. Easton, PA: Mack Publ. Co, **1985**, 1633.
- [140] M. C. Upreti, R. B. Srivastava; *Curr. Sci.* **2003**, 84, 1399.
- [141] H. Dave, P. V. C. Rao, J. D. Desai; *World J. Microbiol. Biotechnol.* **1997**, 13, 655.
- [142] H. S. Yang, J. S. Yoon, M. N. Kim; *Polym. Degrad. Stab.* **2005**, 87, 131.
- [143] H. Eya; *J. Biosci. Bioeng.* **2002**, 94, 186.
- [144] D. L. Kaplan, R. Hartenstein, J. Sutter; *J. Appl. Environ. Microbiol.* **1979**, 38, 551.

- [145] A. Corti, G. Vallini, A. Pera, P. Cion, R. Colara, E. Chielline; Proceeding of second international scientific workshop on 'Biodegradable Polymers and Plastics', Montpellier, France; **1992**, 45.
- [146] B. Ranby, J. F. Rabek; Photodegradation, photo-oxidation and photostabilization of polymers, John Wiley & Sons Ltd., **1975**, ISBN: 0-471-70788-0.
- [147] G. Scott; ACS Symp. Ser. **1976**, 25, 340.
- [148] Z. Osawa, H. Kuroda; Chem. Soc. Jpn. **1986**, 6, 811.
- [149] N. J. Turro; Modern molecular photochemistry. Reading, MA: Addison-Wesley Publishing Co. **1978**.
- [150] T. Otsu, H. Tanaka, H. Wasaki; Polymer, **1979**; 20, 55.
- [151] D. J. Carlsson, D. M. Wiles; J. Macromol. Sci. Rev. Macromol. Chem. **1976**, 14, 65.
- [152] F. Gugumus; In: Zweifel H; editor. Plastics additives handbook. 5th ed. Cincinnati: Hanser; **2001**, 141.
- [153] P. J. Hocking; J. Macromol. Sci. Rev. Macromol. Chem. Phys. **1992**, 32, 35.
- [154] A. L. Andrady, S. H. Hamid, X. Hu, A. Torikai; J. Photochem. Photobiol. B. Biol. **1998**, 46, 96.
- [155] D.S. Allan, N. L. Maecker, D. B. Priddy; Macromolecules **1994**, 27, 7621.
- [156] C. C White, E. Embree, W. E. Byrd, A. R. Patel; J. Res. Natl. Inst. Stand. Technol. **2004**, 109, 465.
- [157] ASTM D4674-89: Standard test method for accelerated testing for color stability of plastics exposed to indoor fluorescent lighting and window-filtered daylight. ASTM International; **1989**.

- [158] N. S. Allen; Degradation and stabilization of polyolefins, Applied Science Publishers, New York **1983**, 204.
- [159] D. Gilead; Intern. J. Polymeric Mater, **1978**, 6, 185.
- [160] J. E. Potts, R. A. Glendinning, W.B Ackart, W.D Niegisch; In: Polymers and ecological problems. Ed.by J.Guillet, Polymer Science and Technology, Vol.3, Plenum Press, New York, **1973**.
- [161] J.R. Haines, M. Alexander; Appl. Microbiol. **1974**, 28, 1084.
- [162] A. Tsuchii, T. Szuki, S. Fukuoda; Rept. of the Fermentation Res. Int, **1980**, 55, 35.
- [163] P. H. Jones, D. Prasad, M. Heskins, M. H. Morgan, J. E. Guillet; Environ. Sci and Technol, **1974**, 8, 919.
- [164] J. E. Guillet, T. W. Regulski, T. B. McAneney; Environ. Sci. and Technol. **1974**, 8, 923.
- [165] A. W. Birley, D. S. Brakman; The degradability of polymers and plastics, PRI Conf, London, **1973**, paper 1/1
- [166] G. Scott, M. F. Yusoff; Polym. Degrad. Stab. **1980**, 2, 309.
- [167] J.V. Gulmine, P. R. Janissek, H. M. Heise, L. Akselrud; Polym. Degrad. Stab. **2003**, 79, 385.
- [168] M Edge; Infrared spectroscopy in analysis of polymer degradation, In Encycl. Anal. Chem., Meyers R.A., Ed. John Wiley and Sons Ltd.: Chichester, **2000**, 7658.
- [169] F. Gugumus; Polym. Degrad. Stab. **1997**, 55, 21.
- [170] V. P. Nekhoroshev, Y. P. Turov, A. V. Nekhorosheva, V. D. Ogorodnikov, K. N. Gaevoi; Russ. J. Appl. Chem. **2006**, 79, 833.
- [171] L. Costa, M. P. Luda, L. Trossarelli; Polym. Degrad. Stab. **1997**, 58, 41.

- [172] E. Andreassen; Infrared and Raman spectroscopy of polypropylene. In Polypropylene: An A-Z reference, Karger-Kocsis J., Ed. Kluwer Publishers: Dordrecht, **1999**, 320.
- [173] A. Rivaton, J. L. Gardette, B. Mailhot, S. Morlat-Therlas; Macromol. Symp. **2005**, 225, 129.
- [174] F. Gugumus; Polym. Degrad. Stab. **1999**, 66, 161.
- [175] M. Piton, A. Rivaton; Polym. Degrad. Stab. **1996**, 53, 343.
- [176] A. C. Kolbert, J. G. Didier, L. Xu; Macromolecules, **1996**, 29, 8591.
- [177] A. Jansson, K. Moller, T. Gevert; Polym. Degrad. Stab. **2003**, 82, 37.
- [178] M. Mirafab, A. R. Horrocks, J. Mwila; Polym. Degrad. Stab. **2002**, 78, 225.
- [179] A. S. F. Santos, J. A. M. Agnelli, D.W. Trevisan, S. Manrich; Polym. Degrad. Stab. **2002**, 77, 441.
- [180] N. Olivares, P. Tiemblo, J. M. Gomez-Elvira; Polym. Degrad. Stab. **1999**, 65, 297.
- [181] D. S. Rosa, J. Sarti, L. H. I. Mei, M. M. Filho, S. Silveira; Polym. Test. **2000**, 19, 523.
- [182] M. Elvira, P. Tiemblo, J. M. Gomez-Elvira; Polym. Degrad. Stab. **2004**, 83, 509.
- [183] S. Mecking; Angew. Chem. Int. Ed. Engl. **2004**, 43, 1078.
- [184] T. U. Gerngross, S. C. Slater; Science **2003**, 299, 822.
- [185] H. Wang, X. Sun, P. Seib; J. Appl. Polym. Sci. **2003**, 90, 3683.
- [186] P. Peter, Klemchuk; Polym. Degrad. Stab. **1990**, 27, 183.
- [187] P. K. Roy, P. Surekha, C. Rajagopal, V. Choudhary; J. Appl. Polym. Sci. **2008**, 108, 2726.

..........

PREPARATION, PROPERTY EVALUATION AND BIODEGRADATION OF LINEAR LOW DENSITY POLYETHYLENE/POLYVINYL ALCOHOL BLENDS

Contents	2.1	<i>Introduction</i>
	2.2	<i>Experimental</i>
	2.3	<i>Results and discussion</i>
	2.4	<i>Conclusion</i>
	2.5	<i>References</i>

2.1 Introduction

Conventional polymers such as polyethylene and polypropylene persist for many years in the environment after disposal. These polymers are characterized by high molecular weight, chemical inertness, hydrophobicity, relative impermeability to oxygen, etc. which make them resistant to microbial attack. These properties, at the same time, impose enormous restrictions on the design and development of biodegradable materials from these polymers [1,2]. It has been estimated that polyethylene biodegrades less than 0.5% in 100 years and about 1% if pre-exposed to sunlight for 2 years [3]. Therefore, recycling and degradation of plastics are important issue for environmental and economic reasons [5,6].

Attempts to produce environmentally degradable, low cost, plastic materials from polyolefines date back to the second half of the 20th century [4]. Griffin, [7,8] introduced the idea of increasing the biodegradability by

adding a biodegradable ingredient to the polymer material. When a biodegradable component is present, microorganisms readily attack it thereby increasing the porosity of the material and resulting in a mechanically weakened matrix. The surface area will also increase making it more susceptible than the original material to all degradation processes including biodegradation [9].

Poly(vinyl alcohol) (PVA) is the only carbon-carbon backbone polymer that is biodegradable under both aerobic and anaerobic conditions [10]. PVA is widely used in the industrial field and recently it has attracted increasing attention as a water-soluble biodegradable polymer. It is used as a moisture barrier film for food supplement tablets that need to be protected from moisture uptake. Most recently, PVA has been used in pharmaceutical and biomedical applications for controlled drug release tests due to its degradable and non-toxic nature [11].

Linear low density polyethylene (LLDPE) is the common name for copolymers of ethylene with α -olefins: butene, hexene, octene and 4-methyl-1-pentene [12]. LLDPE has higher tensile strength and higher impact and puncture resistance than LDPE. It is very flexible and elongates under stress. It can be used to make thinner films, with better environmental stress cracking resistance.

This chapter describes the attempts to improve the biodegradability of LLDPE by blending it with a biodegradable component. LLDPE was blended with PVA and mechanical, thermal and biodegradation properties were investigated. The biodegradability of LLDPE/PVA blends has been studied in culture medium and soil environment over a period of 15 weeks. Changes in

various properties of blends before and after degradation were monitored using FTIR spectroscopy, DSC and SEM among other things.

2.2 Experimental

2.2.1 Materials

Film grade LLDPE (LL20FS010) used in this study was supplied by Reliance Industries Ltd, Mumbai, India. It has a melt-flow index of 1g/10min at 190⁰C and a 2.16kg load. The density of the LLDPE sample is 0.920g/cm³. Hot water soluble polyvinyl alcohol (99% hydrolyzed) used in this study was industrial grade obtained from Rolex Chemical Industries, Mumbai. Molecular formula is (C₄H₁₀O)_n, viscosity at 4% concentration in water at 20⁰C, 3mPa.s.

2.2.2 Blend preparation

Different blends were prepared by melt mixing [13] method using a Thermo Haake PolyLab System (Rheocord 600p) (Fig.2.1). The mixing chamber has a volumetric capacity of 69cm³ and is fitted with roller type rotors. The rotors rotate in opposite directions in order to cause a tearing action on the material mostly by shearing the material against the walls of the mixing chamber. The granules in the desired proportion are fed to the mixing chamber through a vertical chute with a ram. There is a small clearance between the chamber wall and the rotors which rotate at different speeds. In these clearances dispersive mixing takes place. The shape and motion of rotors ensure that all particles undergo high intensive shearing flow in the clearances.



Fig. 2.1 Thermo Haake Polylab system

The mixer consists of three sections and each section is heated and controlled by its own heater and temperature controller. Since mechanical dissipation of heat takes place in the small gap between rotors and chamber, the heat flows to the centre and the temperature of the charge rises. At this point the heater is shut off and circulation of cooling air activated. In this case, the rotor rpm was maintained at 50. LLDPE was added first followed by PVA. The mixing temperature was 195⁰C and the total mixing time was 10 minutes. LLDPE films have been designated as L0, L5, L10, L15, L20, L25 and L30 for pure LLDPE and that containing 5%, 10%, 15%, 20%, 25% and 30% of PVA respectively.

In this work compatibilisation between the blends was not attempted. It is seen from literature that compatibilising a blend increases its resistance to

biodegradation [14]. So inspite of well known methods for compatibilisation [15] the blends were used as such for the studies.

2.2.3 Molding

The LLDPE/PVA blends were compression molded into sheets with the help of a flash mould and an electrically heated hydraulic press. A definite weight of the material was placed in the mould and initially heated for one minute without applying any pressure to ensure uniform heat flow through the material and the molding was subsequently completed by applying pressure for 2 more minutes. The molding temperature and pressure were 195°C and 200MPa respectively. The sheet thus obtained was removed from the press after cooling to room temperature.

2.2.4 Mechanical properties

Changes in mechanical properties, i.e. tensile strength, elongation at break and modulus, were studied according to ASTM D 882-02 [16], in a Universal Testing Machine (Shimadzu Autograph AG-I Series). One grip is attached to a fixed and the other to a movable (power driven) member so that they will move freely into alignment as soon as the machine is started. The test specimen was held tight by the two grips, the lower grip being fixed. Six samples of each specimen were strained at a rate of 50mm/min at room temperature and average values of tensile strength, elastic modulus and elongation at break were determined. The length between the jaws at the start of each test was fixed as 40mm. The tests were undertaken in an air-conditioned environment at 21⁰C and a relative humidity of 65%. The various parameters determined from the tensile testing are:

- 1) Tensile strength: It is measured as the force measured by the load cell at the time of break divided by the original cross sectional area of the sample at the point of minimum cross section.
- 2) Tensile modulus: It is the slope of the linear portion of stress-strain curve.
- 3) Elongation at break: It is the elongation of the specimen at break. It was measured in terms of its initial length (L_0) and final length (L_1) and is given as,

$$\text{Elongation at break} = \frac{(L_1 - L_0)}{L_0} \times 100$$

2.2.5 Water absorption studies

Water absorption studies were carried out according to ASTM D 570 [17]. This test method covers the determination of the relative rate of absorption of water by the blend when immersed. Three moulded specimens (7.5cm×2.5cm) of each composition (L0 to L30) were dried in an oven under vacuum for 24 h at 55⁰C, cooled in a desiccator and immediately weighed to the nearest 0.001g. The conditioned samples were placed in a container of distilled water maintained at room temperature, i.e. 27⁰C. The samples were then retrieved weekly from the water one at a time, gently blotted with tissue paper to remove the excess of water on the surface, weighed to the nearest 0.001g immediately, and replaced in the water. The weighing was repeated at the end of every week for 5 weeks and the average of 3 values was recorded. Percentage increase in weight during immersion was calculated to the nearest 0.01% as follows.

$$\%W_f = W_w - W_c / W_c \times 100$$

where, W_f is the final increased weight percentage, W_w the wet weight and W_c is the conditioned weight of the testing samples.

2.2.6 Degradation studies

The degradation studies on the samples were done in two environments: 1) garden soil and 2) culture medium containing *Vibrio sp.* isolated from marine benthic environment.

2.2.6.1 Biodegradation in culture

Biodegradation of the samples were carried out using a consortium consisting of four PVA degrading *Vibrio sp.* isolated from benthic marine environment, according to ASTM D 5247–92 [18]. Bacterial cultures isolated from sediment samples collected from different locations of Cochin back waters and Mangalavanam mangroves, identified as genus *Vibrio* and maintained in the culture collections of *Microbial Genetic Lab, Dept. of Biotechnology, Cochin University of Science and Technology* were utilized in this study.

2.2.6.1.1 Screening of microorganisms for PVA degradation

PVA minimal agar plates were used for primary screening for PVA degradation [19]. All the isolates were spot inoculated onto PVA minimal agar plates and incubated at 37°C for 2 days and a zone of clearance around the colony after flooding the plates with iodine-boric acid solution [20] indicated PVA degrading ability. PVA degrading *Vibrios* were selected based on the zone diameter around the colonies to form a consortium to conduct the degradation studies.

2.2.6.1.2 Medium for biodegradation studies

Minimal medium was used for testing the degradation of the bioplastics. The PVA minimal medium [19] contains,

PVA	-	0.21 %
MgSO ₄ .H ₂ O	-	0.05 %
NH ₄ NO ₃	-	0.5 %
KH ₂ PO ₄	-	0.1 %
NaCl	-	0.05 %
Yeast extract	-	0.023 %
pH	-	6.8

2.2.6.1.3 Preparation of consortia for biodegradation studies

Four strains (Strain BTTV4, BTTC10, BTTC27 & BTTN18) that produced the largest halo zone (diameter in mm) around the colony on PVA minimal agar medium formed the consortium used to study the microbial degradation of PVA/LLDPE plastic films in shake flask conditions, and were grown to OD₆₀₀ =1.00. The culture suspension was centrifuged to harvest the cells and the cells were resuspended in physiological saline for use as inoculum. 1 ml of each culture was aseptically transferred to the minimal media.

2.2.6.1.4 Preparation of inoculum and shake flask culture

The inoculum was prepared as follows - The individual isolates of the consortium grown overnight at 37^oC at 120 rpm on an Orbitek shaker (Scigenics, India) in nutrient broth (Himedia, Mumbai) pH 7.0 ±0.3 with 1% NaCl, were harvested by centrifugation at 5000rpm (2292g) for 20 minutes, washed with physiological saline and then pooled. 5 ml of this pooled culture

(OD₆₀₀ = 1) was used to inoculate 50mL PVA minimal medium [19] containing strips of LLDPE/PVA blends. Incubation was in an Orbitek environmental shaker (Scigenics Pvt. Ltd, Chennai, India) at 37⁰ C and 120 rpm for a total period of 15 weeks with regular sampling.

The LLDPE/PVA blends were wiped with 70% alcohol to make them bacteria free. They were subjected to microbial degradation using the consortium of PVA-degraders in the PVA minimal medium [19], with LLDPE/PVA blends for a total period of 15 weeks with regular sampling for analyzing the level of degradation. Tensile strength, FTIR spectra and scanning electron micrographs (SEM) of these LLDPE/PVA blends were compared with those of the control specimens (in the absence of bacteria) to indirectly estimate the extent of microbial degradation. The experiments were performed in triplicate.

2.2.6.2 Biodegradation in soil environment

Biodegradability in soil was also tested by burying the samples in garden soil for 15 weeks according to ASTM D 5338-98 [21]. Prior to burying, inoculums of PVA degrading microorganisms were applied to the soil. These inoculums were the same as that used in the culture medium studies.

2.2.7 Spectroscopic studies

Fourier transform infrared (FTIR) spectra of virgin LLDPE and LLDPE/PVA blends (films) were obtained from FTIR-Avatar 370 (Thermo Nicolet) equipment by the absorption of electromagnetic radiation in the frequency range 400-4000 cm⁻¹. Different functional groups and structural features in the molecule absorption at characteristic frequencies. The frequency and intensity of absorption are the indication of the structural features of the molecule.

2.2.8 Thermogravimetric analysis

TGA of PVA/LLDPE blends were done for thermal characterization prior to biodegradation. The thermogravimetric (TG) and derivative thermogravimetric (DTG) analysis of the samples were carried out on a TGA Q-50 (TA Instruments) thermal analyzer under nitrogen atmosphere. Sample weights varied from 5 to 15mg. The thermograms were recorded for the range from room temperature to 800⁰C at a heating rate of 20⁰C/min. The nitrogen gas flow was 50-70cm³/min. The maximum degradation temperature (T_{max}), the onset degradation temperature (T_{onset}), and the percentage residual weight were found out.

2.2.9 Differential scanning calorimetry

Differential scanning calorimetry (DSC) is a technique in which the difference in energy inputs into a substance and a reference material is measured as a function of temperature whilst the substance and the reference material are subjected to controlled temperature program [22]. Crystallinity studies were conducted using a Differential Scanning Calorimeter TA Q-100(TA Instruments) under nitrogen atmosphere. Samples of 5-10mg were taken and heated in nitrogen atmosphere from -50 to 150⁰C at a heating rate of 30⁰C/min and kept at 150⁰C for one minute in order to erase thermal history. Cooling was then performed at a rate of 10⁰C/min from 150⁰C to -50⁰C followed by a second heating from -50 to 150⁰C at the same rate, resulting in endothermic curves. The heat of fusion was calculated by integrating the areas under the endothermic curve. The degree of crystallinity was obtained from the following ratio [23],

$$\% \text{ Crystallinity} = \frac{\Delta H_f}{\Delta H_f^0} \times W_f$$

where ΔH_f is the melting enthalpy of the samples, ΔH_f^0 is the melting enthalpy of 100% crystalline LLDPE and W_f is the weight fraction of LLDPE in the blend.

2.2.10 Scanning electron microscopy

The scanning electron microscope (SEM) is a type of electron microscope that images the sample surface by scanning it with a high energy beam of electrons in a raster scan pattern. A scanning electron microscope (JEOL Model JSM-6390LV) was used in this case to study the surface morphological changes after the biodegradation of the samples. Additionally, SEM was employed to study the fracture surfaces of the biodegraded samples after tensile testing. The fractured ends of the specimens were mounted on a metallic stub and were sputter coated with a thin layer of gold to make them conducting.

2.3 Results and discussion

2.3.1 Mechanical properties

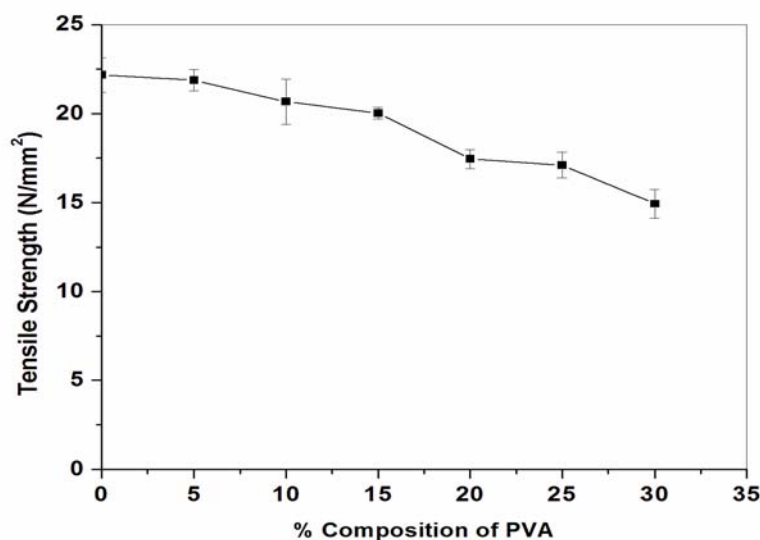


Fig. 2.2 Variation of tensile strength with the concentration of PVA in LLDPE/PVA blends

Fig. 2.2 shows the variation of tensile strength of LLDPE/PVA blends. The tensile strength of these blends tends to decrease on addition of PVA. It can be seen that there is only a slight drop of tensile strength with addition of up to 15% of PVA. The fall in tensile strength is more noticeable beyond a PVA concentration of 15%. The reduction observed was due to the poor interfacial adhesion between the PVA and LLDPE phases which causes poor stress transfer between matrix and the dispersed phase.

Polyvinyl alcohol is highly hydrophilic as it contains hydroxyl groups on its surface whereas LLDPE is nonpolar. Therefore, in such a system, the formation of strong interfacial bonds like hydrogen bonds is not feasible [23]. This is because at higher PVA contents, PVA-PVA interaction becomes more pronounced than PVA-PE interaction.

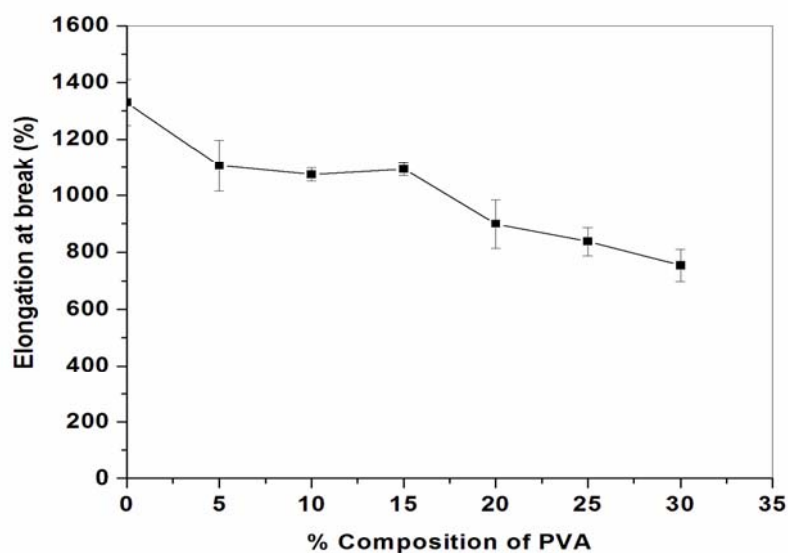


Fig. 2.3 Variation of elongation at break with the concentration of PVA in LLDPE/PVA blends

The elongation at break (Fig.2.3) also shows the same trend as that of tensile strength. The drop in elongation of the blends becomes more drastic as the PVA content is increased. Several researchers [24-26] also report similar trends on mechanical properties of incompatible blends. The absence of a compatibilizer resulted in poor adhesion between PVA particles and LLDPE matrix. This leads to easier crack propagation.

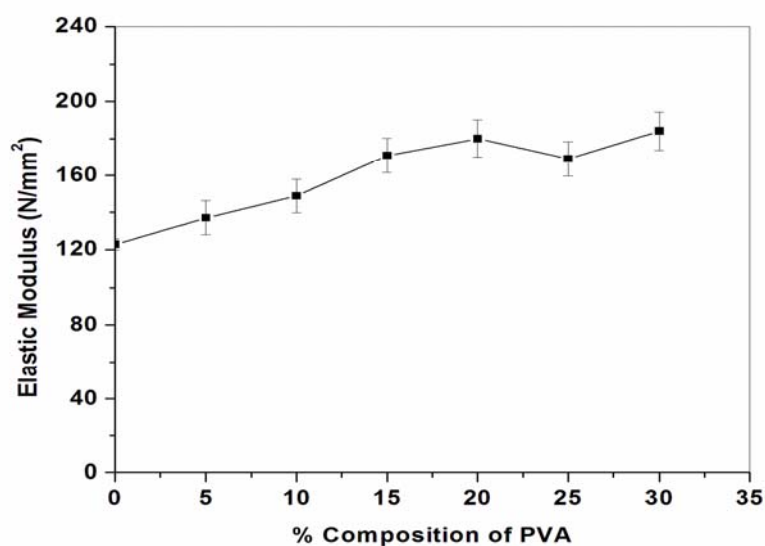


Fig. 2.4 Variation of elastic modulus with the concentration of PVA in LLDPE/PVA blends

Fig. 2.4 shows an increase in elastic modulus of the blends with increase in PVA content. It shows an increase with the increase in PVA content. Modulus increased due to the stiffening effect of PVA, PVA being stiffer than LLDPE. The hydrogen bonds in PVA give it a much higher modulus than semicrystalline polymers such as LLDPE which have no hydrogen bonding. Hence the elasticity of the blend falls and the average stiffness increases as PVA tends to agglomerate within the LLDPE matrix to form three dimensional reticulate structures [15].

2.3.2 Water absorption studies

Fig. 2.5 shows the variation of water absorption of the blends with the time of immersion. From the graph it is clear that blends exhibit somewhat higher water absorption compared to virgin LLDPE. Because of the presence of hydroxyl groups on the surface of PVA, the affinity for water is high. This reduces the moisture barrier property of the blends. Water absorption increases rapidly with increase in PVA content for the first seven days. Beyond that there was only a marginal increase in water absorption up to 35 days. As expected, there were no significant changes in the water uptake of pure LLDPE throughout the immersion period. Therefore that polyvinyl alcohol is responsible for the high moisture uptake of the blends.

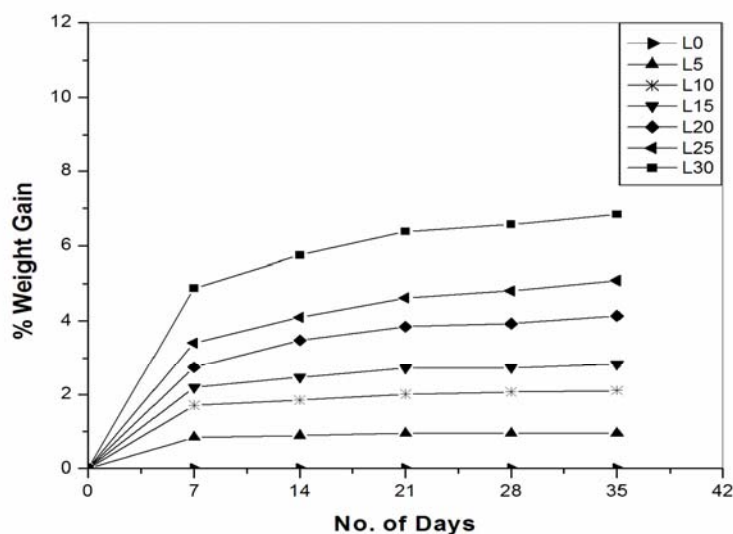


Fig. 2.5 Variation of water absorption of LLDPE/PVA blends with the increase in PVA content

The variation of water absorption with PVA content after 24 hours, 7 days and 35 days immersion in water is shown in Fig. 2.6.

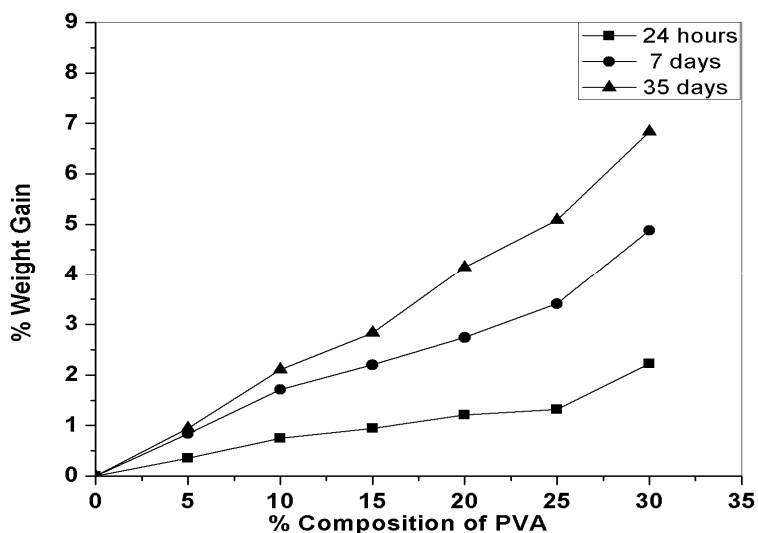


Fig. 2.6 Variation of water absorption with PVA content after 24 hours, 7 days and 35 days immersion in water

Table 2.1 Percentage water absorption of the blends after 5 weeks of immersion in water

Sample	Initial Weight (g)	Weight after 5 weeks(g)	% Water absorption
L0	0.3041	0.3041	0.0
L5	0.2963	0.2991	0.95
L10	0.2932	0.2994	2.11
L15	0.2972	0.3056	2.83
L20	0.3012	0.3137	4.15
L25	0.2949	0.3099	5.09
L30	0.2945	0.3146	6.83

Thus water absorption studies reveal that in the case of blends the uptake of water increases upto 6.83% for the highest concentration (30%) of PVA in the blends (Table 2.1). The hydrophilicity of a polymer is an important factor

influencing its degradability. The indicated increase in hydrophilicity facilitates biodegradation.

2.3.3 Biodegradation studies

2.3.3.1 Culture medium



Fig. 2.7 PVA degrading isolate (*V.neries* , strain BTKB4); Zone of clearance surrounding the colony in PVA agar plates after flooding with iodine -boric acid solution indicates PVA degradation

All the *Vibrio sp.* isolates were screened for PVA degradation employing plate assay method (Fig. 2.7). PVA minimal agar plates were prepared and *Vibrio sp.* were spotted on this plate to detect their PVA degrading ability. The plates were incubated at 37⁰C for 2 days. The presence of a zone of clearance surrounding the colony after flooding with iodine-boric acid solution [20], indicates PVA degrading ability [19]. From the results of primary screening those isolates with largest zones of clearance were selected and subjected to further studies.

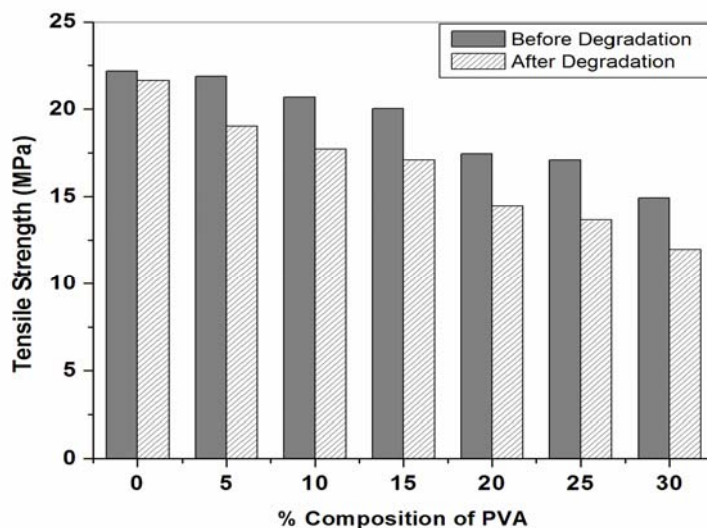


Fig. 2.8 Biodegradability of LLDPE-PVA blends with respect to tensile strength

Fig. 2.8 shows the decrease in tensile strength of LLDPE/PVA blends after biodegradation in culture medium containing *Vibrio sp.* As the PVA content is increased, it becomes a continuous phase in the blend and can be easily accessed by the organisms. At low PVA contents, the PVA may remain encapsulated in the synthetic polymer matrix, thereby making it difficult for the organisms to access and use it as a source of carbon. In such a case, the bacterial growth will be slow or negligible. The bacterial growth was far greater in LLDPE/PVA blends than in virgin LLDPE resulting in considerable loss of tensile strength in the blends.

2.3.3.2 Soil environment

Fig. 2.9 depicts the decrease in tensile strength of LLDPE/PVA blends after degradation in garden soil. Here also, there is decrease in tensile strength indicating degradation by the soil microorganisms. In the soil, water diffuses into the polymer sample, causing swelling and enhancing biodegradation.

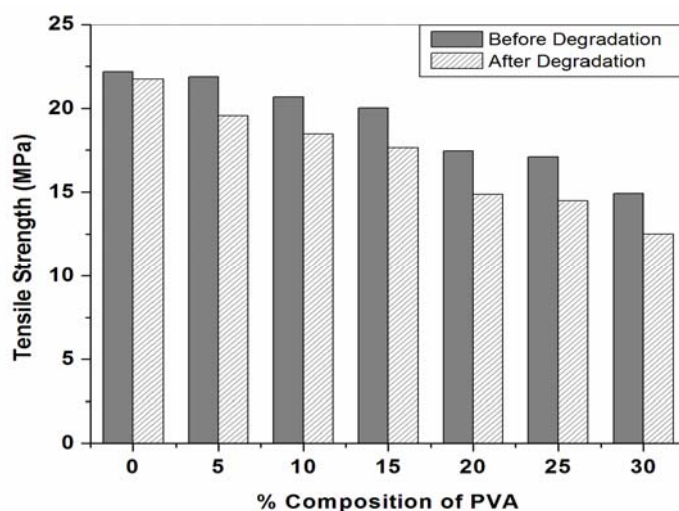


Fig. 2.9 Variation in tensile strength after degradation in garden soil

Table 2.2 shows the percentage decrease in tensile strength of blends after biodegradation in culture medium and in garden soil. From the table it is clear that the extent of degradation is more in the case of culture medium. A maximum percentage loss of tensile strength of 20.16 is noticed in the case of biodegradation in culture. As against this only a 16.34 % loss of is observed in the samples degraded in the soil. Both sets of samples show a steady loss of tensile strength with passage of time indicating biodegradability.

Table 2.2 Percentage decrease in tensile strength of blends after biodegradation and soil degradation

Sample designation	% decrease in tensile strength	
	Biodegradation in culture medium	Biodegradation in soil environment
L0	2.3	1.98
L5	13.2	10.60
L10	14.2	10.64
L15	14.6	11.83
L20	17.2	14.84
L25	20.2	15.42
L30	20	16.34

2.3.4 FTIR analysis

The FTIR spectrum of virgin LLDPE, before and after degradation in culture medium is shown in Fig. 2.10. No substantial changes are seen in virgin LLDPE after degradation.

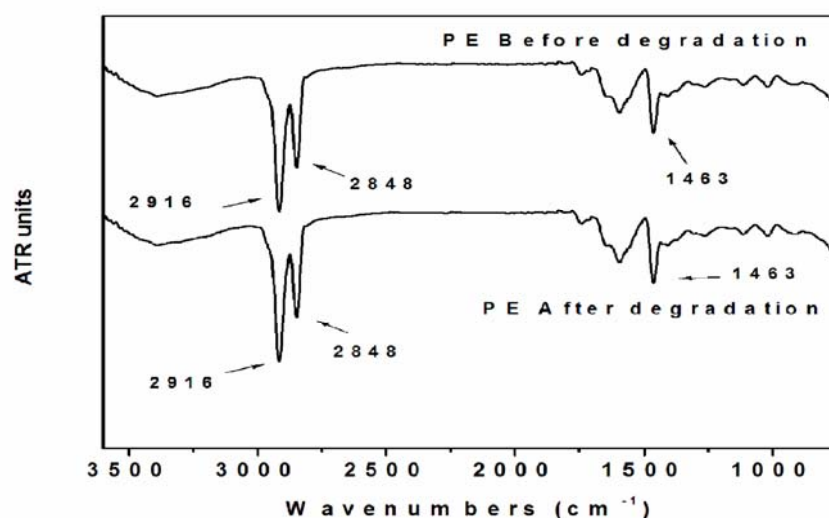


Fig. 2.10 FTIR spectra of neat LLDPE before and after degradation

Fig. 2.11 depicts the spectra of LLDPE/PVA blends before and after 15 weeks of incubation in culture medium containing *Vibrio sp.* From the spectra it is clear that the peak intensities of films at 2916-2848 cm⁻¹, 1463-1473 cm⁻¹ after degradation in culture medium have increased considerably. The peaks at 2916-2848 cm⁻¹ and 1463-1473 cm⁻¹ are due to symmetrical stretching vibration of C-H bonds and bending vibration of middle intensity C-H bond. The increase in the intensity of these peaks is owing to the fracture of polyethylene chains in degradable environments which result in the increase in terminal group numbers [27]. The peaks at 1020-1100 cm⁻¹ correspond to C-O symmetrical stretching and C-O

asymmetrical stretching vibrations in PVA. The peak at 1643 cm^{-1} also corresponds to PVA. Degradation of PVA led to the increase in intensity of these peaks.

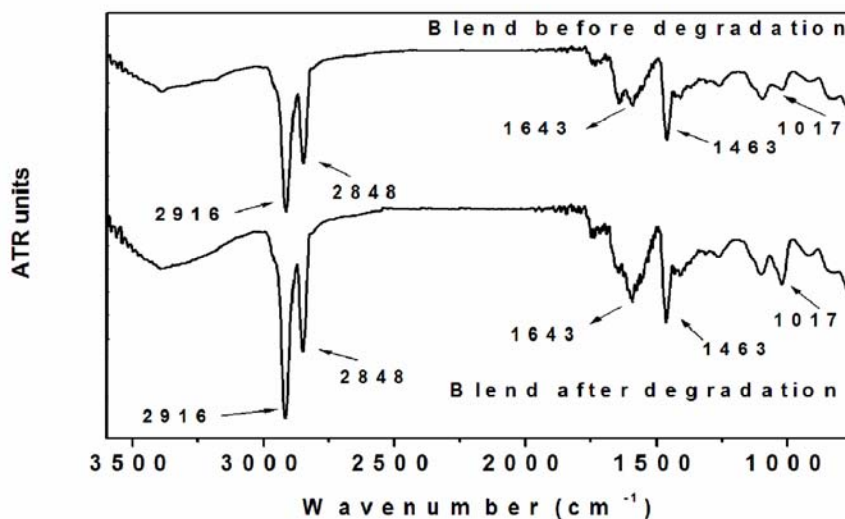


Fig. 2.11 FTIR spectra of LLDPE/PVA blends before and after degradation

2.3.5 Thermogravimetric analysis

The thermogravimetric (TG) and derivative thermogravimetric (DTG) traces for neat LLDPE and LLDPE/PVA blends in nitrogen atmosphere are shown in Fig. 2.12 and 2.13 respectively. From the figures, it is evident that all the samples exhibit a two-stage degradation process, except for neat LLDPE. In the temperature range 220°C to 420°C there is a decrease in the weight of the LLDPE/PVA blend which is not noticed in the case of neat LLDPE.

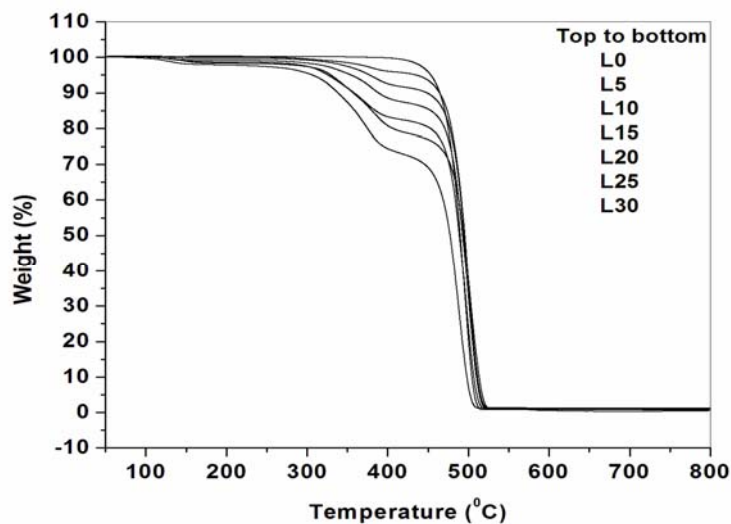


Fig. 2.12 Thermogravimetric analysis curves of neat LLDPE and LLDPE/PVA blends

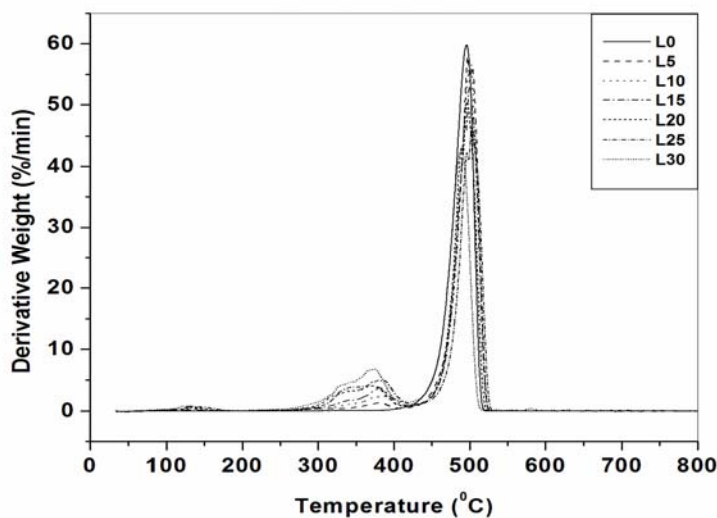


Fig. 2.13 Derivative thermogravimetric curves of neat LLDPE and LLDPE/PVA blends

This first degradation stage is due to water evaporation from the decomposition of hydroxyl groups [15]. The second degradation stage between 420°C to 520°C is due to chain scission of the carbon-carbon bonds in the main chain. The presence of PVA does not affect the degradation temperature

of LLDPE but causes a slowdown of the degradation rate. The two separated DTG maxima in the blend indicate that a separation of phases has occurred between the LLDPE and PVA components [15]. The maximum degradation temperature (T_{\max}), the onset degradation temperature (T_{onset}), and the percentage residual weight are shown in Table 2.3.

Table 2.3 TGA data of virgin LLDPE and LLDPE/PVA blends. The maximum degradation temperature (T_{\max}), the onset degradation temperature (T_{onset}) and the percentage residual weight are shown

Sample designation	Maximum degradation temperature (T_{\max})	Onset degradation temperature (T_{onset})	%Residual weight
L0	495.9	448.75	1.781
L5	490.4	435.19	1.168
L10	495.8	442.96	1.263
L15	496.2	446.90	1.058
L20	495.7	447.77	.9153
L25	496.6	448.70	.5718
L30	491.6	451.78	.4336

The maximum degradation temperature of the blend is almost the same as that of pure LLDPE. This means that addition of PVA to LLDPE does not adversely affect the thermal stability of LLDPE. The residual weight decreases as the PVA content is increased.

2.3.6 Crystallinity studies

Crystallinity is a state of greater order implying a long range periodic geometric pattern of atomic spacings. In semicrystalline polymers such as polyethylene, the degree of crystallinity influences the degree of stiffness,

hardness and heat resistance [28]. Crystallinity can be calculated from a differential calorimetry curve by dividing the measured heat of fusion by the heat of fusion of 100% crystalline material.

LLDPE is a semi crystalline thermoplastic polymer which, upon application of heat, undergoes a process of fusion or melting wherein the crystalline character of the polymer is destroyed. While polymers melt over a temperature range due to differences in the size and regularity of the individual crystallites, the melting point of a polymer is generally reported as a single temperature at which the melting of the polymer is complete. An additional parameter for the characterization of LLDPE is its percent crystallinity.

From the DSC scans of LLDPE and LLDPE/PVA blends, enthalpy of fusion (ΔH_f), enthalpy of crystallization (ΔH_c), melting temperature (T_m) and % crystallinity were evaluated. The percent crystallinity was calculated on the assumption that the heat of fusion of 100% crystalline LLDPE is 289 J/g [29]. The blend shows a fall in heat of fusion compared to virgin LLDPE. Hence a lower degree of crystallinity is exhibited by the LLDPE/PVA blend. The lowering of crystallinity in LLDPE/PVA blends is understandable in the light of the intrusion of the bulky PVA groups into the crystallite formation [30,31] and the hydrophilic nature of PVA. Heat of crystallization is also seen to be lower for the blends compared to LLDPE. The melting and crystallization temperatures of LLDPE (Table 2.4) have not been affected to any serious extent by the presence of PVA in the concentration range studied. Hence it can be safely assumed that the interaction between LLDPE and PVA is minimal [32]. In Table 2.4 T_c stands for crystallization temperature.

Table 2.4 DSC analysis data of neat LLDPE and LLDPE/PVA blends

Sample designation	T _m (°C)	T _c (°C)	Heat of fusion (J/g)	Heat of crystallisation (J/g)	% Crystallinity
L0	123.43	111.62	96.35	85.18	33.34
L5	123.65	111.76	91.88	79.40	30.20
L10	123.51	111.41	86.71	76.78	27.00
L15	123.36	111.56	83.20	71.32	24.47
L20	123.38	111.91	78.74	70.47	21.79
L25	123.41	111.97	73.68	64.90	19.12
L30	123.40	112.28	68.16	60.13	16.50

After 15 weeks of incubation in the culture medium containing *Vibrio sp.*, the biodegraded samples were again analysed for crystallinity. The results obtained for all compositions of LLDPE/PVA blends are tabulated in Table 2.5.

Table 2.5 DSC comparison data of blends before and after degradation obtained from the second heating thermograms: A-before degradation, B-after degradation

Sample Designation	Heat of fusion (J/g)		% Crystallinity	
	A	B	A	B
L0	96.35	96.93	33.34	33.54
L5	91.88	92.69	30.20	30.47
L10	86.71	89.75	27.00	27.94
L15	83.20	87.03	24.47	25.59
L20	78.74	84.21	21.79	23.31
L25	73.68	78.11	19.12	20.27
L30	68.16	73.93	16.50	17.91

From the table it is clear that as the PVA content increases the heat of fusion and crystallinity decrease for LLDPE/PVA blends. In all the blends the heat of fusion and crystallinity increases after biodegradation. Albertsson [33]

and Kestelman *et al* [34] noticed a similar change in the crystallinity of polyethylene after biodegradation.

2.3.7 Surface morphological studies

Fig. 2.14 and 2.15 show the SEM photographs of neat LLDPE and LLDPE/PVA blends before and after degradation in culture medium containing *Vibrios sp.*

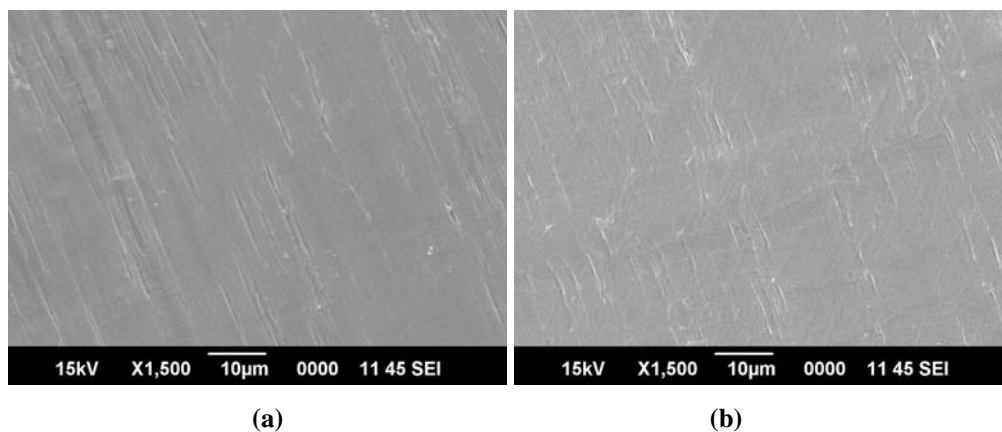


Fig. 2.14 Scanning electron micrographs of (a) neat LLDPE before degradation; (b) neat LLDPE after degradation

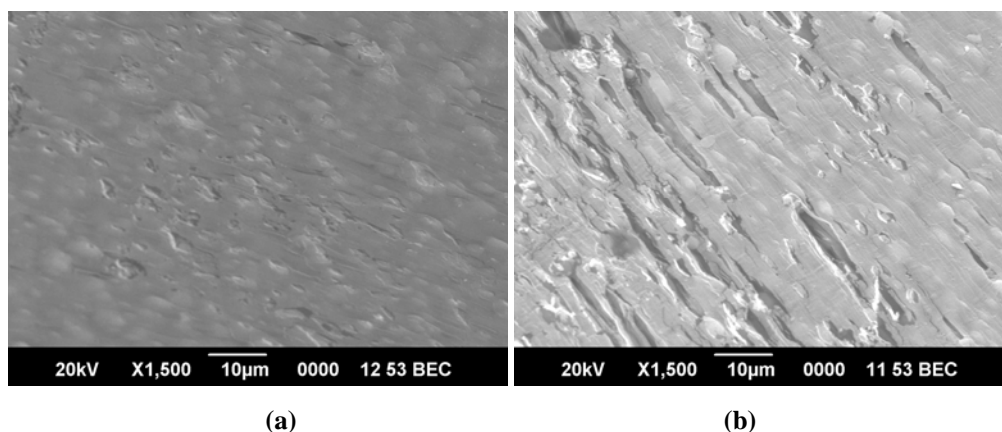


Fig. 2.15 Scanning electron micrographs of (a) LLDPE/PVA blend before degradation; (b) LLDPE/PVA blend after degradation

There are no noticeable changes in morphology of virgin LLDPE when subjected to microbial attack. Scanning electron microscopy shows that surfaces of LLDPE/PVA blends prior to biodegradation exhibit a rough surface with no surface defects. The surface roughness increases in the blends with degradation. There are cracks and grooves visible in the blends after degradation in culture medium containing *Vibrios*. These defects are the result of consumption of the biodegradable component by microbes. Such surface destruction can facilitate the transport of degrading factors to the polymer bulk and further accelerate the total degradation occurring in the environment.

2.4 Conclusions

- The blending of PVA with LLDPE has lead to a marginal loss of mechanical properties such as tensile strength and elongation at break. But the modulus of the blends increased as the PVA content is increased.
- Thermogravimetric analysis shows that addition of PVA does not adversely affect the thermal stability of LLDPE.
- Differential scanning calorimetry studies shows that the percentage crystallinity of the blends is lower than that of neat LLDPE.
- Water absorption values of the blends were higher than for neat LLDPE indicating increased affinity of the blends towards microbial attack.
- When these blends are subjected to biodegradation in soil environment and a culture medium, microbial activity is indicated by fall in tensile properties, spectroscopic studies, crystallinity increase and surface defects.

- Biodegradation in the culture is more rapid than soil degradation. The blends are remarkably more biodegradable than pure LLDPE.
- The FTIR analysis and morphology of the degraded samples give ample evidence for degradation of LLDPE/PVA blends.
- The study has established that blending with PVA has improved the biodegradability of LLDPE.

2.5 References

- [1] D. Bikiaris, J. Prinos; *Polym. Degrad. Stab.* **1997**, 58, 215.
- [2] Y. Otake, T. Kobayashi, H. Asabe, N. Murukami, K. Ono; *J. Appl. Polym. Sci.* **1995**, 56, 1789.
- [3] F. Khabbaz, A. C. Albertsson; *J. Appl. Polym. Sci.* **2001**, 79, 2309.
- [4] E. Chiellini, A. Corti, G. Swift; *Polym. Degrad. Stab.* **2003**, 81, 341.
- [5] M. Pracella, F. Pazzagli, A. Galeski; *Polym. Bull.* **2002**, 48, 67.
- [6] U. S. Ishiaku, K. W. Pang, M. S. Lee, I. Z. A. Mohd; *Eur. Polym. J.* **2002**, 38, 393.
- [7] G. J. L. Griffin; *J. Polym. Sci. Polym. Symp.* **2007**, 57, 281.
- [8] G. J. L. Griffin; *Pure. Appl. Chem.* **1980**, 52, 399.
- [9] J. E. Glass, G. Swift; *ACS Symposium Series* **1990**, 433, 61.
- [10] M. Shuichi, T. Noriyasu, T. Atsuko, N. Kimihito, T. Kazunobu; *Macromolecules*, **1999**, 32, 7753.
- [11] N. A. Peppas, Y. Huang, M. Torres-Lugo, J. H. Ward, J. Zhang; *Annual Rev. Biomedical Engineering*, **2000**, 2, 9.

- [12] Prasad; Polymer Engineering and Science **1938**, 8, 1716.
- [13] S. Wei, G. Shiyi, F. Changshui, X. dong, R. Quan; J. Mater. Sci. **1999**, 34, 5995.
- [14] S. T. Sam, H. Ismail, Z. Ahmad; Polymer-Plastics Technology and Engineering, **2011**, 50, 851.
- [15] H. Ismail, R. Nordin, Z. Ahmad, A. Rashid; Iranian Polymer Journal, **2010**, 19, 297.
- [16] ASTM D 882–02. Standard test method for tensile properties of thin plastic sheeting, **1997**.
- [17] ASTM D 570-98. Standard Test Method for Water Absorption of Plastics **2003**
- [18] ASTM D 5247–92. Standard test method for determining the aerobic biodegradability of degradable plastics by specific microorganisms **2003**.
- [19] T. Mori, M. Sakimoto, T. Kagi, T. Sakai; Biosci. Biotechol. Biochem. **1996**, 16, 1205.
- [20] J. H. Finley; Anal. Chem. **1961**, 33, 1925.
- [21] ASTM D 5338 – 98. Standard Test Method for Determining Aerobic Biodegradation of Plastic Materials Under Controlled Composting Conditions **2003**.
- [22] J. M. Margolis ed., Instrumentation for thermoplastics processing, Hanser Publishers, Munich, Vienna, New York, Oxford Univ. Press, **1988**, 54.
- [23] L. Mascia; Thermoplastics, Materials Engineering, Applied Science, Essex, England, **1982**, 75.
- [24] Greco, A. Maffezzoli; Polym. Test. **2008**, 27, 61.
- [25] O. Breuer, R. Tchoudakov, M. Narkis, A. Siegmann; J. App. Polym. Sci. **1997**, 64, 1097.

- [26] S. Joseph, S. Thomas; Eur. Polym. J. **2003**, 39, 115.
- [27] W. Shujun, Y. Jiugao, Y. Jinglin; Journal of Polymers and the Environment **2006**, 14, 65.
- [28] R. Chandra, R. Rustgi; Polym. Degrad. Stab. **1997**, 56, 185.
- [29] R. E. Lavengood, L. Nicolais, M. Narkis; J. Appl. Polym. Sci. **1973**, 17, 1173.
- [30] M. A. Cole; A protocol for conducting Soil Burial Studied with Biodegradable Plastics. University of Illinois Urbana-Champaign, Department of Agronomy, **1989**, March 3.
- [31] R. Greco, P. Musto, F. Riva, G. Maglio; J. Appl. Polym. Sci. **1989**, 37, 789.
- [32] G. Pedroso, D. S. Rosa; Carbohydrate Polymers **2005**, 59, 1.
- [33] C. Albertsson; In Int. Conf: on the Advances in the Stabilization and Controlled Degradation of Polymers, ed. A. V. Patnis, Technomic, West Chester, PA, **1986**.
- [34] V. N. Kestelman, V. L. Yaravenko, E. I. Melnikova; Int. Biodete. Bull. **1972**, 81, 15.

.....✪.....

HYDROTHERMAL SYNTHESIS OF NANO-TiO₂ PHOTOCATALYST AND ITS CHARACTERIZATION

Contents	3.1 <i>Introduction</i>
	3.2 <i>Experimental</i>
	3.3 <i>Results and discussion</i>
	3.4 <i>Conclusion</i>
	3.5 <i>References</i>

3.1 Introduction

Studies on the photochemical activity of pigments in commercial polyolefins have been mainly concerned with white pigments. Titanium dioxide (TiO₂) is the most widely studied of these, since it is technically outstanding in many respects [1]. Anatase, brookite and rutile are the three crystalline forms of titania. Among these crystalline forms anatase-TiO₂ deserves more attention by virtue of its use as pigment [2] and gas sensors [3], catalysts [4,5] and photocatalysts [6–8] in applications related to pollution control and in photovoltaics [9]. The catalytic and other properties of these materials strongly depend on the crystallinity, surface morphology, the particle sizes and preparation methods.

TiO₂ nanoparticles have real advantages in relation to photocatalytic activity. Different preparation processes for them have been reported, such as sol–gel process [10], hydrolysis of inorganic salts [11], ultrasonic technique [5] and hydrothermal process [12–15].

This chapter describes a rapid hydrothermal synthesis method to produce phase pure, monodisperse anatase particles with small grain size and high specific surface area at low temperature. Hydrothermal processing of either amorphous titania or a titanium containing precursor has been shown to be an ideal method for producing ultrafine (grain size < 10nm) anatase crystallites with high specific surface areas and high crystallinity, a property that is essential for photocatalytic reactions [16].

3.2 Experimental

3.2.1 Chemicals

Titanium-iso-propoxide, $[\text{Ti}(\text{OPr}^i)_4]$ purchased from Alpha was used as titanium source for TiO_2 photocatalyst preparation. $\text{Ti}(\text{OPr}^i)_4$ was used without further purification. Glacial acetic acid ($\text{C}_2\text{H}_4\text{O}_2$, 99.5%) was used as a solvent. Distilled water was used for the hydrolysis of $\text{Ti}(\text{OPr}^i)_4$.

3.2.2 Experimental set up



Fig. 3.1 Experimental setup for the synthesis of nanoanatase

Since the experiments were carried out on a small scale, a 500ml Borosil beaker was used for the reaction. A magnetic stirrer was used for stirring. The speed of the stirrer was maintained at 60 rpm.

3.2.3 Preparation of nano-TiO₂ photocatalyst by hydrothermal method

The most popular technique to hydrolytically prepare nanocrystalline titania is hydrothermal processing, i.e., crystallization at elevated temperature and pressure in the presence of water. This technique can be more appropriately called “solvothermal” processing because a liquid other than water is used as the solvent even if water is present for hydrolysis [17]. Hydrothermal crystallization is carried out in a sealed autoclave. A heating mantle or oven is used to raise the temperature above the standard boiling point of the solvent, at which point the evaporating solvent begins to generate a pressure inside the sealed vessel exclusively due to the refluxing solvent. Hydrothermal reaction times are often as short as 2 h and are rarely longer than 1-2 days. The following procedure was employed in this case.

10ml Ti(OPrⁱ)₄ was dissolved in 20ml acetic acid by stirring. After stirring for 10 minutes, 200ml distilled water was added dropwise from a burette at a rate of 1ml/min. The stirring without heating was continued till a clear solution was obtained. The clear solution was then transferred into a Teflon-lined autoclave. The autoclave was then maintained at 110⁰C overnight without shaking or stirring. After the autoclave naturally cooled to room temperature, the sample solution was transferred into a beaker and subjected to solvent evaporation at 110⁰C for 2h. It was then dried in oven at 110⁰C for a few minutes in a current of air. The sample was then calcined at 400⁰C in the muffle furnace for different time intervals to ensure a crystalline product.

During this processing titanium (IV) alkoxide reacts with water and forms Ti-O-Ti bridges to create solid TiO₂, according to the reaction;

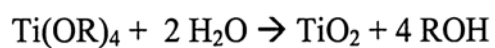


Fig. 3.2 The solution obtained after hydrothermal treatment in an autoclave



Fig. 3.3 TiO₂ nano particles obtained after calcinations at 400⁰C

3.2.4 Characterization of nanotitania

3.2.4.1 X-Ray diffraction

The crystalline phase of the hydrothermally synthesized TiO₂ nanoparticles was analyzed by X-ray powder diffraction (XRD) pattern obtained from Bruker D8 Advance Model Diffractometer with Cu K α radiation in the region $2\theta = 10\text{--}80^\circ$ and Ni filter operating at 30kV and 20mA. The crystallite size of the anatase particles was calculated from the X-ray diffraction peak using Scherrer's equation [18,19];

$$d_{hkl} = k\lambda / (\beta \cos (\theta))$$

where d_{hkl} is the average crystallite size (nm), λ is the wavelength of the Cu K α radiation applied ($\lambda = 1.54\text{\AA}$), θ the Bragg's angle of diffraction, β the full-width at half maximum intensity of the peak observed at $2\theta = 25.3^\circ$ (converted to radians) [20] and k the constant usually taken as 0.94.

3.2.4.2 Bulk density

The bulk density of the material was determined as per ASTM D 1895-96. Bulk density is defined as the weight per unit volume of a material. It is primarily used for powders or pellets. The test can provide a gross measure of particle size and dispersion, which can affect material flow consistency.

Procedure

The small end of the funnel is closed with hand or a suitable flat strip and $115 \pm 5 \text{ cm}^3$ of samples are poured into the funnel. Open the bottom of the funnel quickly and allow the material to flow freely into the cup. If caking occurs in the funnel, the material may be loosened with a glass rod. After the material has passed through the funnel immediately scrape off the excess on the top of the cup

with a straight edge without shaking the cup. Weigh the material nearest to 0.1g and determine bulk density.

3.2.4.3 BET studies

Surface area of the titanium dioxide nano particles as well as commercial titania were measured using BET method. Measurements were carried out under nitrogen atmosphere using ASAP 2000 model, surface area and porosity analyzer. Surface area was determined using the equation,

$$S_{\text{BET}} = 4.353 V_m$$

where S_{BET} is the surface area in m^2/g and V_m is the molar volume of adsorbate gas (N_2) at STP.

3.2.4.4 Fourier transform infrared spectroscopy

FTIR spectra of the commercial and synthesized TiO_2 in powder form was recorded in the range 400 to 4000 cm^{-1} .

3.2.4.5 Scanning electron microscopy

The surface morphology of TiO_2 was examined using a scanning electron microscope. The synthesized and commercial TiO_2 samples were sputter-coated with a thin layer of gold and examined under scanning electron microscope.

3.3 Results and discussion

3.3.1 X-Ray diffraction

The XRD pattern is shown in Figs. 3.4 to 3.8. All the sharp peaks observed belong to anatase- TiO_2 . Rutile and brookite phases were absent as

their characteristic d-spacing values were not observed. Apparently, a complete anatase TiO₂ crystalline phase was obtained.

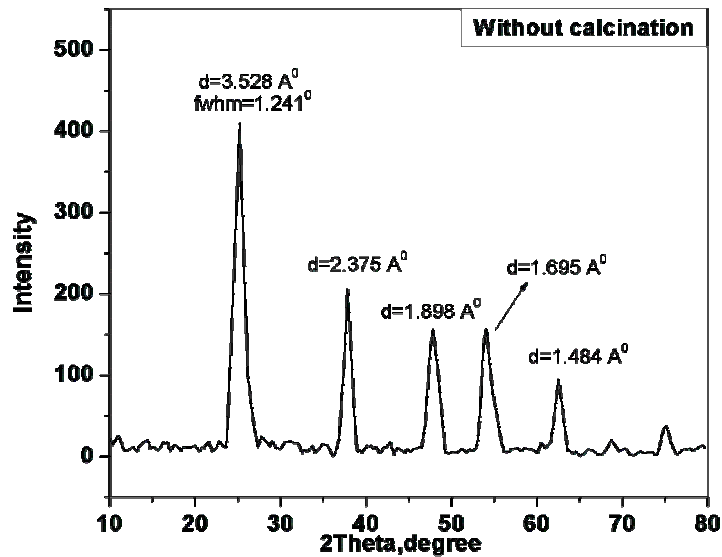


Fig. 3.4 XRD pattern of hydrothermally synthesized nano-TiO₂ powder without calcination

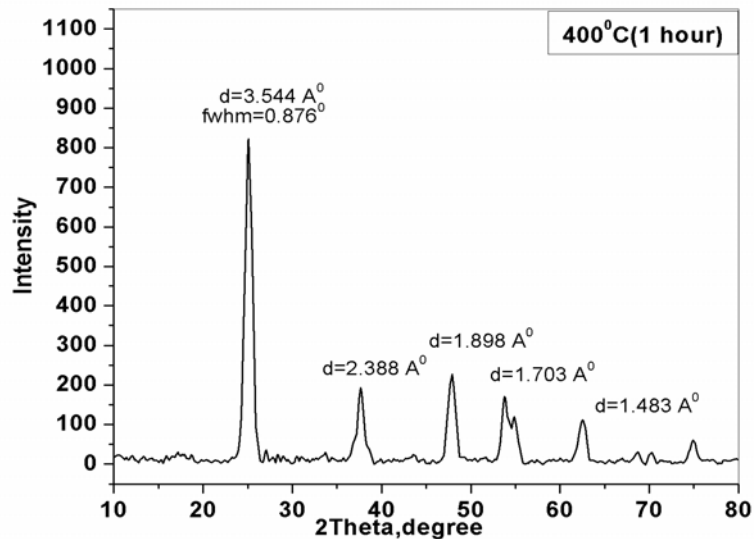


Fig. 3.5 XRD pattern of hydrothermally synthesized nano-TiO₂ powder with calcination at 400°C for 1 hour

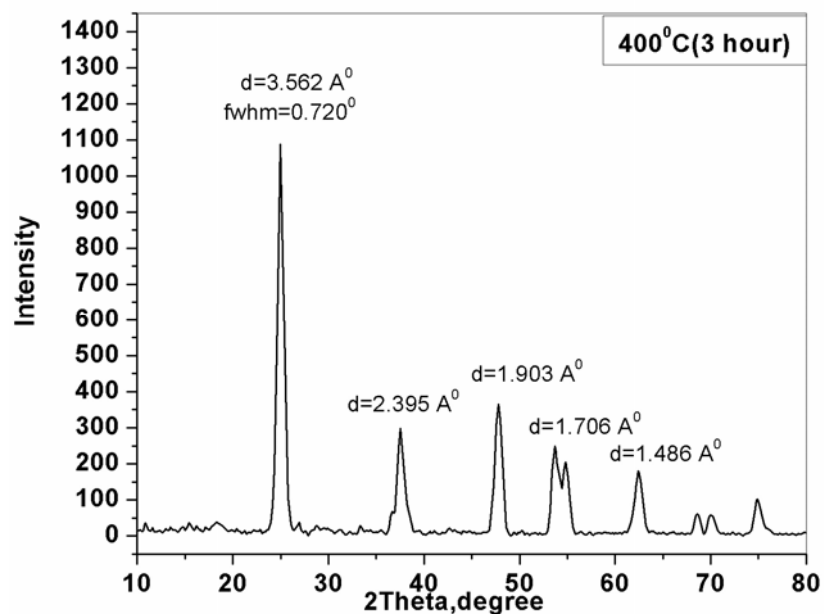


Fig. 3.6 XRD pattern of hydrothermally synthesized nano-TiO₂ powder with calcination at 400°C for 3 hours

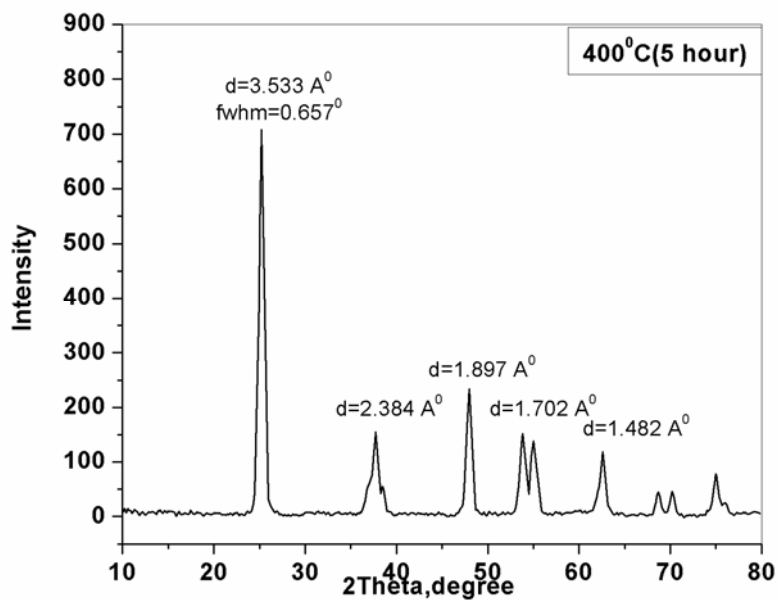


Fig. 3.7 XRD pattern of hydrothermally synthesized nano-TiO₂ powder with calcination at 400°C for 5 hours

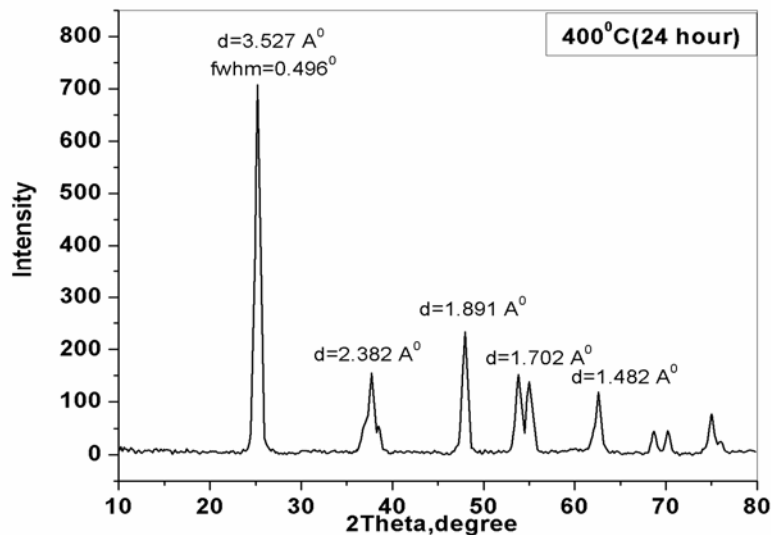


Fig. 3.8 XRD pattern of hydrothermally synthesized nano-TiO₂ powder with calcination at 400°C for 24 hours

Details of X-Ray diffraction studies are given in Table 3.1. Average crystallite size of TiO₂ was estimated by Scherrer's equation. The average crystallite size of the nano-TiO₂ (without calcinations) was estimated to be 6 nm and it is much lower than most other commercially available titania samples.

Table 3.1 Data of X-Ray diffraction studies

Catalyst	Calcination time (hour)	2θ (°)	Cos θ	β (°)	Crystallite size (nm)
A0	0	25.220	0.97	1.241	6.56
A1	1	25.108	0.97	0.876	9.29
A3	3	24.981	0.97	0.720	11.31
A5	5	25.188	0.97	0.657	12.39
A24	24	25.233	0.97	0.496	16.43

[A0 = Anatase sample without calcination, A1= Anatase sample after 1hour calcination, A3 = Anatase sample after 3hour calcination, A5 = Anatase sample after 5hour calcination, A24 = Anatase sample after 24hour calcination.]

The variation of β value and crystallite size with calcination time is shown in Figs. 3.9 and 3.10 respectively. The gradual narrowing of XRD lines with the increase in calcinations time (Fig. 3.9) reflects a corresponding increase in the average crystallite size (Fig. 3.10).

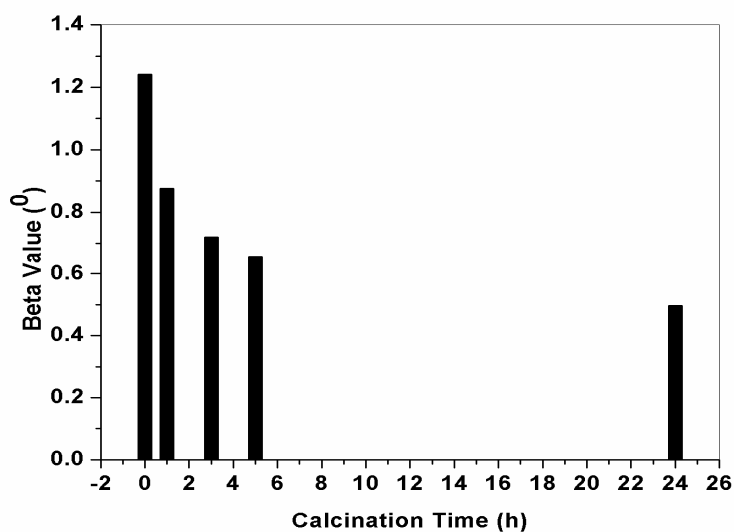


Fig. 3.9 Variation of β value with calcination time

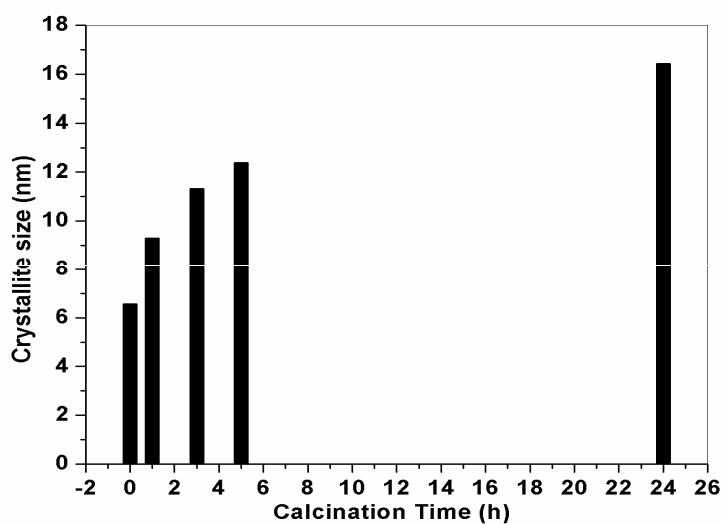


Fig. 3.10 Variation of crystallite size with calcination time

3.3.2 Bulk density

The bulk density of the commercial and synthesized samples is given in Table 3.2. It is found that the bulk density of the synthesized anatase (A0-A24) is higher than that of commercial anatase (A). This is due to the smaller particle size of synthesized anatase compared to that of commercial anatase.

Table 3.2 Bulk densities of the prepared anatase samples

Samples	Bulk density (g/cm ³)
A	0.979
A0	1.296
A1	1.282
A3	1.173
A5	1.136
A24	1.104

The variation of bulk density with calcination time is shown in Fig.3.11. Bulk density of the synthesized anatase samples decreases with increase in calcination time. This is due to the increase in particle size.

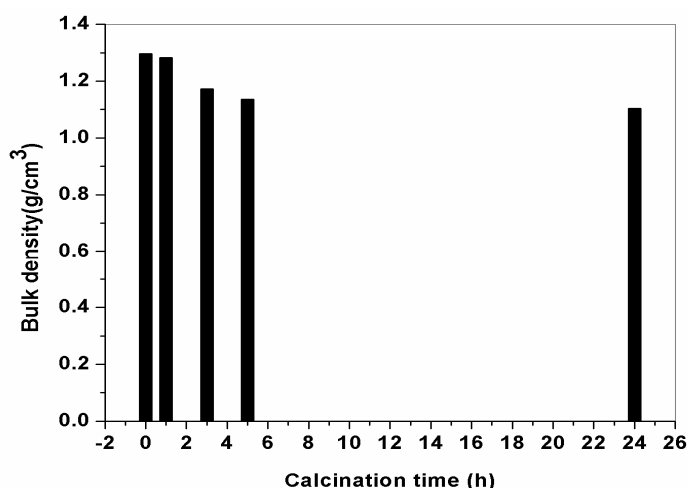


Fig.3.11. Variation of bulk density with calcination time

3.3.3 BET studies

Table 3.3 gives the BET adsorption results of nano and commercial anatase. From the table it is clear that nanoanatase has higher surface area than that of commercial anatase. Higher the surface area, lower the particle size. It is very well known that the photocatalytic effect of a catalyst is dependent on the crystallite size and surface area. The smaller the particles, the larger will be its specific surface area and the higher photocatalytic activity [21].

Table 3.3 Surface area of the TiO₂ samples

Samples	Surface area (m ² /g)
Commercial anatase	110
Nanoanatase	310

3.3.4 Infrared spectroscopy

The FTIR spectrum of nano and commercial forms of TiO₂ are shown in Figs. 3.12 and 3.13 respectively. In the FTIR spectrum, the broad band at 3360 cm⁻¹ is attributed to bound water. The peak at 1624 cm⁻¹ is due to vibration frequency corresponding to the bending of water molecule (O-H bending vibration). Ti-(O-C) vibration is observed as a small band around 1053 cm⁻¹. The sharp band observed at 930 cm⁻¹ is attributed to Ti-O stretching vibration.

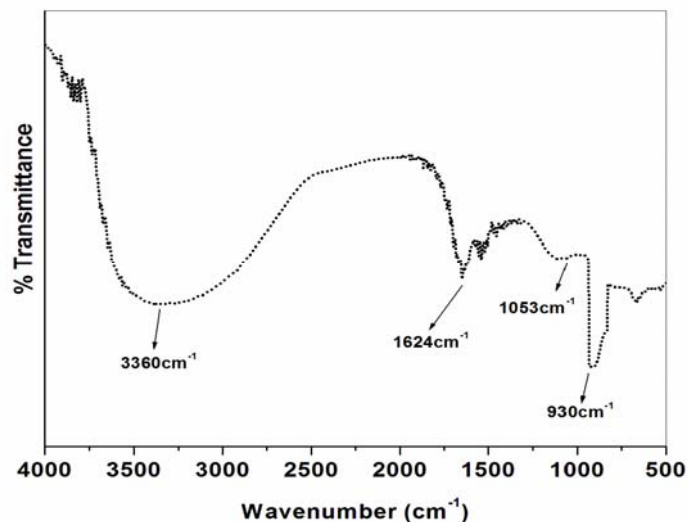


Fig. 3.12 FTIR spectrum of synthesized nano-TiO₂ particle dried at 110⁰C

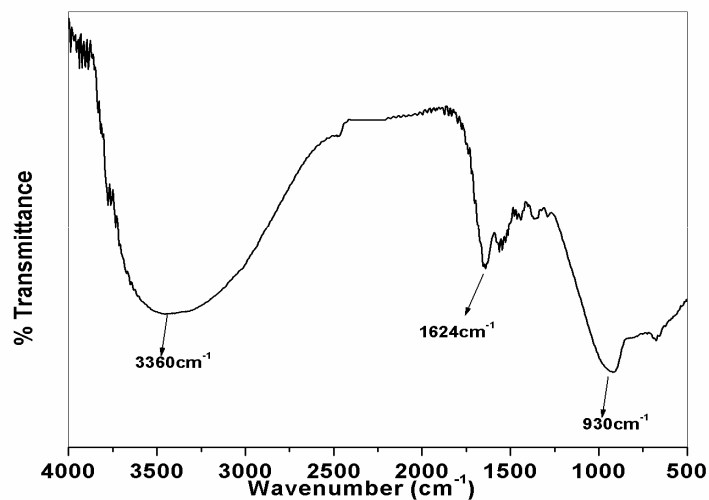


Fig. 3.13 FTIR spectrum of commercial-TiO₂

3.3.5 Scanning electron microscopy

The surface morphology of TiO₂ was examined by a JEOL JSM-6390LV Model scanning electron microscope. The scanning electron

micrographs of the synthesized nano and commercial forms of TiO_2 are shown in Figs. 3.14 and 3.15. These micrographs show that the synthesized TiO_2 has lower particle size than the commercial TiO_2 . From the micrographs it is clear that anatase particles are spherical in shape.

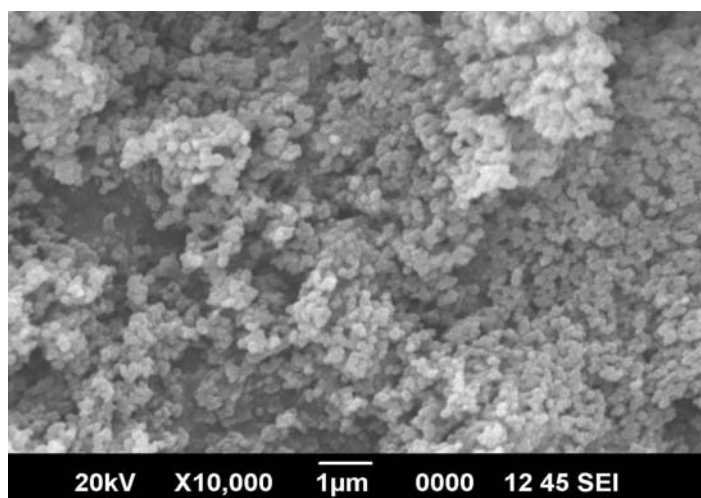


Fig. 3.14 Typical SEM micrograph of hydrothermally synthesized nanoanatase particle

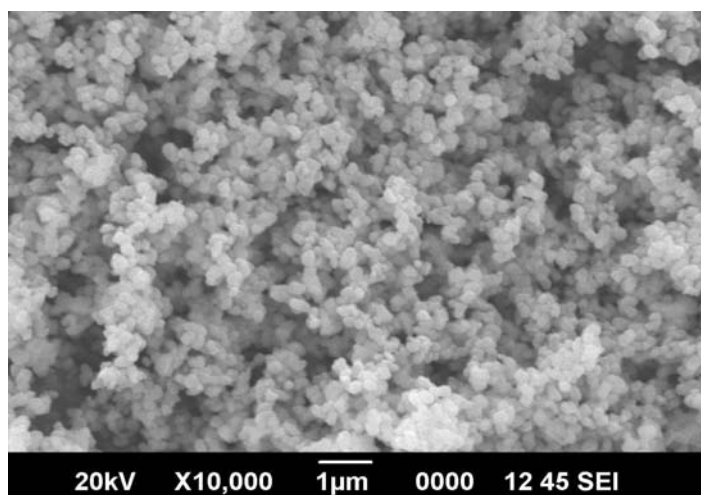


Fig. 3.15 Typical SEM micrograph of commercial anatase particle

3.4 Conclusions

- Nanoanatase having photocatalytic activity was successfully prepared by hydrothermal method under controlled conditions.
- XRD studies showed that anatase was the only crystalline phase in the nano TiO₂ powder.
- The crystallite size of titania was calculated to be 6nm from the XRD results.
- Crystallite size increases as the calcination time of the synthesized anatase is increased.
- Anatase without any calcination showed the smallest crystallite size.
- From BET method the surface area was found to be 310m²/g which is higher than that of commercial anatase (110m²/g). Higher the surface area, lower the particle size.
- The smaller particle size and larger specific surface area indicates higher photocatalytic activity.
- SEM shows that nanoanatase prepared by this method is spherical in shape.

3.5 References

- [1] KING; *Plastics and Polymers*,**1968**.
- [2] J.G. Balfour; *Technological Applications of Dispersions*, Marcel Dekker, New York, **1994**.
- [3] Y.C. Yeh, T.T. Tseng, D.A. Chang; *J. Am. Ceram. Soc.* **1989**,72 ,1472.
- [4] C.G. Bond, S. F. Tahir; *Appl. Catal.* **1991**,71, 1.
- [5] P.S.Awati, S.V.Awate, P.P.Shah, V.Ramaswamy; *Catal.Comm.***2003**,4, 393.

- [6] Hagfeldt, M. Gratzel; Chem. Rev. **1995**,95,49.
- [7] Y.H. Hsien, C.F. Chang, Y.H. Chen, S. Cheng; Appl. Catal., B Environ. **2001**, 31, 241.
- [8] C. Lizama, J. Freer, J. Baeza, H.D. Mansilla; Catal. Today, **2002**, 76, 235.
- [9] N. Serpane, J. Texier, A.V. Emeline, P. Pichat, H. Hidaka, J. Zhao; J. Photochem. Photobiol., A Chem. **2000**,136,145.
- [10] G. Colon, M.C. Hidalgo, J.A. Navio; Catal. Today. **2002**, 76, 91.
- [11] Y. Zhang, G. Xion, N. Yao, W. Yang, X. Fu; Catal. Today. **2001**, 68,220.
- [12] X.M. Wu, L. Wang, Z.C. Tan, G.H. Li, S.S. Qu; J. Solid State Chem. **2001**, 156, 220.
- [13] E. Vigil, J.A. Ayllon, A.M. Peiro, R.R. Clemente; Langmuir, **2001**,17,891.
- [14] H. Zhang, M. Finnegan, J.F. Banfield; Nano Lett. **2001**, 1, 81.
- [15] X. Ju, P. Huang, N. Xu, J. Shi; J. Membr. Sci. **2002**, 202, 63.
- [16] J.Ovenstone; Journal of Materials Science. **2001**, 36, 1325.
- [17] A.Rabenau, C.Angewandte; International Edition English, **1985**, 24, 1026.
- [18] B. D. Cullity; Elements of X-Ray Diffraction, Addison Wesley, **1978**.
- [19] L. E. Alexander; X-ray diffraction methods in Polymer Science, John Wiley, New York, **1968**.
- [20] L.Q. Jing, Z. L. Xu, X. J. Sun, J. Shang, W. M. Cai; Appl. Surf. Sci. **2001**, 180, 308.
- [21] M. Asilturk, F. Sayilkan, S. Erdemoglu, M. Akarsu, H. Sayikan, M. Erdemoglu, E. Arpac; Journal of Hazardous Materials, **2005**.

..........

EFFECT OF TiO₂ ON THE WEATHERING AND BIODEGRADATION OF LLDPE/PVA BLENDS CONTAINING VEGETABLE OIL

Contents	4.1	<i>Introduction</i>
	4.2	<i>Experimental</i>
	4.3	<i>Results and discussion</i>
	4.4	<i>Conclusion</i>
	4.5	<i>References</i>

4.1 Introduction

Polyethylene of enhanced environmental degradability is prepared by blending with biodegradable additives, photo-initiators or by copolymerization. Incorporation of pro-oxidant additives is a promising step to overcome the environmental degradation by polyethylene films. Pro-oxidants accelerate photo oxidation and consequent polymer chain cleavage rendering the product more susceptible to biodegradation.

Due to favourable characteristics such as inexpensiveness, non-toxicity, stability and high photoactivity, TiO₂ has become an excellent choice for a photocatalyst [1,2]. As photocatalysts, rutile and anatase phases of TiO₂ have also been investigated. It is recognised that the photocatalytic activity of the anatase phase which has a more negative conduction edge potential (higher potential energy of photogenerated electrons) is superior to that of rutile [3].

The different effects of micro- and nano-sized titania particles on the degradation of polyethylene were investigated by first Allen et al [4], nano sized particles being found to be the more active. A small particle size increases the available surface area for reaction and lowers the probability of electron-hole recombination after the initial photo-excitation event. Further, the band gap is increased by nano-scale quantum isolation effects so that the photo-activation spectrum shifts to shorter wavelengths. Hence, for pigmented paints and plastics exposed to the weather, titanium dioxide plays an important part in determining the overall rate of degradation. In all cases, the degradation results in the pigment particles being exposed at the surface resulting in loss of gloss, colour fade and chalking [5].

In this chapter, we have investigated the effect of titanium dioxide and vegetable oil either acting alone or in combination on the degradation behaviour of LLDPE/PVA blends. The weathering performance of nanoanatase and two commercial crystalline forms of TiO₂ (rutile and anatase) in commercial polyethylene in the absence as well as presence of vegetable oil is also examined. The extent of degradation was then monitored by physical property measurements, weight loss determination, thermal, MFI, spectroscopic and morphological studies.

4.2 Experimental

4.2.1 Materials

Titanium dioxide (anatase and rutile grades) was purchased from M/S Travancore Titanium Products, Thiruvananthapuram. Nano-TiO₂ photo catalyst was synthesized by hydrothermal method as described in Chapter-3. Glycerol (C₃H₈O₃) was purchased from S.D Fine Chemicals, Ltd, Mumbai. Food grade sunflower oil was used for the study.

4.2.2 Sample preparation

The PVA was melt blended with LLDPE in an internal mixer, Haake Rheometer (Rheocord 600p) as described in Chapter-2. Initial studies with LLDPE/PVA blends reveal that PVA degrades at an early stage to give a discoloured and inferior product. Hence it is decided to employ a PVA stabilizer. Several suitable PVA plasticizers capable of enhancing its thermal stability, such as glycerol, ethylene glycol and its dimer and trimer, amine alcohols, and polyvalent hydroxyl compounds have been proposed and utilized in industrial processes [6]. In this study glycerol (15 w/w of PVA) was added as a plasticizer. This lowers the melting point of PVA into a processable range [7]. It also helps to better disperse PVA into the LLDPE matrix. Oils and fats are mostly triglycerides. Triglycerides containing unsaturated acids are more susceptible to autoxidation. This reaction is believed to take place via the formation of a free radical, followed by the production of hydroperoxides[8]. Since free radical formation catalyses the photooxidation reactions of polyethylene, vegetable oil (1 w/w of LLDPE) was also added to the blends.

Varying amounts of nano and commercial forms of TiO₂ (0.25% - 1% w/w) were added to LLDPE/PVA blends during mixing. Blends containing different proportions of LLDPE, PVA and metal oxides were compression molded into sheets to form thin films. Molded samples, cut into strips according to ASTM D 882, were used for all the tests. The details of film samples prepared along with their designation are presented in Table 4.1. LLDPE/PVA (sample-L10 from Chapter-2) blends containing glycerol alone have been designated as F and those containing both glycerol and vegetable oil as FV. Samples containing additionally anatase, rutile and nanoanatase have

been designated as FVA, FVR and FVN respectively, the numerical suffix indicating the percentage concentration of the oxide additive.

L10 + Glycerol = F

L10 + Glycerol + Veg. Oil = FV

L10 + Glycerol + Veg. Oil + Rutile = FVR

L10 + Glycerol + Veg. Oil + Anatase = FVA

L10 + Glycerol + Veg. Oil + Nano-anatase = FVN

L10 + Glycerol + Rutile = FR

L10 + Glycerol + Anatase = FA

L10 + Glycerol + Nano-anatase = FN

Table 4.1 Details of formulations and their sample designation

Sample designation	LLDPE (g)	PVA (g)	Glycerol (g)	Vegetable oil (g)	TiO ₂ (g)
F	45	4.5	0.675	—	—
FV	45	4.5	0.675	0.45	—
FVA-0.25	45	4.5	0.675	0.45	0.1125
FVA-0.50	45	4.5	0.675	0.45	0.225
FVA-0.75	45	4.5	0.675	0.45	0.3375
FVA-1	45	4.5	0.675	0.45	0.45
FA-0.50	45	4.5	0.675	—	0.225
FVR-0.25	45	4.5	0.675	0.45	0.1125
FVR-0.50	45	4.5	0.675	0.45	0.225
FVR-0.75	45	4.5	0.675	0.45	0.3375
FVR-1	45	4.5	0.675	0.45	0.45
FR-0.50	45	4.5	0.675	—	0.225
FVN-0.25	45	4.5	0.675	0.45	0.1125
FVN-0.50	45	4.5	0.675	0.45	0.225
FVN-0.75	45	4.5	0.675	0.45	0.3375
FVN-1	45	4.5	0.675	0.45	0.45
FN-0.50	45	4.5	0.675	—	0.225

4.2.3 Degradation studies

4.2.3.1 Natural weathering

Polyethylene films were mounted on racks at an angle of 30-45° facing the south direction as per ASTM D 1435-99 [9]. These experiments were started in the month of May 2010 in Kochi (Kerala, India) and continued for 600 hours. Samples after weathering were retrieved at regular intervals of 120, 240, 360, 480, and 600 hours, respectively, to evaluate the effect of weathering time on degradation. Average relative humidity in the atmosphere was 70% and the average temperature was 33°C.

4.2.3.2 Degradation studies in culture medium and in garden soil

The weathered samples were then subjected to biodegradation and soil degradation studies. Biodegradation of the samples were carried out using a consortium of bacteria (Chapter-2 section-2.2.6) according to ASTM D 5247–92. The procedure adopted for the preparation of the inoculum was described in Chapter 2. The degradation studies were continued for 15 weeks. Soil burial tests were conducted in garden soil for the same time period.

4.2.4 Evaluation of extent of degradation

Samples with a gauge length of 100 mm and width of 10 mm were cut from the films for tensile strength measurements as per ASTM D 882-85. Six samples were tested for each experiment and the average value was taken.

Structural changes upon exposure were investigated using FTIR spectroscopy. FTIR spectra were recorded at regular intervals using a Thermo Nicolet (Avatar 370) spectrophotometer in the spectral region between 400 and 4000 cm⁻¹. For each sample a total of 32 scans were averaged at a

resolution of 4 cm^{-1} . Carbonyl index (CI) which provides a useful means of monitoring the extent of PE oxidation was calculated from the following equation [10, 11].

$$\text{Carbonyl index (CI)} = \frac{\text{Absorption at } 1715\text{cm}^{-1} \text{ (the maximum of carbonyl peak)}}{\text{Absorption at } 2020\text{cm}^{-1} \text{ (internal thickness band)}}$$

The thermal properties were investigated using a Differential Scanning Calorimeter TA Q-100 (TA Instruments). The studies were done under nitrogen atmosphere.

The Melt Flow Index of samples before and after degradation was measured on a MFI tester (CEAST Extrusion Plastometer) at 190°C as per ASTM D 1238-01. The extrudates were cut at regular intervals after the application of 2.16 kg of dead weight. Ten extrudates were collected and the average value reported.

Scanning electron microscopy was performed to investigate the changes in the morphology due to outdoor exposure. Sample surfaces were sputtered with gold using usual techniques and then analyzed in a JEOL (JSM-6390LV) electron microscope. Weight loss of the samples on degradation was also recorded.

4.3 Results and discussion

4.3.1 Effect of glycerol and vegetable oil

Fig. 4.1 shows the torque versus mixing time curves for three classes of LLDPE/PVA (90/10) blends, viz. Case I-without any additives, Case II-with glycerol and Case III-with glycerol and vegetable oil. After 2 min, LLDPE melted leading to lower torque values from the initial high value. When PVA

was added to the molten LLDPE (after 2 min) torque showed a sudden increase due to the resistance offered by PVA in the LLDPE matrix. Later, the torque gradually dropped and reached a steady value as PVA melted (Case I). For Cases II and III containing glycerol with and without vegetable oil (added after addition of PVA) the equilibrium torque after addition of the additives is lower than that for Case I. Hence vegetable oil and glycerol act as a plasticizer and a higher degree of mixing occurs in the presence of these additives, vegetable oil showing a greater effect.

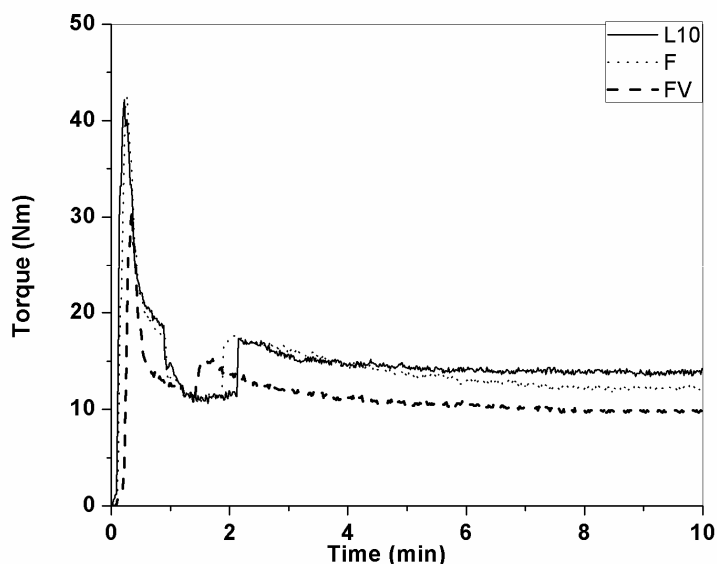


Fig. 4.1 Torque versus mixing time for LLDPE/PVA blends with or without glycerol and/or vegetable oil containing 10 %PVA.

SEM micrographs reveal that the interaction of PVA and LLDPE is improved (Fig.4.3) in the presence of both glycerol and vegetable oil. Unlike the LLDPE/PVA blend shown in Fig. 4.2 where the PVA appears to form separate domains, in the second micrograph, the PVA particles appear to be

better assimilated into the LLDPE matrix without any sharp boundary lines. Therefore, samples with glycerol (15w/w of PVA) and vegetable oil (1w/w of PE) were exclusively used for further investigations.

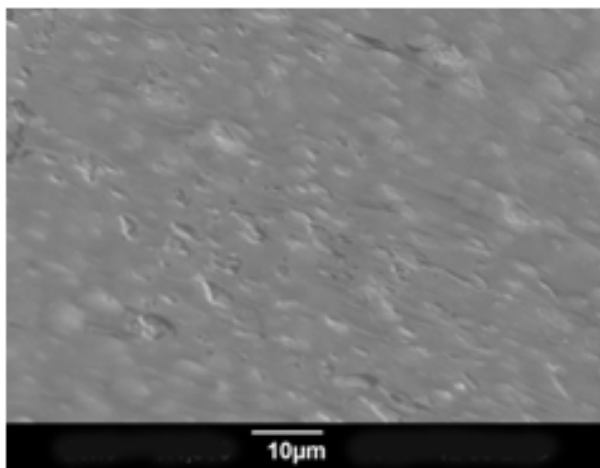


Fig. 4.2 SEM micrograph (1500X) of LLDPE/PVA blends without glycerol and vegetable oil

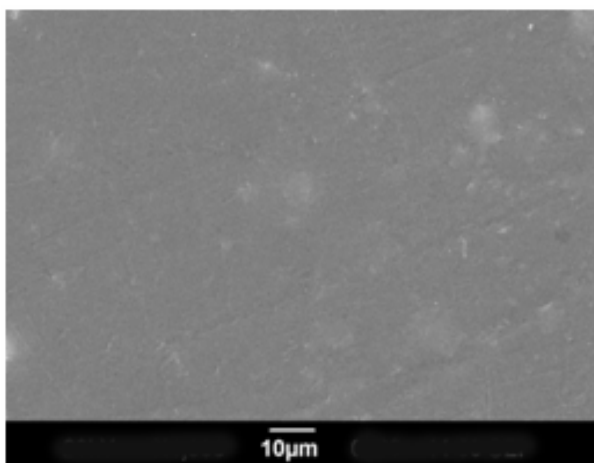


Fig.4.3 SEM micrograph (1500X) of LLDPE/PVA blends containing glycerol and vegetable oil

4.3.2 Effect of TiO₂

Fig.4.4 shows the effect of TiO₂ content (0.25-1%) on the tensile properties of LLDPE/PVA blends containing glycerol and vegetable oil. Three types of TiO₂ viz. rutile (R), anatase (A) and nanoanatase (nA) were employed for the study.

The tensile strength shows a steep rise on addition of 0.25% of TiO₂ irrespective of the type of TiO₂. But on addition of higher amounts, rutile and anatase give lower tensile strengths. Only nanoanatase showed a steady high value of tensile strength on addition of greater percentages. The lower particle size of true nanomaterial and a greater level of dispersion must be responsible for this.

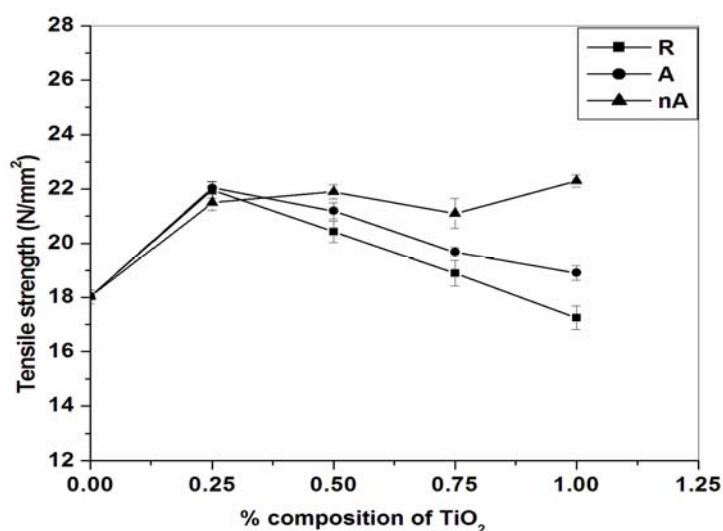
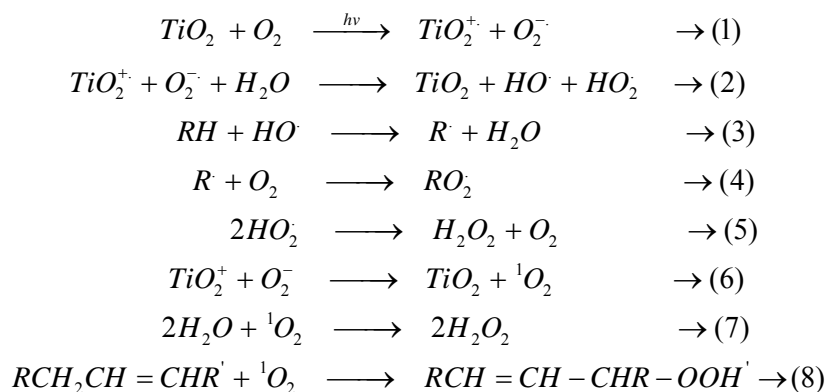


Fig.4.4 Variation of tensile strength of blend F with the addition of varying amounts of TiO₂

The mechanism of the transition metal catalyzed degradation of PE has been described in the literature as a free radical chain mechanism proceeding

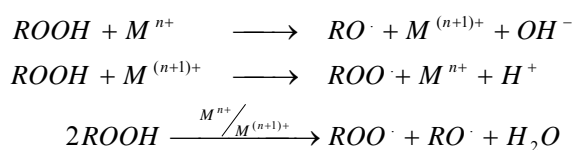
from the formation of hydro peroxides along the polymer backbone through reaction of the polymer with molecular oxygen [12-14] (Scheme 4.1). According to Albertsson [15], in the presence of metal catalyst, these peroxides are readily decomposed to form reactive intermediates. The catalytic activity of the metal was reported to correlate with the redox potential of the metal and requires several oxidation states of comparable energy for the metal. The peroxide decomposition products react further to yield volatile low molecular weight fragments.



Scheme 4.1 Catalysis of PE degradation by transition metal oxides [14]

The formation of the oxygen radical anion and, possibly, other excited state species, can occur via the electron transfer from excited state TiO_2 to molecular oxygen. These species can react with water to form perhydroxyl or hydroxyl radicals which may subsequently abstract a proton from the polymer and initiate degradation [14]. It has been suggested further that singlet oxygen may be produced in the presence of TiO_2 and this can react with water to produce hydrogen peroxide or, alternatively, it may attack unsaturated centres in the polymer to produce hydroperoxide species [14].

The presence of the metal compound will catalyse the hydroperoxide decomposition step of the oxidation mechanism. It is well known that metal compounds react further with the carboxylic acid groups according to the mechanisms shown in Scheme 4.2.



Scheme 4.2 Examples of reactions of metal catalysts with hydroperoxides [15]

4.3.3 Outdoor weathering studies and degradation by microorganisms

Figs. 4.5, 4.6 and 4.7 show the variation in tensile strength of the blends containing rutile, anatase and nanoanatase respectively. The tensile strength initially shows substantial improvement on addition of TiO₂ to the glycerol modified blend. All the cases to be discussed in subsequent sections refer to blends containing glycerol.

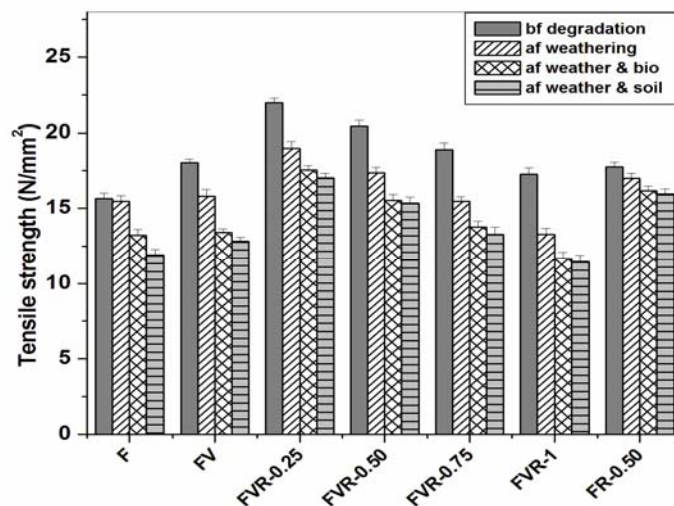


Fig.4.5 Variation of tensile strength of blends with the addition of varying amounts of commercial rutile

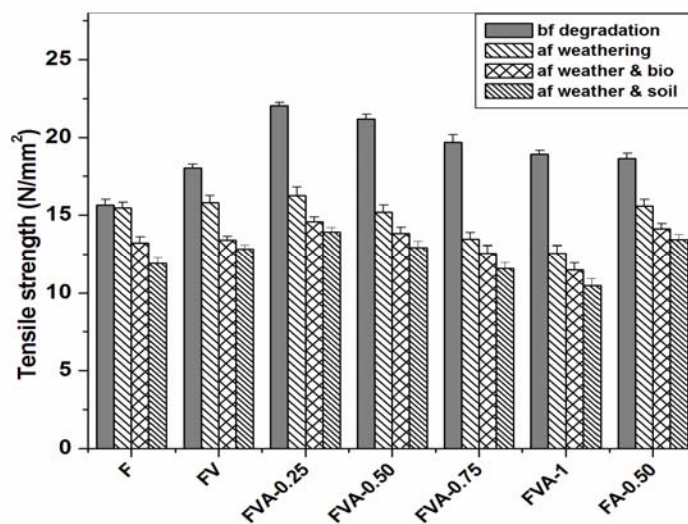


Fig.4.6 Variation of tensile strength of blends with the addition of varying amounts of commercial anatase

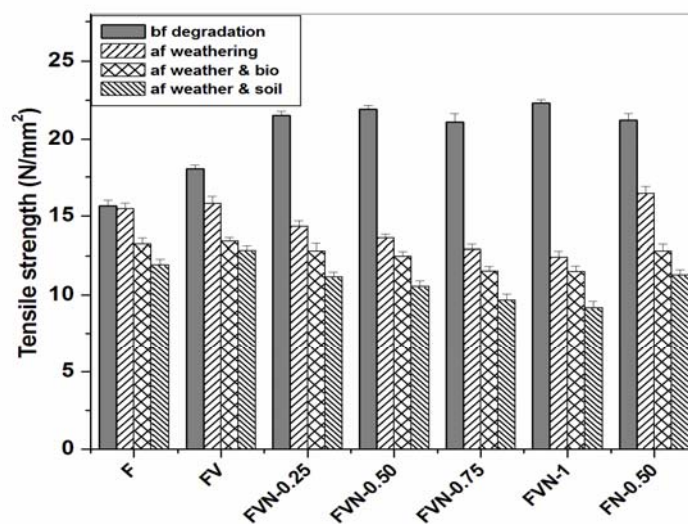


Fig.4.7 Variation of tensile strength of blends with the addition of varying amounts of nanoanatase

On weathering of the blends containing only TiO₂, the greatest reduction in tensile properties was observed in the case of samples containing the nano form of TiO₂. For the case of 0.50% of TiO₂ only (Fig.4.8 and Table-4.2), the tensile strength decreased by 4.28% for samples containing rutile (FR-0.50), 16.42% for anatase (FA-0.50) and 22.5% for nanoanatase (FN-0.50) after 600 hours of weathering. Although the three forms of TiO₂ (rutile, anatase and nanoanatase) played a significant role in promoting the photo-oxidative degradation of LLDPE films the decrease is greatest in the case of samples containing nanoanatase pigment.

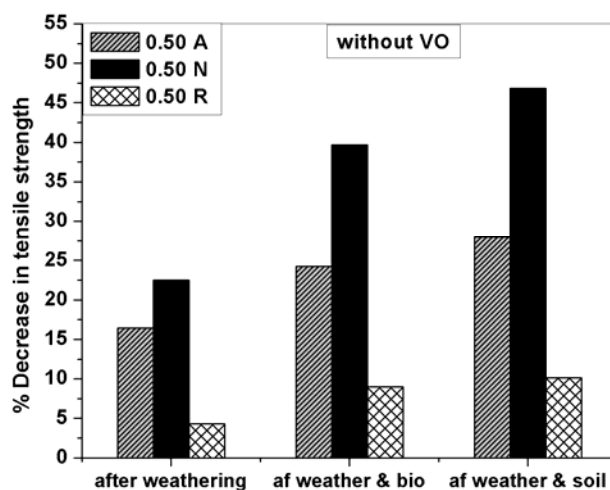


Fig.4.8 Percentage decrease in tensile strength of samples containing 0.50% of TiO₂ only

The samples containing a mixture of vegetable oil and TiO₂ (Fig.4.9) showed considerable decrease in tensile strength during outdoor exposure. The stiffness and brittleness of the materials increased considerably within a month of exposure time. We can see that there is a continued decrease in tensile

strength after biodegradation and soil degradation also. This effect is also more in the case of samples containing both TiO_2 and vegetable oil.

For the case of 0.50% of TiO_2 and vegetable oil, (Fig.4.9 and Table-4.2), the tensile strength decreased by 15.03% for samples containing rutile (FVR-0.50), 28.36% for anatase (FVA-0.50) and 37.89% for nanoanatase (FVN-0.50) which means that vegetable oil played a significant role in the degradation of LLDPE (Figs. 4.8 and 4.9). Vegetable oil undergoes auto-oxidation by which free radicals are generated. These, in turn, initiate oxidation of LLDPE.

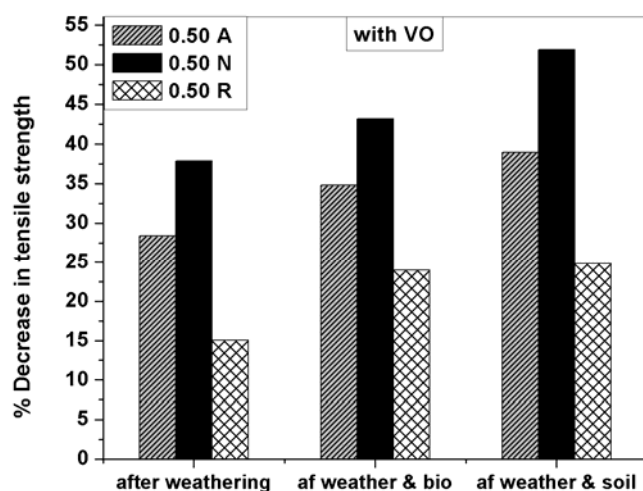


Fig. 4.9 Percentage decrease in tensile strength of samples containing 0.50% of TiO_2 and vegetable oil.

Table 4.2 Percentage decrease in tensile strength of the samples after weathering

Sample designation	Tensile strength (N/mm ²)		
	Before weathering	After weathering	% decrease
F	15.63	15.45	1.15
FV	18.03	15.79	12.42
FVR-0.25	21.97	18.98	13.61
FVR-0.50	20.42	17.35	15.03
FVR-0.75	18.89	15.45	18.21
FVR-1	17.25	13.27	23.07
FR-0.50	17.74	16.98	4.28
FVA-0.25	22.04	16.25	26.27
FVA-0.50	21.19	15.18	28.36
FVA-0.75	19.67	13.45	31.62
FVA-1	18.90	12.54	33.65
FA-0.50	18.63	15.57	16.42
FVN-0.25	21.5	14.32	33.39
FVN-0.50	21.9	13.6	37.89
FVN-0.75	21.1	12.9	38.86
FVN-1	22.3	12.4	44.39
FN-0.50	21.2	16.43	22.5

Outdoor exposure also affected the elongation of the blends (Figs. 4.10, 4.11 and 4.12) adversely. The elongation at break decreased for all samples containing vegetable oil as well as its combination with TiO₂, the rate being much higher in the case of samples containing the nano form of TiO₂. The decrease in elongation is basically due to increased degree of cross-linking with temperature, which finally leads to the embrittlement of the sample. The polymer chains take up oxygen and lead to the formation of hydroperoxide which breaks down to give oxygenated products. It should be mentioned that after six months of exposure it was not possible to test the films because these samples had physically broken down in the environment or did so during

handling. Further, effects like chalking, loss of gloss, embrittlement and flaking occurred for samples exposed to longer time periods.

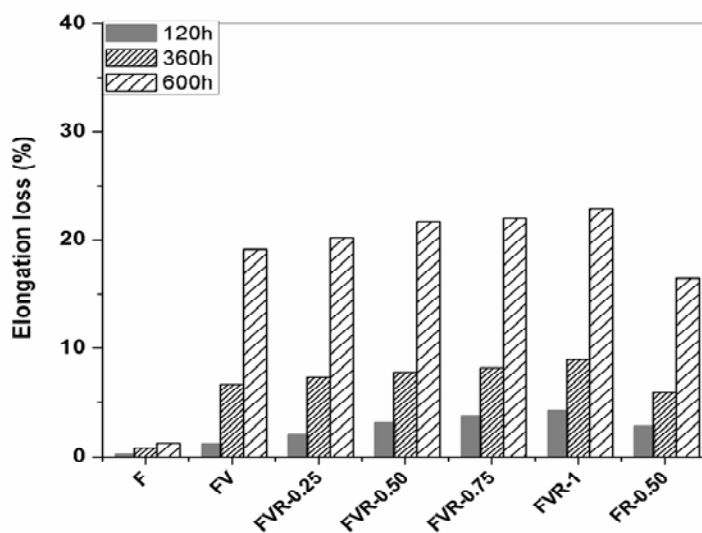


Fig. 4.10 Percentage elongation loss of the samples containing varying amounts of commercial rutile

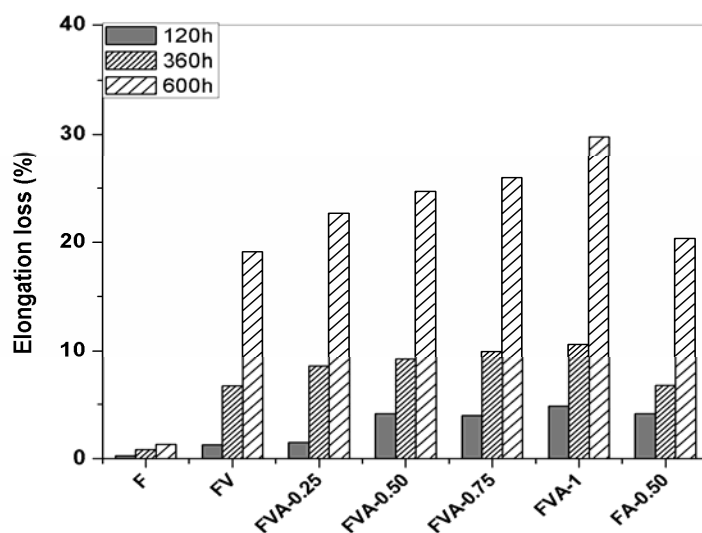


Fig. 4.11 Percentage elongation loss of the samples containing varying amounts of commercial anatase

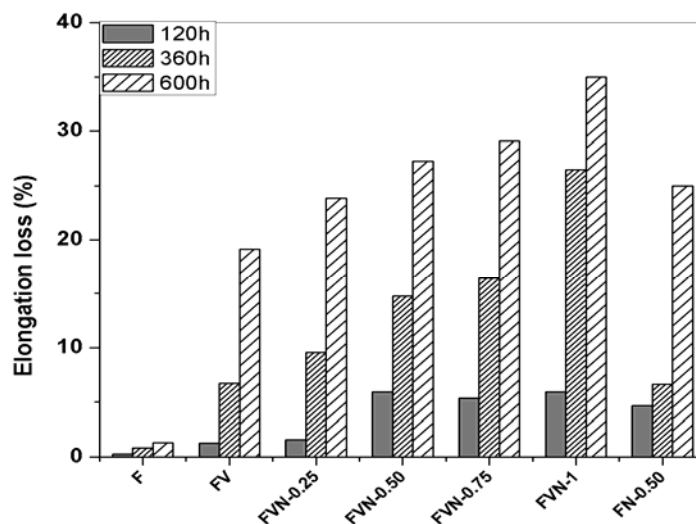


Fig.4.12 Percentage elongation loss of the samples containing varying amounts of nanoanatase

The percentage elongation loss of the samples after 600 hours of weathering is given in Table 4.3. For the case of 0.50% of TiO₂ only (Table-4.3), a maximum of 16.51% elongation loss is observed for samples containing rutile (FR-0.50), 20.36% for anatase (FA-0.50) and 24.98% for nanoanatase (FN-0.50). Here also the elongation loss is highest in the case of samples containing nanoanatase pigment.

For the case of 0.50% of TiO₂ and vegetable oil, (Table-4.3), a maximum of 21.74% elongation loss is observed for samples containing rutile (FVR-0.50), 24.66% for anatase (FVA-0.50) and 27.27% for nanoanatase (FVN-0.50) which means that vegetable oil played a significant role in the degradation of LLDPE.

Table 4.3 Percentage elongation loss of the samples after weathering

Sample designation	Elongation loss (%)
F	1.32
FV	19.14
FVR-0.25	20.22
FVR-0.50	21.74
FVR-0.75	22.03
FVR-1	22.91
FR-0.50	16.51
FVA-0.25	22.67
FVA-0.50	24.66
FVA-0.75	25.93
FVA-1	29.77
FA-0.50	20.36
FVN-0.25	23.85
FVN-0.50	27.27
FVN-0.75	29.10
FVN-1	34.97
FN-0.50	24.98

The discolouration of the samples shown in Fig. 4.13 provides a good indication of the photo-oxidative degradation. This is similar to the results reported by Sastry et.al [16] and Sharma et.al [17].

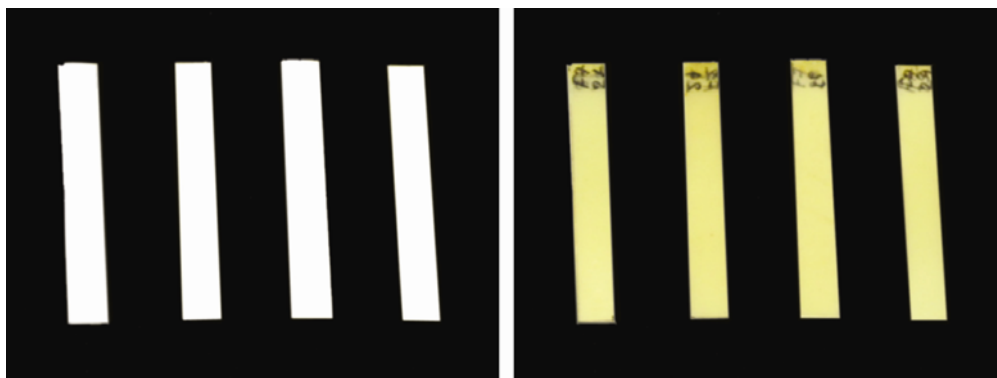


Fig. 4.13 Discoloration of the samples after 600 hours of outdoor exposure

4.3.4 Spectroscopic studies

Figs. 4.14 to 4.19 show FTIR spectra of samples containing 0.50% of rutile, anatase or nanoanatase each before weathering as well as after weathering in the absence as well as presence of vegetable oil.

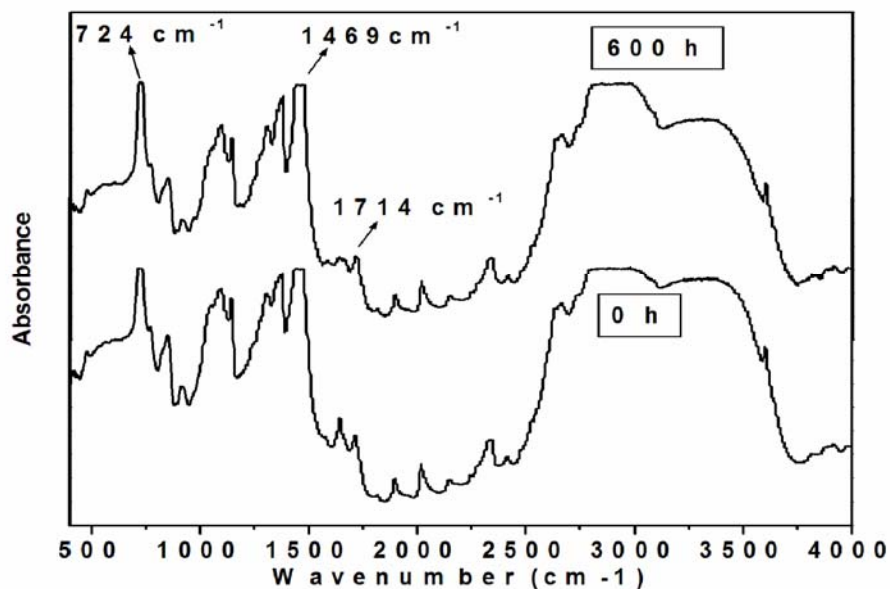


Fig. 4.14 FTIR spectra of samples containing 0.50% of rutile only

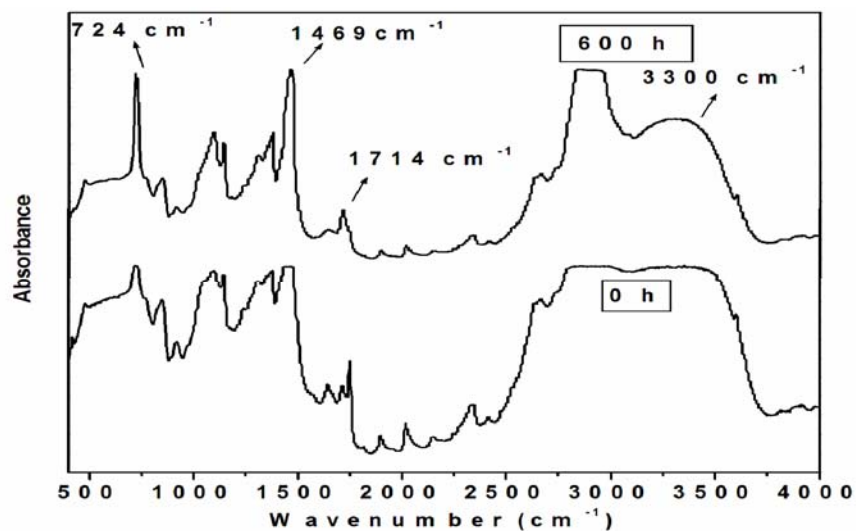


Fig. 4.15 FTIR spectra of samples containing vegetable oil and 0.50% of rutile

From the figures it can be seen that the absorption band around 1714 cm^{-1} which can be assigned to the C=O stretching vibration of a keto group, grows in intensity with extended outdoor exposure. A broadening of the band at this point indicates the formation of more than one oxidation product. Hence these carbonyl bands can be assigned to C=O stretching vibrations arising from aldehydes and/or esters (1733 cm^{-1}), carboxylic acid groups (1700 cm^{-1}) and γ -lactones (1780 cm^{-1}) [18-21]. The absorption band around 720 cm^{-1} and 1469 cm^{-1} also increases in intensity. These bands correspond to the characteristic absorption of the crystalline and amorphous bands and bending vibrations of C-H bonds. The increase in intensity of these peaks was owing to the fracture of the polyethylene chain in degradable environments. Increase in intensity is maximum in the case samples containing both nano-TiO₂ and vegetable oil.

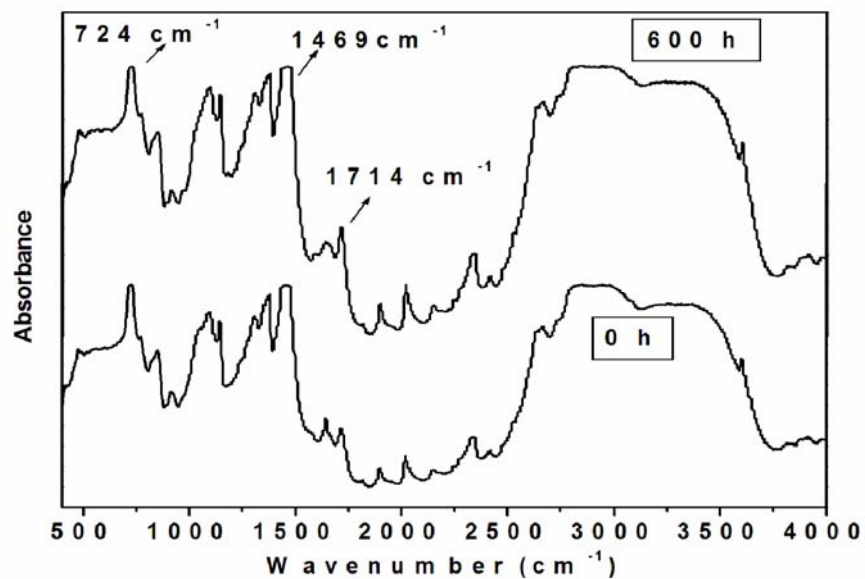


Fig. 4.16 FTIR spectra of samples containing 0.50% of anatase only

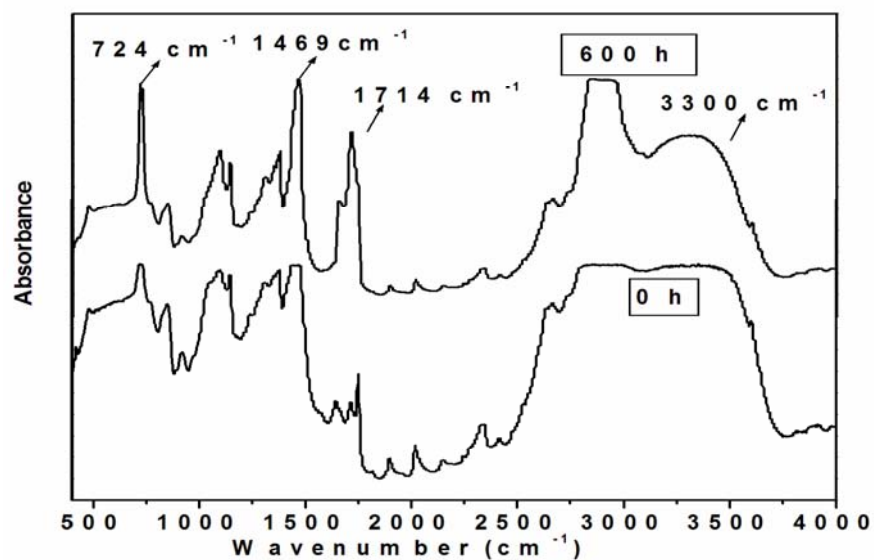


Fig.4.17 FTIR spectra of samples containing vegetable oil and 0.50% of anatase

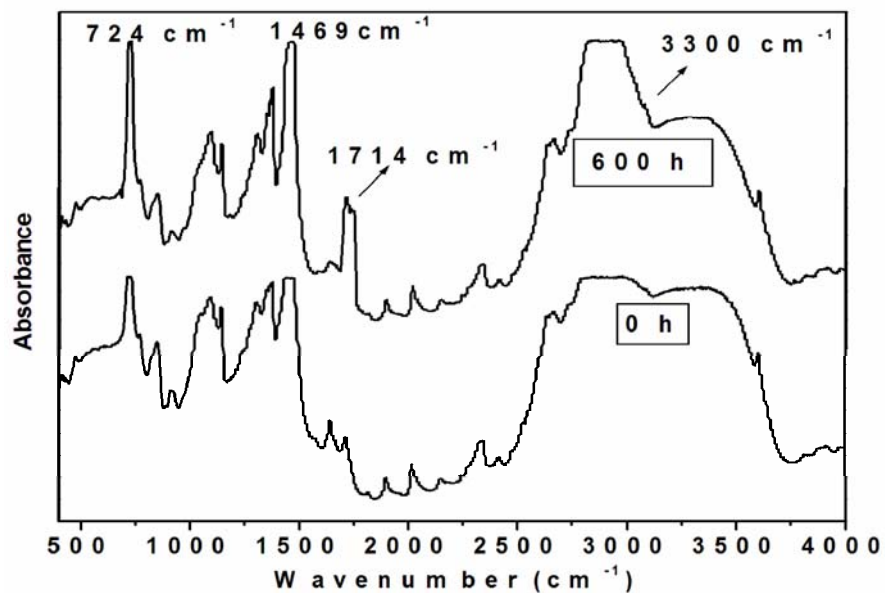


Fig.4.18 FTIR spectra of samples containing 0.50% of nanoanatase only

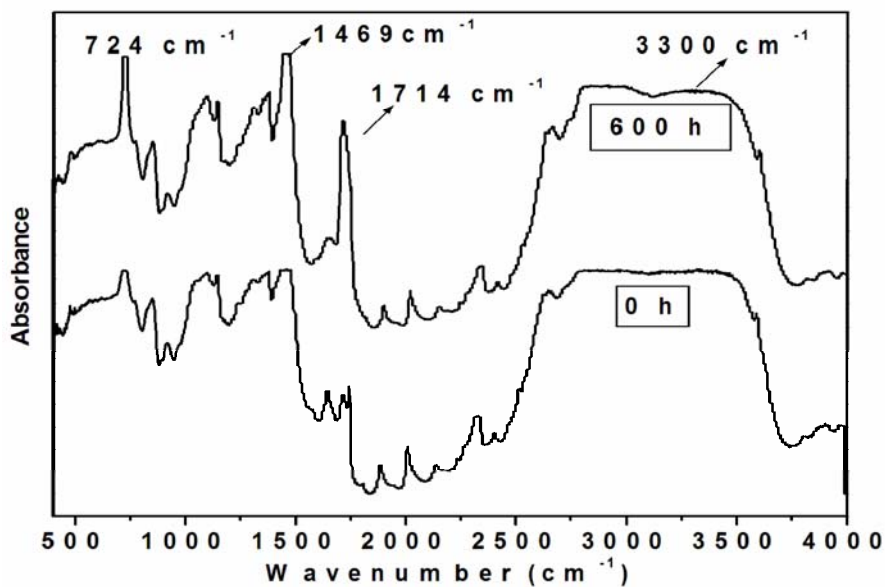


Fig.4.19 FTIR spectra of samples containing vegetable oil and 0.50% of nanoanatase

Fig. 4.20 depicts the variation of carbonyl index value as a function of exposure time for LLDPE/PVA samples containing varying amounts of TiO₂ in the presence as well as absence of vegetable oil. The carbonyl index, defined as the ratio between the integrated band absorbance of the carbonyl around 1714 cm⁻¹ and that of the PE-Polymer bands characterizes the degree of oxidation for each polyethylene sample. Moderate extents of photo-oxidation of PE are known [22-24] to result in accumulation of carbonyl functionalities in polymer. After the initial stage of photo-oxidation, results reported in the literature show the accumulation of carbonyl groups in PE to be auto accelerating.

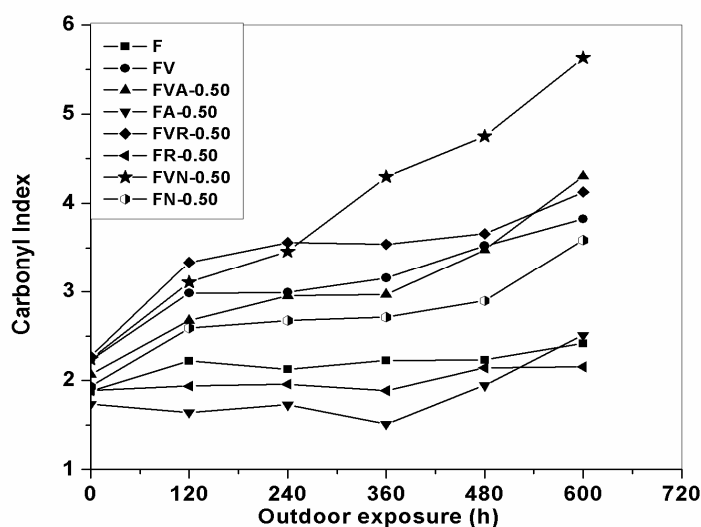


Fig. 4.20 Variation of carbonyl index value as a function of exposure time

Fig. 4.21 shows the percentage increase in carbonyl index (CI) of the samples with exposure time for various cases. Samples containing nanoanatase have a higher carbonyl index compared to samples containing commercial rutile and anatase, indicating a faster rate of carbonyl builds up in the former case. The presence of nano TiO₂ presumably accelerated the atmospheric oxidation of the samples.

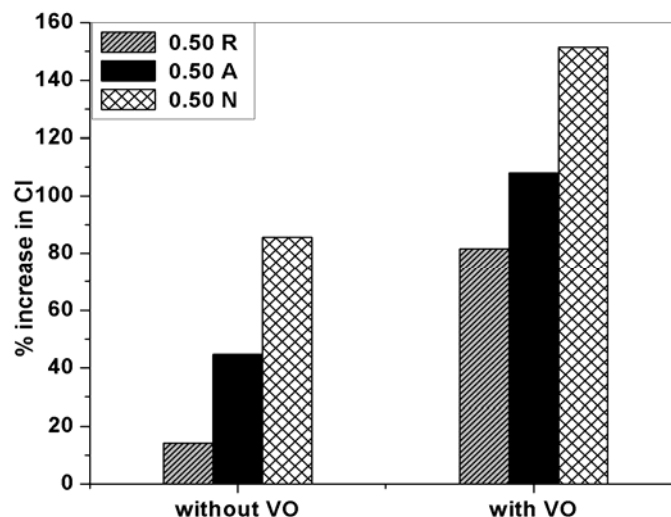


Fig.4.21 The percentage increase in carbonyl index (CI) of the samples containing 0.50% TiO₂ after weathering in the presence and absence of vegetable oil

In the case of samples containing 0.50% of TiO₂ only, CI increased by 14.2% for sample containing rutile (FR-0.50), 44.67% for sample containing anatase (FA-0.50) and 85.66% for sample containing nanoanatase (FN-0.50). This means that all the three forms of TiO₂ (rutile, anatase and nanoanatase) promote the photo-oxidative degradation of LLDPE films, nanoanatase being outstanding.

In the case of samples containing 0.50% TiO₂ and vegetable oil, the CI increased by 81.60% for sample containing rutile (FVR-0.50), 107.97% for sample containing anatase (FVA-0.50) and 151.41% for sample nanoanatase (FVN-0.50). This means that vegetable oil also plays a significant role in the degradation of LLDPE. This is more clearly understood from the Figs. 4.20 and 4.21.

Pro-oxidants like vegetable oil promote photooxidation. During photo-oxidation process, auto-oxidation of the chain takes place resulting in the

formation of free radicals. Samples containing only vegetable oil show considerable photoactivity, sometimes superior to those containing additionally rutile/anatase. Most commercial TiO₂ grades are known to have a stabilizing effect on polymers exposed to light [14]. This is the reason why compositions containing both vegetable oil and commercial rutile/anatase show only moderate photodegradation. Here, the pro-oxidant activity of vegetable oil is somewhat offset by these substances. However, the nano form of anatase shows significant photoactivity far superior to the other cases.

MFI which is related to molecular weight was also determined for all the formulations at 190^oC under a load of 2.16kg as per ASTM D 1238-01. The increase in MFI as a result of outdoor exposure is quantified in Table 4.4. From the table it can be seen that the increase in MFI is highest in the case of samples containing the nano form of TiO₂. In this case, MFI has shown an increase of 6.8 over the nondegraded sample. It is noteworthy that nanoanatase even in the absence of vegetable oil leads to substantial increase of 6.7 in MFI.

Table 4.4 Effect of outdoor exposure on MFI of the samples containing 0.50% TiO₂

Sample designation	MFI(g/10 min with a 2.16kg load)	
	Before Exposure	After Exposure (600h)
F	0.8	1.0
FV	1.0	2.0
FVR-0.50	0.9	3.5
FR-0.50	0.9	3.2
FVA-0.50	0.9	5.1
FA-0.50	0.9	4.8
FVN-0.50	0.9	7.7
FN-0.50	0.9	7.6

4.3.5 Thermal studies

Referring to Figs. 4.22 to 4.24 which show DSC scans, the weathering and biodegradation process led to a slight broadening of the polyethylene melting endotherm. This resulted in increased ΔH_f values. LLDPE is a semicrystalline polymer in which both crystalline and amorphous regions coexist. Due to the gradual depletion of the amorphous phase, the crystallinity of the samples increased. This increase could also be partially attributed to the changes in the crystallite sizes, molecular weight differences that were brought about by chain breaking and secondary recrystallization [25]. The broadening of the peaks is more noticeable in the case of samples containing nanotitania. Since the amorphous form is more prone to degradation the increasing percentage of crystalline material and consequently the endothermic heat of melting is an indication of a greater level of degradation. Preferential degradation in the amorphous regions of the blends is observed both in the case of photo-oxidation and subsequent biodegradation.

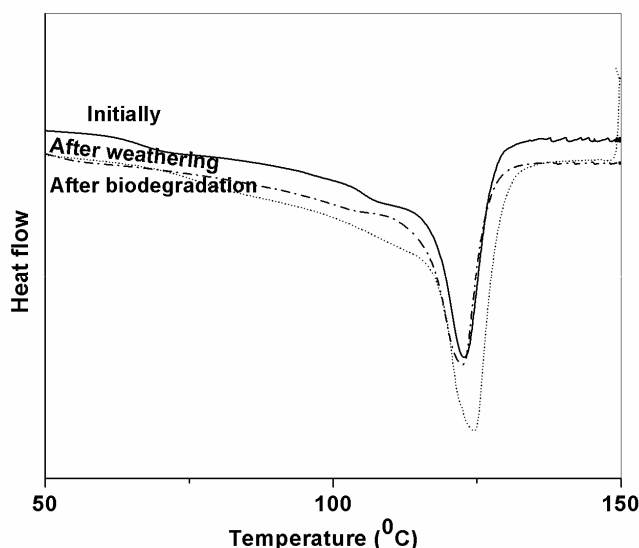


Fig. 4.22 The heating scans of samples containing commercial rutile

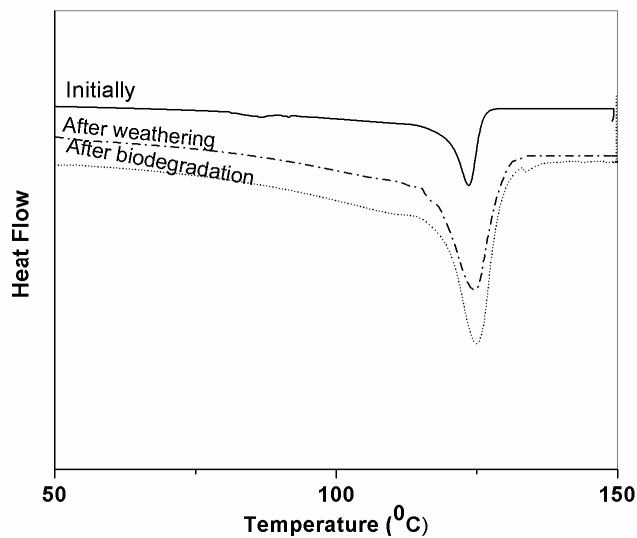


Fig. 4.23 The heating scans of samples containing commercial anatase

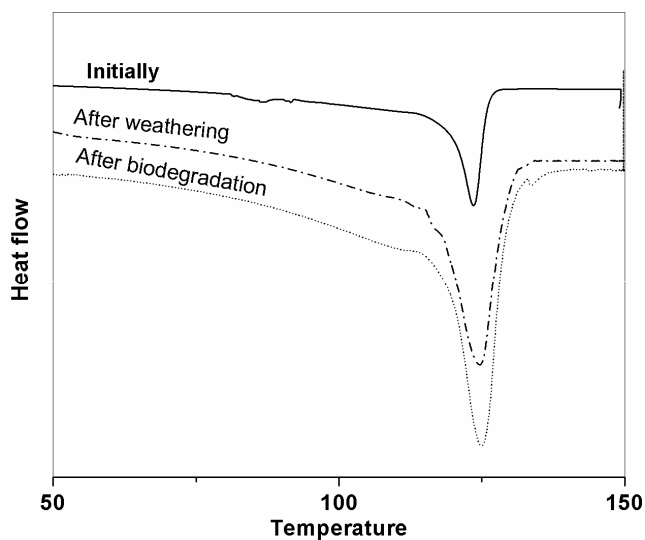


Fig. 4.24 The heating scans of samples containing nanoanatase

4.3.6 Percentage weight loss

Table 4.5 shows the weight loss of the samples during outdoor weathering. The weight loss rate was much higher for samples containing nanoanatase and

vegetable oil than for commercial forms of TiO₂. The weight loss data indicate that the photocatalytic degradation of films led to bond scission producing a mass of volatile intermediates.

Table 4.5 Percentage weight loss of the samples after weathering (600h), biodegradation (15 weeks) and soil degradation (15 weeks)

Sample designation	% Weight Loss		
	Weathering	Biodegradation	Soil degradation
F	8.14	3.21	5.85
FV	11.31	4.01	6.15
FVR-0.50	23.62	6.22	7.98
FR-0.50	20.83	4.35	6.15
FVA-0.50	32.16	10.78	13.36
FA-0.50	29.27	8.15	11.91
FVN-0.50	44.67	15.62	18.13
FN-0.50	41.34	13.84	15.28

4.3.7 Morphological studies

The SEM micrographs of the samples after weathering are shown in Figs. 4.25 to 4.30. The surface of the samples before degradation was smooth without cracks or holes and free of any kind of defects. After weathering, the samples containing pro-oxidants appear to have numerous cracks. On subsequent biodegradation/soil degradation, cavities are seen all over the surface indicating microbial activity. Although these cavities suggest massive degradation it must be noted that the extent of degradation as estimated by weight loss and loss of mechanical properties is much higher in the case of photo degradation. This is especially so in the case of samples containing nanoanatase and vegetable oil. These samples show crater-like cavities. It can be assumed that the greater the

extent of photo degradation, greater the extent of subsequent biodegradation. Weathering leads to physical embrittlement of the PE, leaving a porous and mechanically weakened plastic. This accelerates the degradation of PE by diffusion of oxygen, moisture, and enzymes into the porous PE matrix. In a combined degradation process involving photo and biodegradation the bulk of the degradation is found to occur during photo degradation.

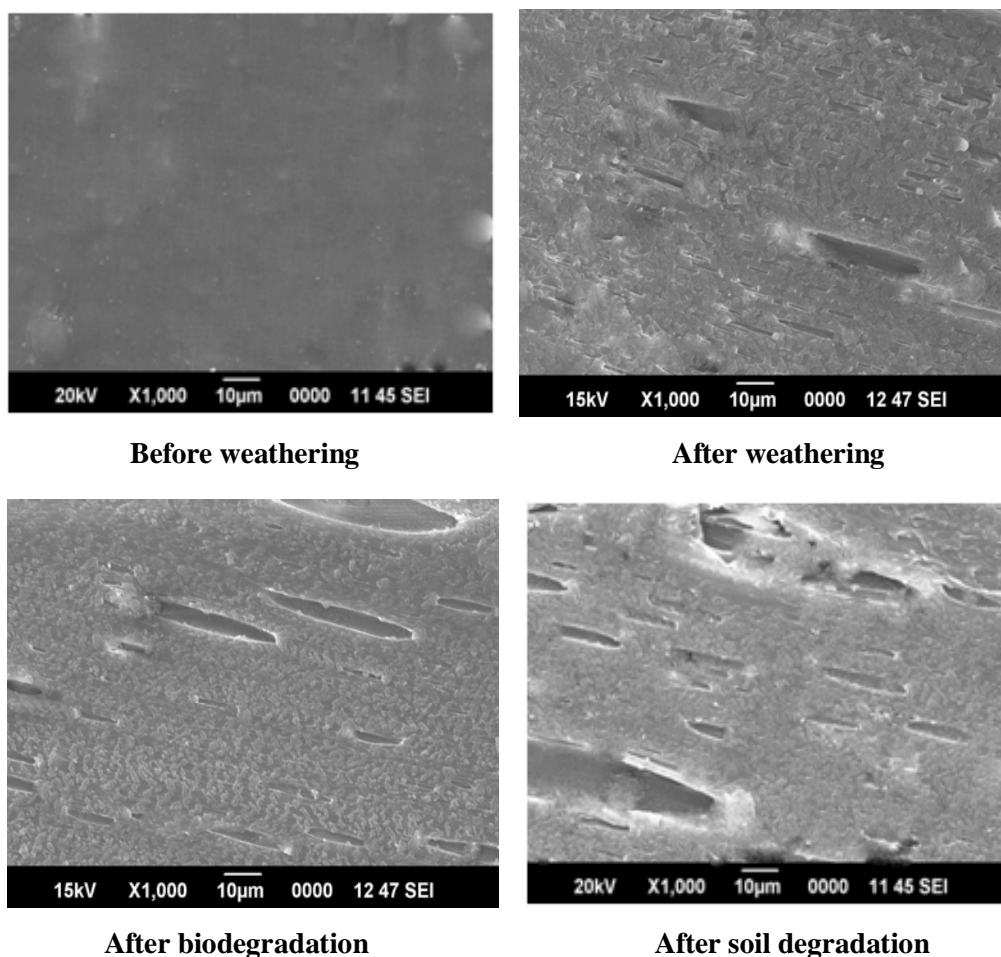


Fig. 4.25 Scanning electron micrographs of LLDPE/PVA blends with rutile only

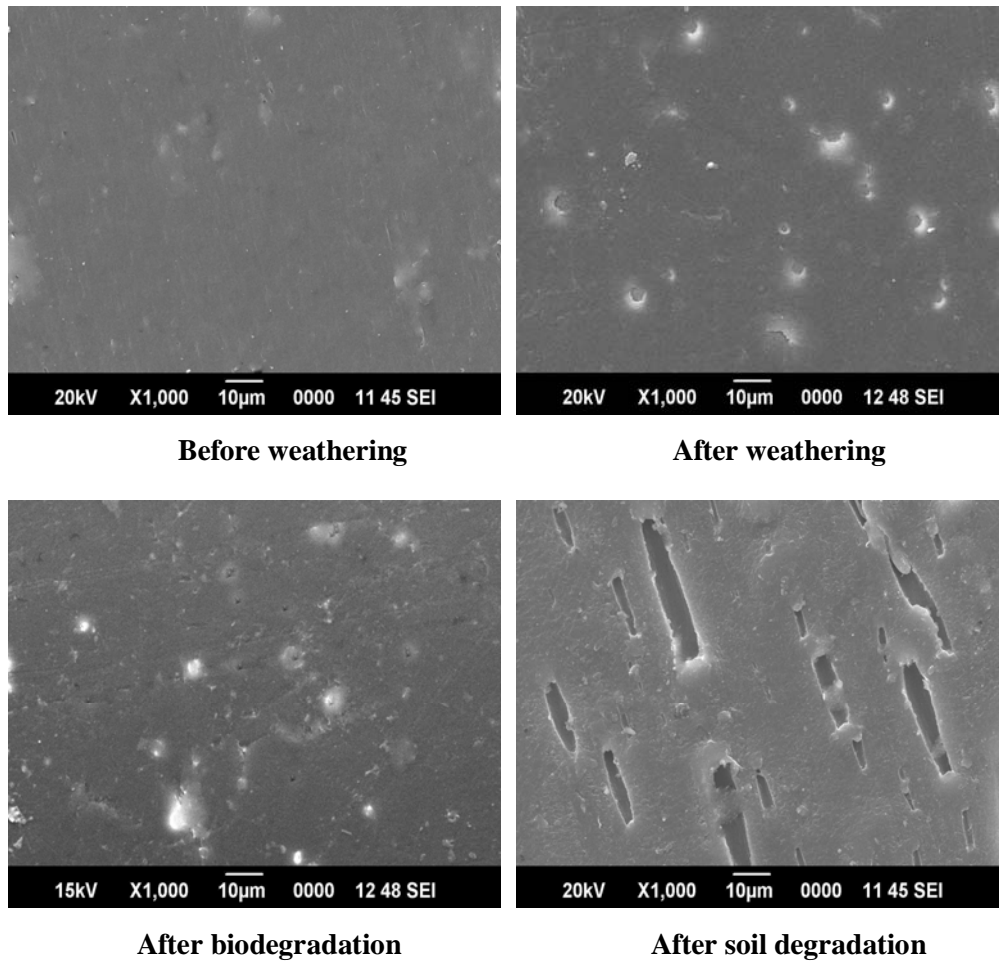


Fig.4.26 Scanning electron micrographs of LLDPE/PVA blends with rutile and vegetable oil

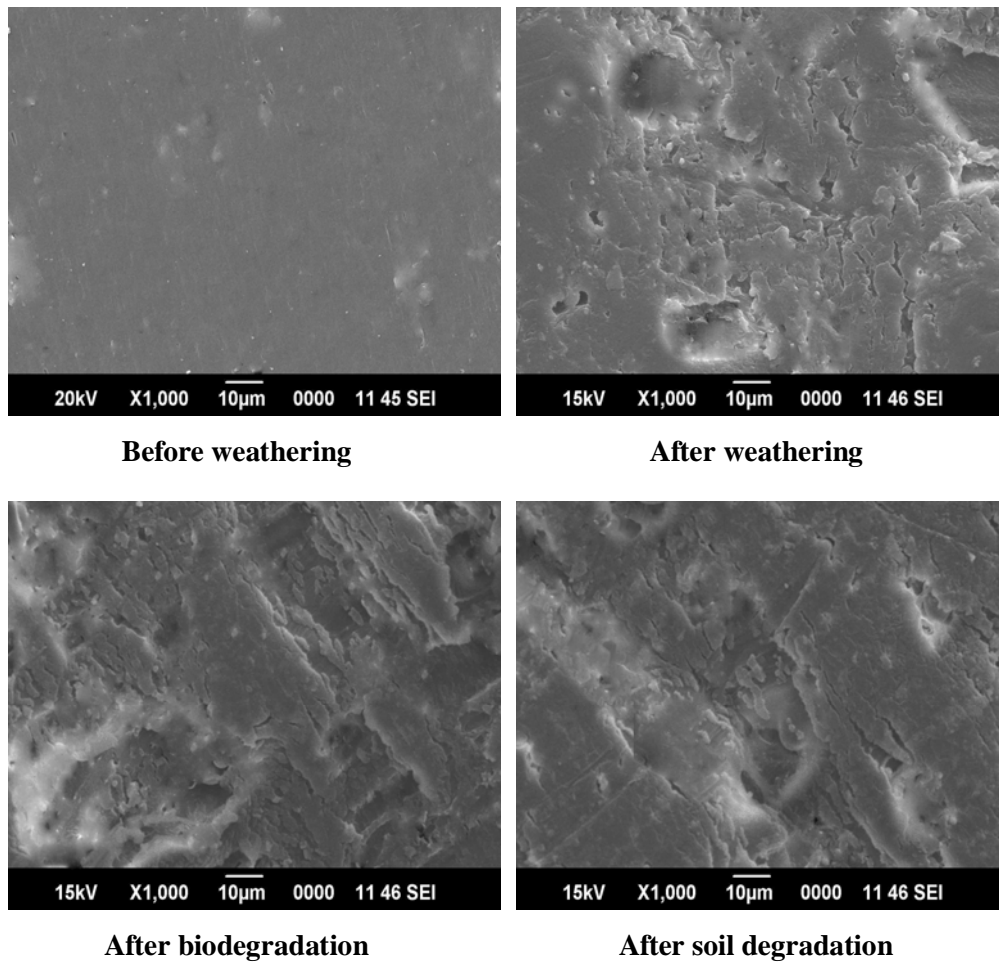


Fig.4.27 Scanning electron micrographs of LLDPE/PVA blends with anatase only

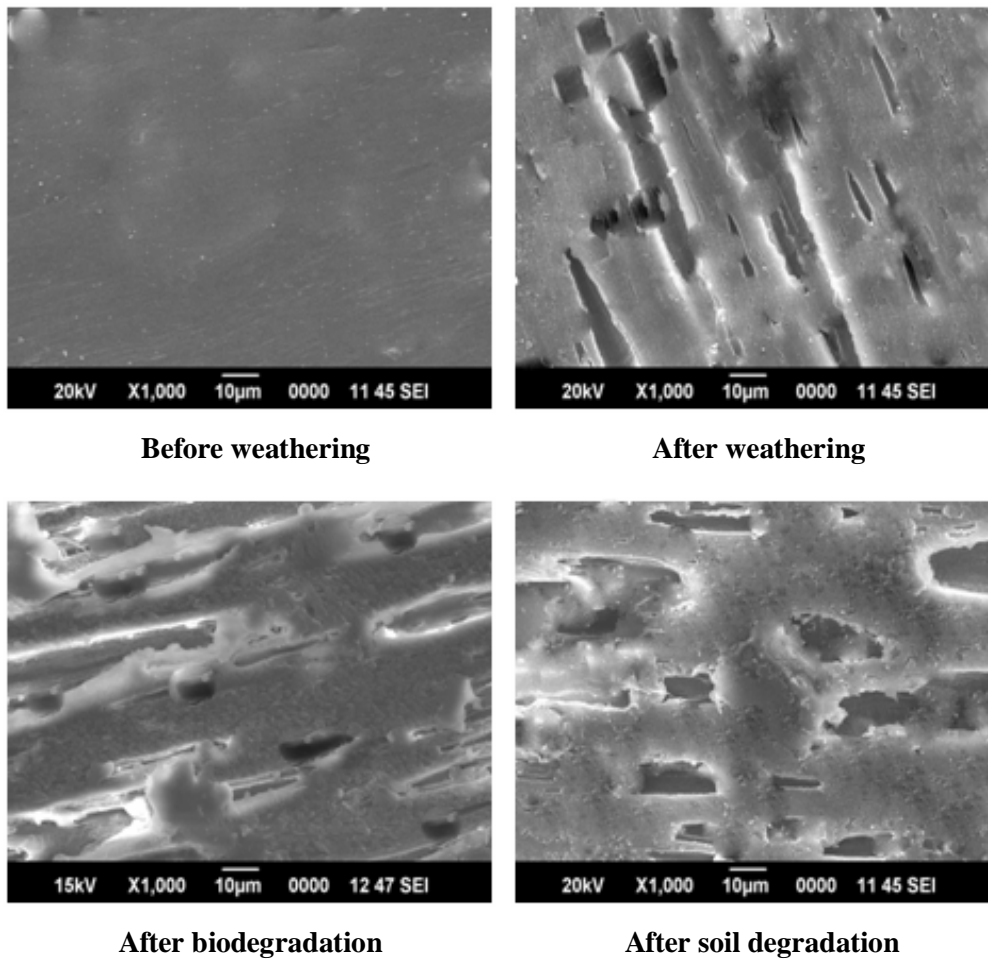


Fig. 4.28 Scanning electron micrographs of LLDPE/PVA blends with anatase and vegetable oil

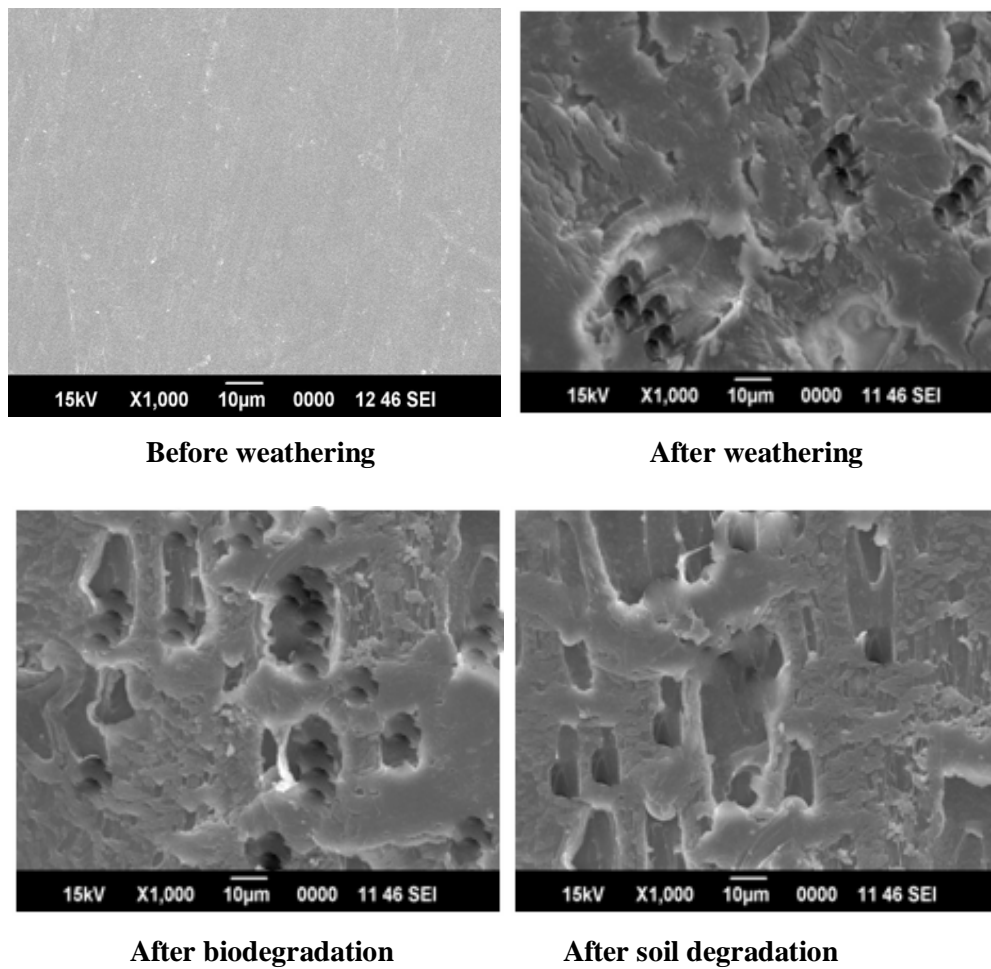


Fig.4.29 Scanning electron micrographs of LLDPE/PVA blends with nanoanatase only

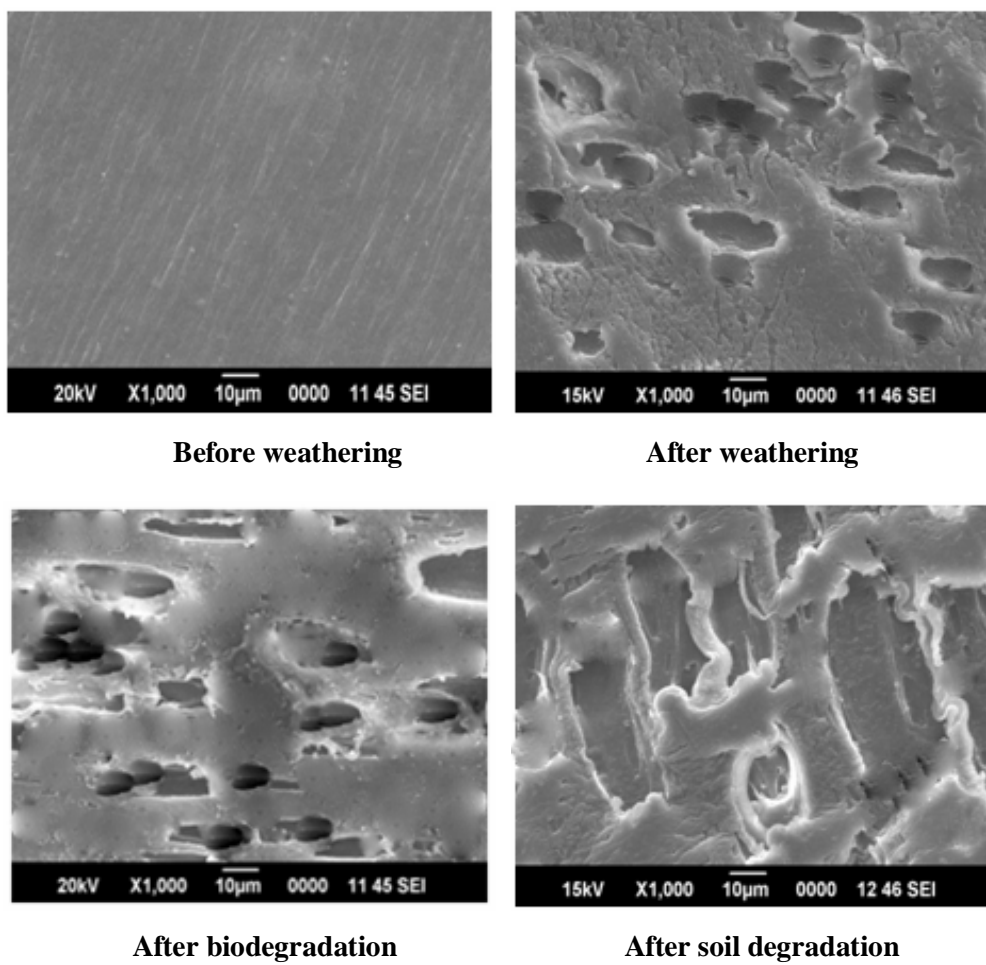


Fig.4.30 Scanning electron micrographs of LLDPE/PVA blends with nanoanatase and vegetable oil

SEM images suggest that the degradation of PE matrix starts from PE-TiO₂ interface and leads to the formation of cavities around TiO₂ particle aggregates [26]. It is understood that active oxygen species generated on TiO₂ surface diffuse to etch out the polymer matrix. Examination of the micrographs shows numerous holes in the film which scatter light and cause whitening. This indicates that in the vicinity of the titania the polymer gets totally degraded to water and carbon dioxide or other volatile substances. Loss of pigment particles from degraded polymers containing titania has been attributed to erosion of the polymer due to photo-catalysis [27]. Both photo- and UV-degradations lead to physical embrittlement of the PE, leaving a porous and mechanically weakened plastic. This will accelerate the degradation of the PE by diffusion of oxygen, moisture, and enzymes into the porous PE matrix. The photosensitised oxidation of commercial polyolefins by white pigments, such as TiO₂ and ZnO, occurs at the surface of the material. The polymer gradually erodes away leaving the pigment exposed. This phenomenon is commonly referred to as ‘chalking’ [28].

4.4 Conclusions

- Miscibility of PVA and LLDPE is improved in the presence of both glycerol and vegetable oil.
- Unlike the LLDPE/PVA blend where the PVA appears to form separate domains, the PVA particles appear to be better assimilated into the LLDPE matrix without any sharp boundary lines in the presence of both glycerol and vegetable oil.
- The incorporation of TiO₂ as the key pro-degradant has increased the rate of degradation tremendously.

- Vegetable oil is also capable of accelerating the oxidation of LLDPE/PVA blends during weathering.
- A greater extent of oxidation was observed during weathering, primarily due to TiO₂, in the case of compositions containing a combination of TiO₂ and vegetable oil.
- The pro-oxidant activity is maximum in the case of samples containing nanoanatase particles and vegetable oil.
- The discolouration of the samples provides an indication of the photo-oxidative degradation of the sample.
- The pores seen in scanning electron micrographs are an indication of degradation

4.5 References

- [1] H. Qin, C. Zhao, S. Zhang, G. Chen, M. Yang; Polym. Degrad. Stab. **2003**, 81, 497.
- [2] X. Zhao, Z. Li, Y. Chen, L. Shi, Y. Zhu; Journal of Molecular Catalysis A: Chemical, **2007**, 268, 101.
- [3] Fujishima, T.N. Rao, D.A. Tryk; J.Photochem. Photobiol. C Photochem. Rev. **2000**, 1, 1.
- [4] N.S. Allen, M.Edge, A.Otega, G. Sandoval, C.M. Liauw, J. Verran, J. Stratton, R.B.McIntyre; Polym.Degrad. Stab. **2004**, 85, 927.
- [5] J. H. Braun; Progress in Organic Coatings, **1987**, 15, 249.
- [6] E. F. Petrushenko, P. S. Vakanyan, V. A. Pakhrenko; Plast. Massy. **1988**, 11, 23.
- [7] Famili, L. M. Robeson, J. F. Nangeroni; U.S Patent 5369168.

- [8] E. N. Frankel; Pray. Lipid Res. **1980**, 19, 1.
- [9] ASTM D 1435 – 99 Practice for Outdoor Weathering of Plastics
- [10] W. Sung, Z. L. Nikolov; Ind. Eng. Chem. Res. **1992**, 31, 2332.
- [11] C. Albertson, S. V. Anderson, S. Karlsson; Polym. Degrad. Stab. **1987**, 18, 73.
- [12] D. J. Carlsson, D. M. Wiles; Macromolecules. **1971**, 4, 179.
- [13] M. U. Amin, G. Scott; Eur. Polym. J. **1973**, 9, 219.
- [14] N. S. Allen, Degradation and Stabilisation of Polyolefins, Applied Science Publishers, New York, London, **1983**.
- [15] C. Albertsson, C. Benenstedt, S. Karlsson; J. Appl. Polym. Sci. **1994**, 51, 1097.
- [16] P. K. Sastry, D. Satyanarayana, D. V. M. Rao; J. Appl. Polym. Sci. **1998**, 70, 2251.
- [17] N. Sharma, H. Ismail, U. S. Ishiaku, Z. A. M. Ishak; 2nd Colloquium on Lignocellulose 99. Penang (Malaysia), Universiti Sains Malaysia, **1999**.
- [18] F. Khabbaz, A. C. Albertsson, S. Karlsson; Polym. Degrad. Stab. **1998**, 61, 229.
- [19] R. Setnescu, S. Jipa, Z. Osawa; Polym. Degrad. Stab. **1998**, 60, 377.
- [20] F. Khabbaz, A. C. Albertsson, S. Karlsson; Polym. Degrad. Stab. **1999**, 63, 127.
- [21] Valadez-Gonzalez, J. M. Cervantes-Uc, L. Veleza; Polym. Degrad. Stab. **1999**, 63, 253.
- [22] G. Scott; J. Polym. Sci. Symp. **1976**, 57, 357.
- [23] M. U. Amin, G. Scott, L. M. K. Tillekeratne; Eur. Polym. J. **1975**, 11, 85.
- [24] G. Scott; Chem. Soc. Div. Org. Coat. Plast. Chem. Prepr. **1975**, 35, 163.
- [25] P. K. Roy, P. Surekha, C. Rajagopal, V. Choudhary; J. Appl. Polym. Sci. **2008**, 108, 2726.

- [26] Z. Xu, L. Zongwei, C. Yi, S. Liyi, Z. Yongfa; Applied Surface Science. **2008**, 254, 1825.
- [27] N. S. Allen, M. Edge, J. Verran, J. Stratton, J. Maltby, C. Bygott; Polym Degrad. Stab. **2008**, 93, 1632.
- [28] G. Kaempf, W. Papenroth, R. Holm; J. Paint Technol. **1974**, 46, 56.

.....❧.....

EFFECT OF PRO-OXIDANT ACTIVITY OF TiO₂ ON THE UV AND BIODEGRADATION OF LLDPE/PVA BLENDS

Contents	5.1	<i>Introduction</i>
	5.2	<i>Experimental</i>
	5.3	<i>Results and discussion</i>
	5.4	<i>Conclusion</i>
	5.5	<i>References</i>

5.1 Introduction

Some additives and impurities may catalyze the breaking of polymer chains by a series of UV-initiated free radical reactions [1]. In polyolefins, the effect of UV-rays on the formation of chemical functional groups and their role in polymer chain breaking has been widely reported [2]. Photo-oxidation leads to an increase in the low molecular weight fraction by chain scission, thereby facilitating subsequent biodegradation [3]. It also leads to an increase in the surface area through increased porosity. In addition, the formation of carbonyl groups on the surface increases its hydrophilicity. Consequently, the possibility of further degradation and ultimate mineralization of plastic material is enhanced [4].

Due to characteristics such as low cost, photo stability, non-toxicity, and high-reactivity, TiO₂ has been generally regarded as the best photocatalyst [5]. In addition to the ability to scatter efficiently all the wavelengths of visible radiation, titanium dioxide pigments show strong absorption of UV, for rutile,

below 400 nm and anatase, below 370 nm. The absorbed UV radiation releases electrons and positive holes in the titanium dioxide crystals, some of which diffuse to the surface, resulting in the production of free radicals-hydroxy, peroxy, singlet oxygen, etc. These, in turn, can attack the polymer causing photo-oxidation and leading to photocatalytic degradation [6, 7]. Surprisingly TiO₂ also acts as a photostabilizer under certain conditions when appropriate grades of TiO₂ are used [8].

In this chapter, LLDPE/PVA films containing commercial and nano forms of TiO₂ and/or vegetable oil were prepared and photocatalytic degradation under ultraviolet light was investigated followed by biodegradation and soil degradation.

5.2 Experimental

5.2.1 Materials and sample preparation

The materials used and the methods adopted for the preparation of test samples were described in Chapter 4

5.2.2 Photo-degradation procedure

Samples were UV-irradiated using a low pressure mercury vapor discharge lamp (TUV 30W, $\lambda = 253.7\text{nm}$) in air atmosphere at room temperature. Samples were mounted on racks positioned 5cm from the lamps and the temperature in the cabinet was maintained at $30\pm 2^\circ\text{C}$. Sampling was carried out at regular intervals of 120, 240, 360, 480, and 600 hours, respectively, and the degradation was monitored by various techniques. TiO₂ photocatalyst absorbs only UV light ($\lambda < 387\text{ nm}$); thus only UV-light plays a role in the solar degradation of PE-TiO₂ composites.

The UV-degraded samples were then subjected to bio and soil-degradation studies as described in Chapter-4.

5.2.3 Evaluation of extent of degradation

The methods adopted for evaluating the extent of degradation are described in Chapter 4

5.3 Results and discussion

5.3.1 UV degradation studies and degradation by microorganisms

Figs. 5.1, 5.2 and 5.3 show the variation in tensile strength of the blends containing rutile, anatase and nano-anatase respectively. The tensile strength shows substantial improvement on addition of TiO₂ to the glycerol modified blend.

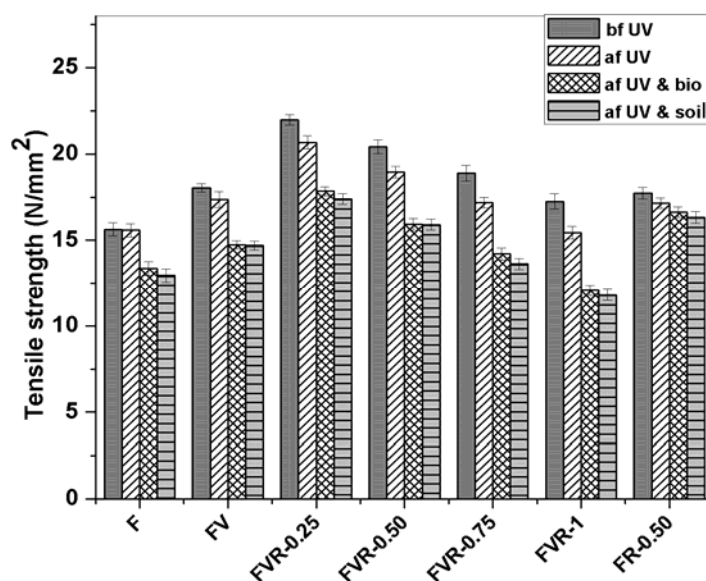


Fig.5.1 Variation of tensile strength of blends with the addition of varying amounts of commercial rutile

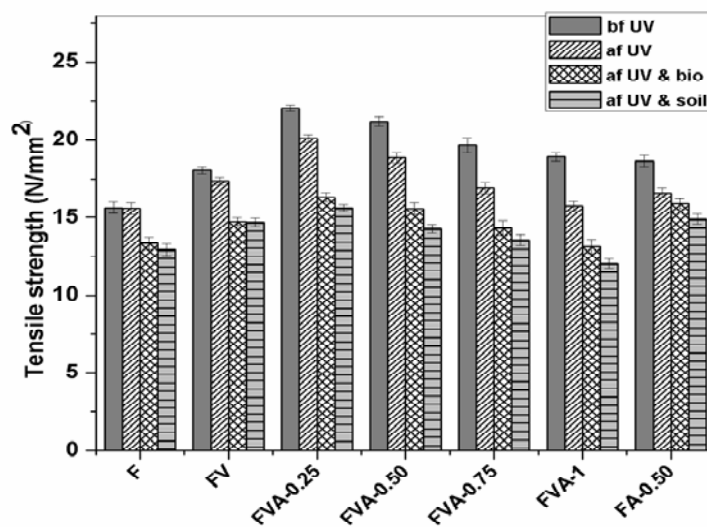


Fig.5.2 Variation of tensile strength of blends with the addition of varying amounts of commercial anatase

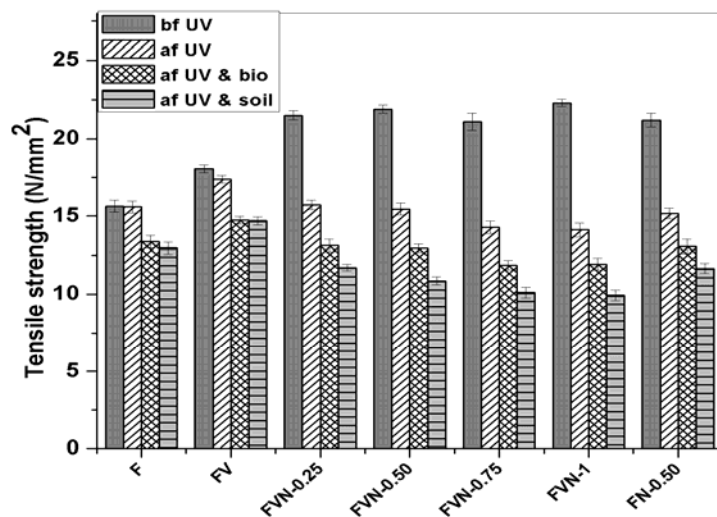


Fig.5.3 Variation of tensile strength of blends with the addition of varying amounts of nanoanatase

After UV exposure, the greatest reduction in tensile properties was observed in the case of samples containing the nano form of TiO₂. For the case of 0.50% of TiO₂ (Fig.5.4), the tensile strength decreased by 3.33% for samples containing rutile (FR-0.50), 10.84% for anatase (FA-0.50) and 28.49% for nanoanatase (FN-0.50). All three forms of TiO₂ (rutile, anatase and nanoanatase) played a significant role in promoting the photo-oxidative degradation of LLDPE films the decrease is more in the case of samples containing nanoanatase.

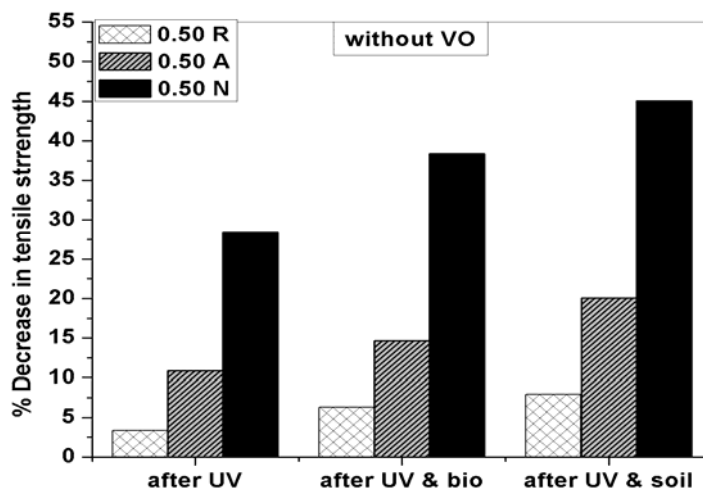


Fig.5.4 Percentage decrease in tensile strength of samples containing 0.50% of TiO₂ only (VO = vegetable oil)

For the case of 0.50% of TiO₂ and vegetable oil, (Fig.5.5), the tensile strength decreased by 7.15% for samples containing rutile (FVR-0.50), 11.14% for anatase (FVA-0.50) and 29.45% for nanoanatase (FVN-0.50) which means that vegetable oil played a significant role in the degradation of LLDPE. Vegetable oil undergoes auto-oxidation by which free radicals are generated [9]. These, in turn, initiate oxidation of LLDPE.

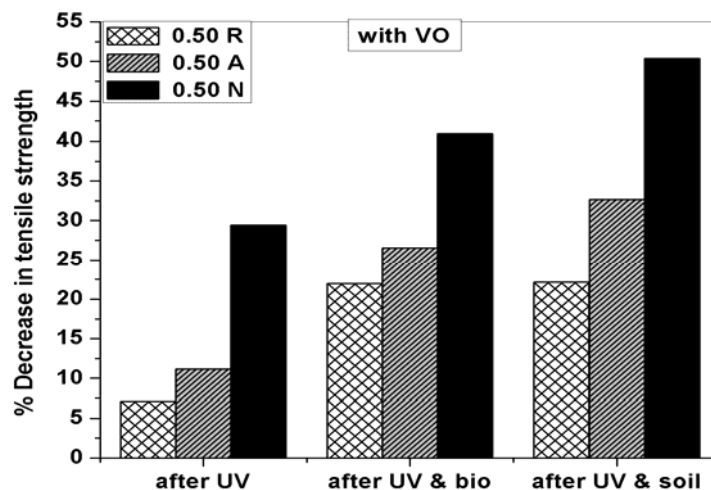


Fig.5.5 Percentage decrease in tensile strength of samples containing 0.50% of TiO₂ and vegetable oil (VO)

Table 5.1 Percentage decrease in tensile strength of the samples after UV exposure

Sample designation	Tensile strength (N/mm ²)		
	Before UV exposure	After UV exposure	% decrease
F	15.63	15.58	0.32
FV	18.03	17.37	3.66
FVA-0.25	22.04	20.10	8.80
FVA-0.50	21.19	18.83	11.14
FVA-0.75	19.67	16.92	13.98
FVA-1	18.90	15.74	16.72
FA-0.50	18.63	16.61	10.84
FVR-0.25	21.97	20.68	5.87
FVR-0.50	20.42	18.96	7.15
FVR-0.75	18.89	17.19	8.99
FVR-1	17.25	15.44	10.49
FR-0.50	17.74	17.15	3.33
FVN-0.25	21.5	15.72	26.88
FVN-0.50	21.9	15.45	29.45
FVN-0.75	21.1	14.28	32.32
FVN-1	22.3	14.11	36.72
FN-0.50	21.2	15.16	28.49

The elongation at break (Figs. 5.6, 5.7 and 5.8) decreased for all samples containing vegetable oil as well as its combination with TiO₂, the rate being much faster in the case of samples containing the nano form of TiO₂. The decrease in elongation is basically due to increased degree of cross-linking with temperature, which finally leads to the embrittlement of the sample.

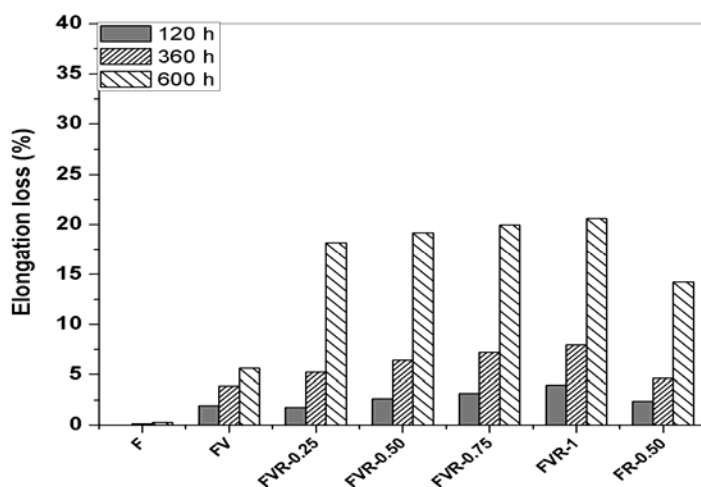


Fig.5.6 Percentage elongation loss of the samples containing varying amounts of commercial rutile

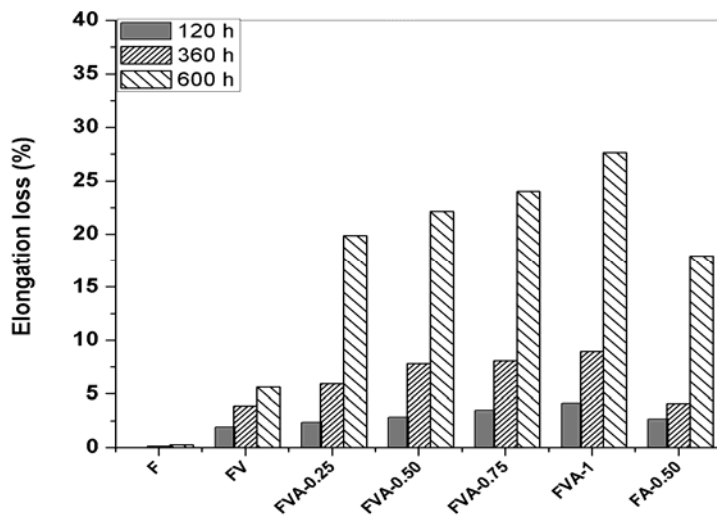


Fig.5.7 Percentage elongation loss of the samples containing varying amounts of commercial anatase

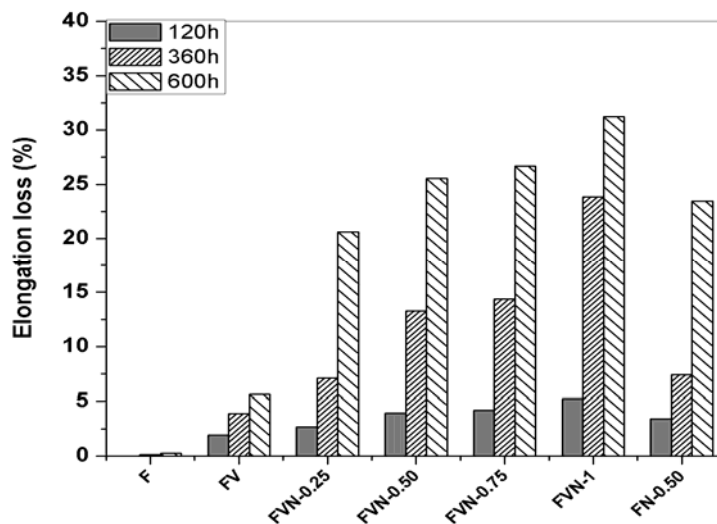


Fig.5.8 Percentage elongation loss of the samples containing varying amounts of nanoanatase

The percentage elongation loss of the samples after 600 hours of UV exposure is given in Table 5.2. For the case of 0.50% of TiO_2 only (Table-5.2), a maximum of 14.22% elongation loss is observed for samples containing rutile (FR-0.50), 17.94% for anatase (FA-0.50) and 23.43% for nanoanatase (FN-0.50). Here also the elongation loss is highest in the case of samples containing nanoanatase pigment.

For the case of 0.50% of TiO_2 and vegetable oil, (Table-5.2), a maximum of 19.15% elongation loss is observed for samples containing rutile (FVR-0.50), 22.15% for anatase (FVA-0.50) and 25.54% for nanoanatase (FVN-0.50) which means that vegetable oil played a significant role in the degradation of LLDPE.

Table 5.2 Percentage elongation loss of the samples after UV exposure

Sample designation	Elongation loss (%)
F	0.26
FV	5.64
FVR-0.25	18.16
FVR-0.50	19.15
FVR-0.75	19.96
FVR-1	20.63
FR-0.50	14.22
FVA-0.25	19.87
FVA-0.50	22.15
FVA-0.75	24.04
FVA-1	27.66
FA-0.50	17.94
FVN-0.25	20.62
FVN-0.50	25.54
FVN-0.75	26.67
FVN-1	31.21
FN-0.50	23.43

The discolouration of the samples before and after photo-degradation is shown in Fig. 5.9. This provides a good indication of the photo-oxidative degradation of the sample.

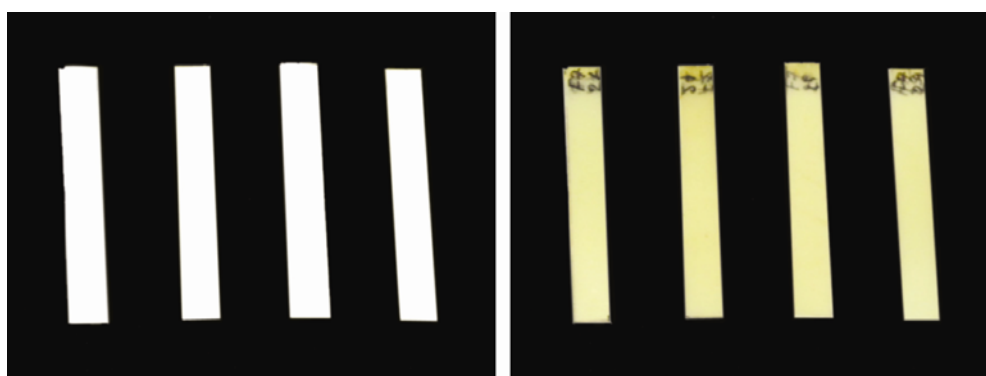


Fig.5.9 Discolouration of the samples before and after 600 hours of UV exposure

5.3.2 Spectroscopic studies

Figs. 5.10 to 5.15 show FTIR spectra of samples containing 0.50% of rutile, anatase or nanoanatase each before UV exposure as well as after UV exposure in the presence or absence of vegetable oil.

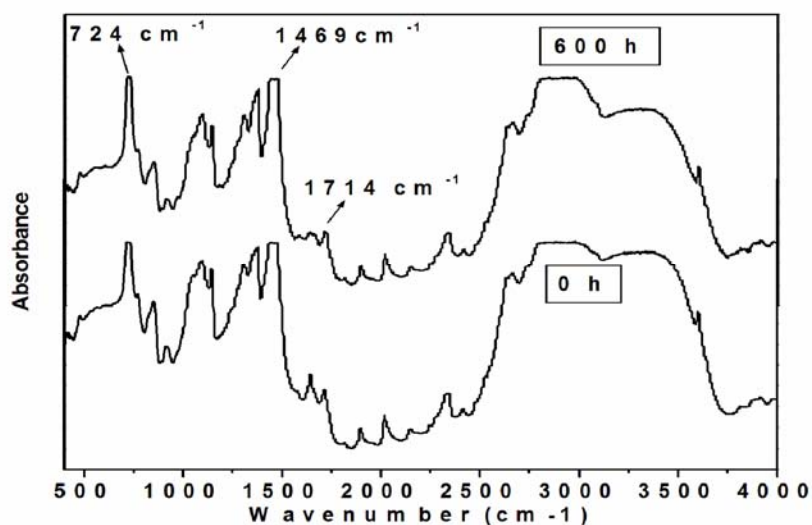


Fig.5.10 FTIR spectra of samples containing 0.50% of rutile only

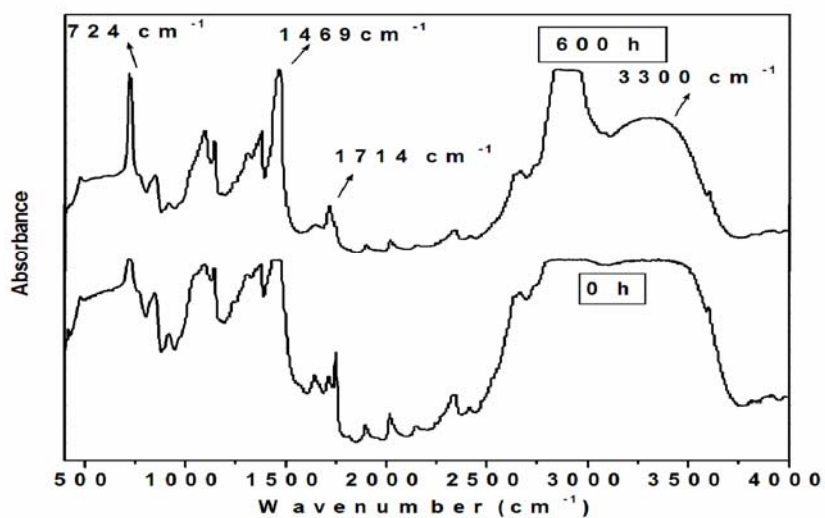


Fig.5.11 FTIR spectra of samples containing vegetable oil and 0.50% of rutile

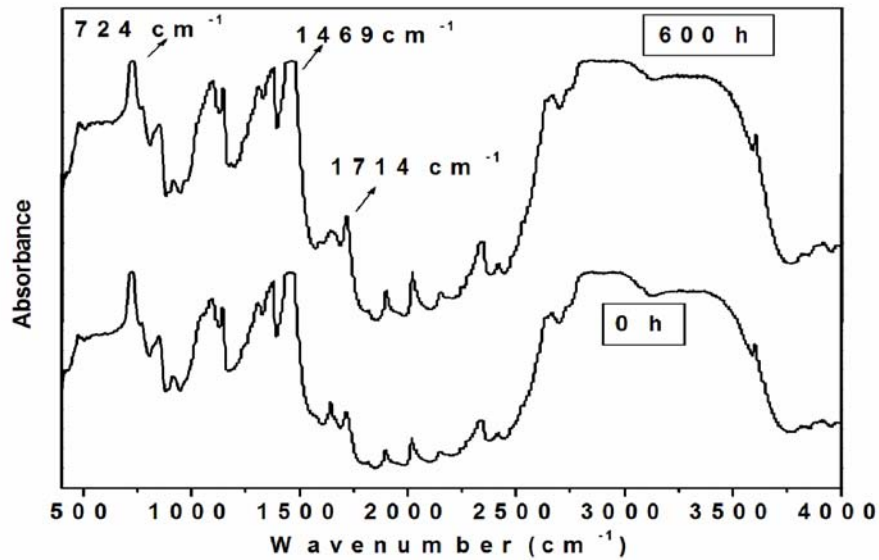


Fig.5.12 FTIR spectra of samples containing 0.50% of anatase only

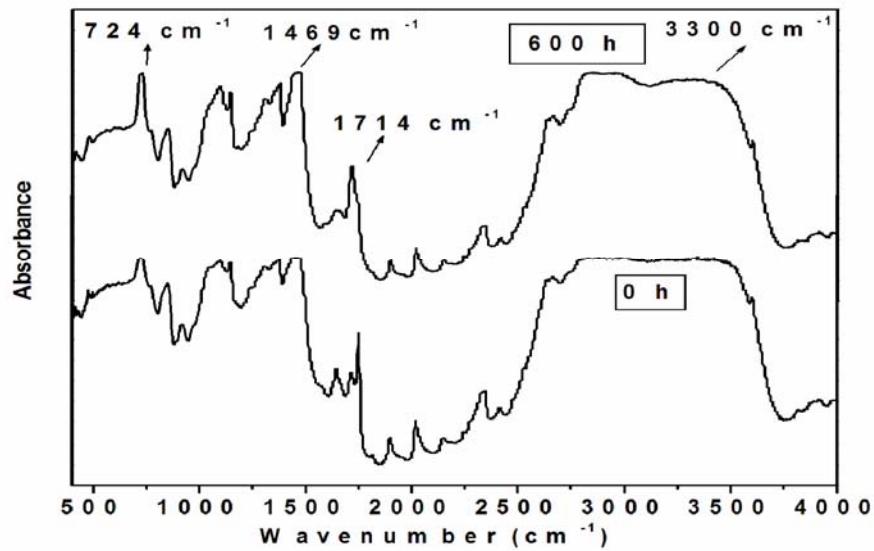


Fig.5.13 FTIR spectra of samples containing vegetable oil and 0.50% of anatase

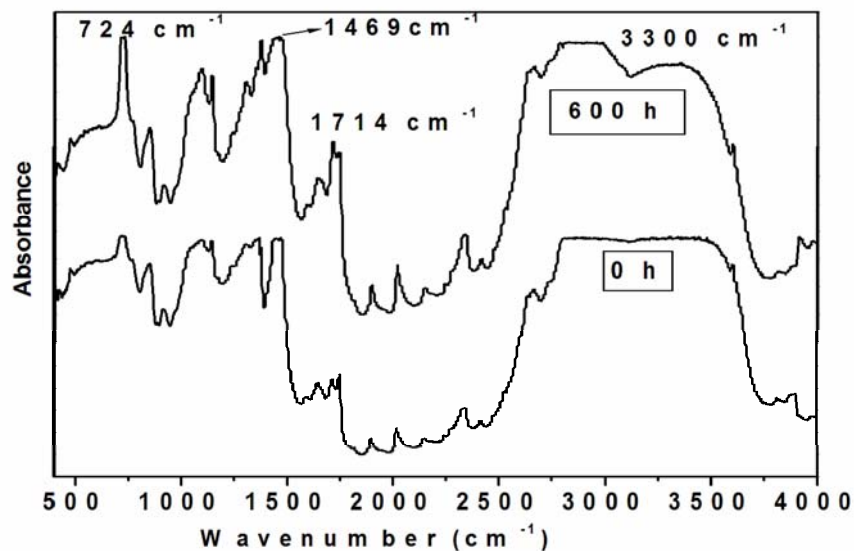


Fig.5.14 FTIR spectra of samples containing 0.50% of nanoanatase only

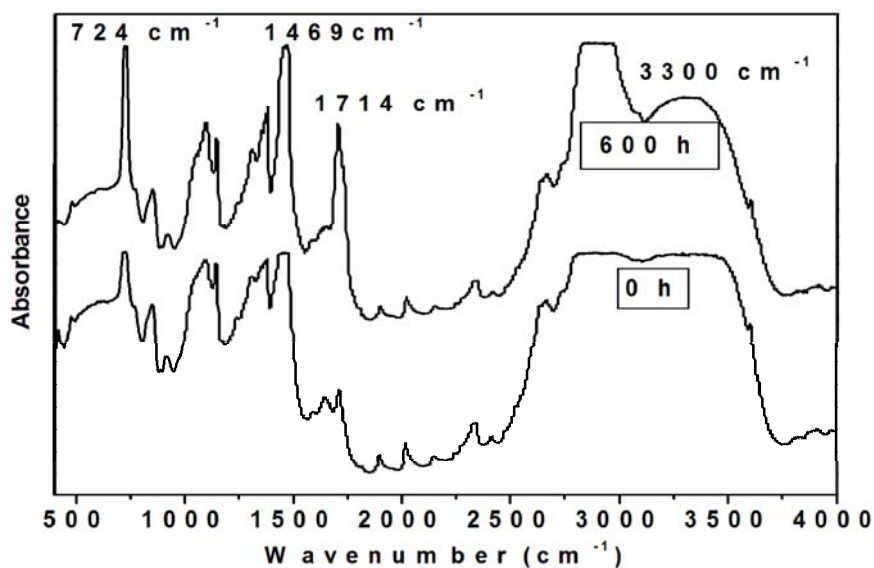


Fig.5.15 FTIR spectra of samples containing vegetable oil and 0.50% of nanoanatase

The FTIR spectra show significant changes, especially in the carbonyl (1785-1700 cm^{-1}), amorphous (1300 cm^{-1}), and hydroxyl regions (3400 cm^{-1}).

The absorption band around 1714 cm⁻¹ which can be assigned to the C=O stretching ketonic functionality, increases in intensity and exhibits band broadening. This carbonyl band is a result of overlapping of absorption bands due to several functional groups like ketones, carboxylic acids, aldehydes, esters and peroxy-carboxylic acids. The overlap of all these bands results in the observed band broadening [10–13]. The band broadening is more in the case of samples containing a combination of both TiO₂ and vegetable oil. The absorption bands around 724 cm⁻¹ and 1469 cm⁻¹ also increase in intensity. These bands correspond to rocking vibrations of -CH₂ groups and bending vibrations of C-H bonds. The increase in the absorbance of these bands was also more pronounced for samples containing TiO₂ and vegetable oil rather than only TiO₂. The increase in intensity of these peaks can be attributed to the fracture of the polyethylene chains in the degrading environment. Comparing the three forms of TiO₂, the nano TiO₂ showed greater extend of degradation in a reasonable time frame which is evident from carbonyl index values.

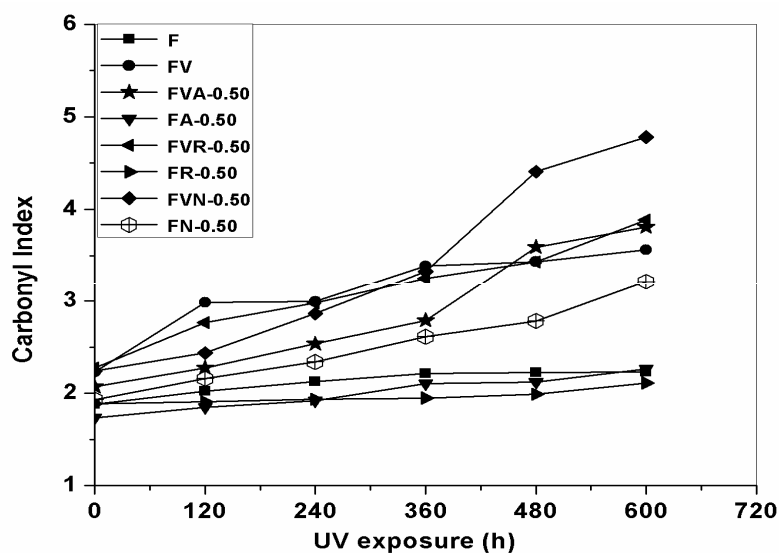


Fig.5.16 Variation of carbonyl index value as a function of exposure time

Fig. 5.16 displays the variation of carbonyl index value as a function of exposure time for LLDPE/PVA samples containing varying amounts of TiO₂ in the presence as well as absence of vegetable oil. The carbonyl index values are more for samples containing nanoanatase, which indicates a better rate of degradation of the polymer when compared to those containing commercial rutile or anatase.

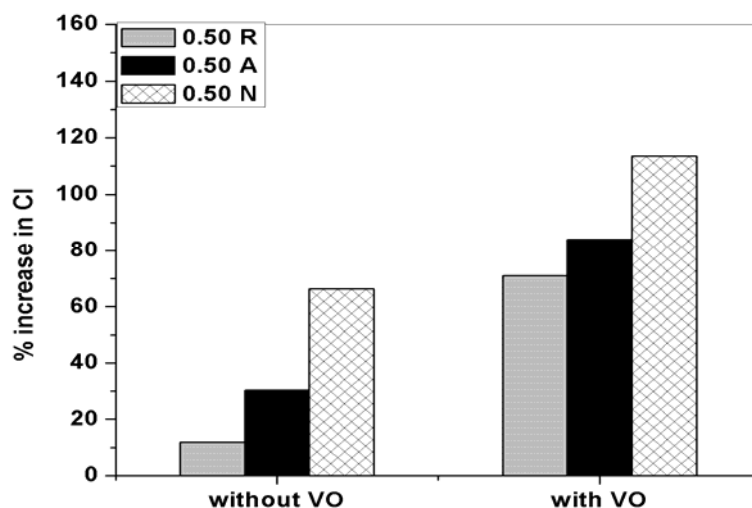


Fig.5.17 Percentage increase in carbonyl index (CI) of the samples containing 0.50% TiO₂ after UV exposure in the presence and absence of vegetable oil.

Fig. 5.17 shows the percentage increase in carbonyl index for various cases. In the case of samples containing 0.50% of TiO₂ only, CI increased by 11.92% for samples containing rutile (FR-0.50), 30.37% for anatase (FA-0.50) and 66.36% for nanoanatase (FN-0.50). This means that all the three forms of TiO₂ (rutile, anatase and nanoanatase) promote the photo-oxidative degradation of LLDPE films.

In the case of samples containing 0.50% TiO₂ and vegetable oil, the CI increased by 71.04% for sample containing rutile (FVR-0.50), 84.01% for anatase (FVA-0.50) and 113.53% for nanoanatase (FVN-0.50). This means that vegetable oil also plays a significant role in the degradation of LLDPE. This is more clearly understood from the Figs. 5.16 and 5.17.

The increase in MFI as a result of UV exposure is quantified in Table 5.3. From the table it can be seen that the increase in MFI is highest in the case of samples containing the nano form of TiO₂. In this case MFI has shown an increase of 6.2 over the nondegraded sample. It is noteworthy that nanoanatase even in the absence of vegetable oil leads to a substantial increase of 5.9 in MFI.

Table 5.3 Effect of UV exposure on Melt Flow Index of the samples containing 0.50% TiO₂

Sample designation	MFI(g/10 min with a 2.16kg load)	
	Before Exposure	After Exposure (600h)
F	0.8	0.9
FV	1.0	1.3
FVR-0.50	0.9	2.8
FR-0.50	0.9	2.6
FVA-0.50	0.9	4.7
FA-0.50	0.9	4.4
FVN-0.50	0.9	7.1
FN-0.50	0.9	6.8

5.3.3 Thermal Studies

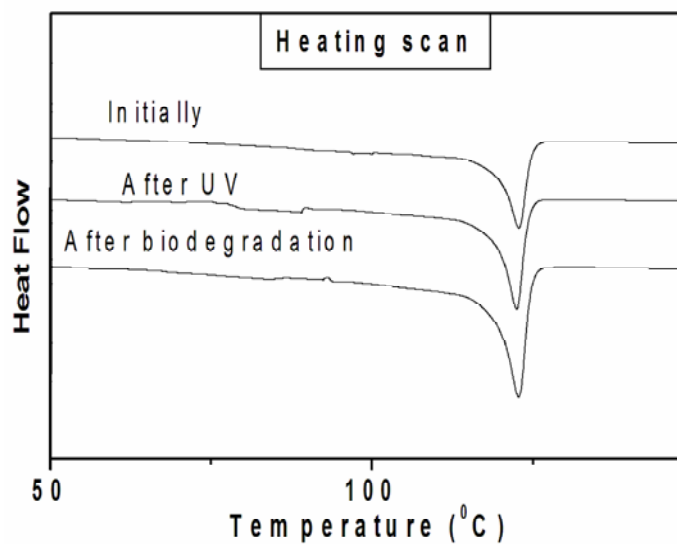


Fig. 5.18 The heating scans of samples containing commercial rutile

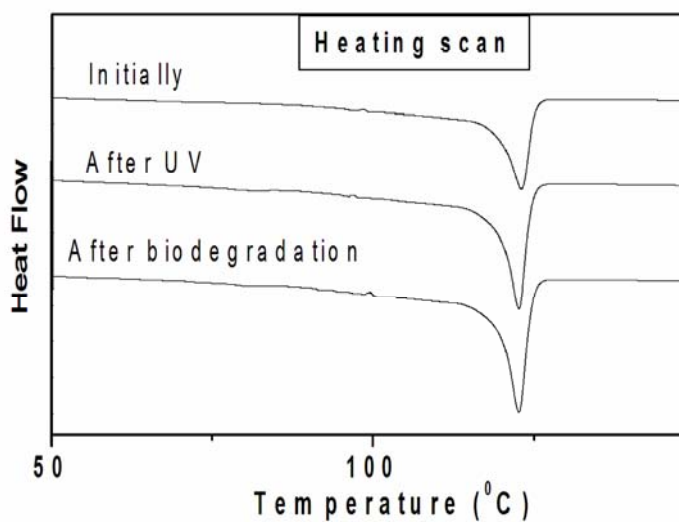


Fig. 5.19 The heating scans of samples containing commercial anatase

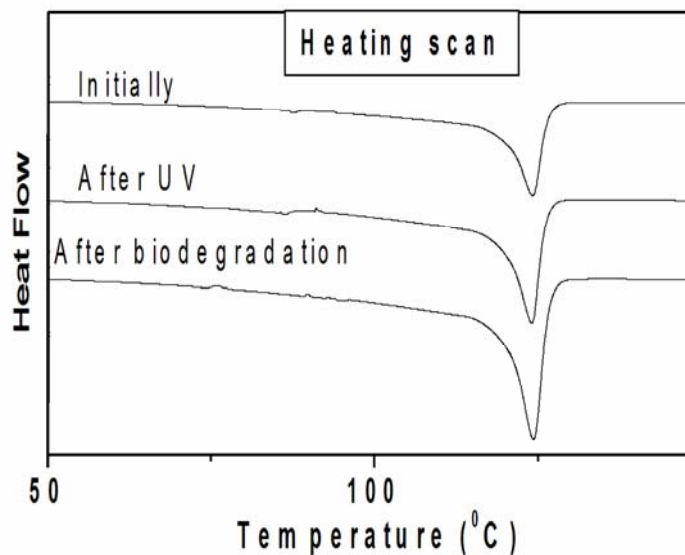


Fig. 5.20 The heating scans of samples containing nanoanatase

Referring to Figs. 5.18 to 5.20 which show DSC scans, the UV exposure and biodegradation process led to a slight broadening of the polyethylene melting endotherm. LLDPE is a semicrystalline polymer in which both crystalline and amorphous regions coexist. Due to the gradual depletion of the amorphous phase, the crystallinity of the samples increased. This increase could also be partially attributed to the changes in the crystallite sizes, molecular weight differences that were brought about by chain breaking and secondary recrystallization [14]. The broadening of the peaks is more noticeable in the case of samples containing nanotitania. Since the amorphous form is more prone to degradation the increasing percentage of crystalline material and consequently the endothermic heat of melting is an indication of a greater level of degradation.

5.3.4 Percentage weight Loss

Table 5.4 shows the weight loss of the samples after UV exposure. The weight loss was much higher for samples containing nanoanatase and vegetable oil than for commercial forms of TiO₂. The weight loss data indicate that the UV degradation of films led to bond scission and a mass of volatile intermediates.

Table 5.4 Percentage weight loss of the samples after UV exposure, biodegradation and soil degradation

Sample designation	%Weight Loss		
	UV exposure	Biodegradation	Soil degradation
F	4.21	2.43	4.24
FV	6.13	3.08	5.31
FVR-0.50	14.26	4.72	6.03
FR-0.50	13.28	3.15	4.82
FVA-0.50	19.31	9.02	11.92
FA-0.50	16.22	6.45	10.06
FVN-0.50	24.46	13.94	16.71
FN-0.50	21.43	12.16	14.97

5.3.5 Morphological studies

It can be seen that there are some deep cavities on the film surface with the extension of irradiation time. The photodegradation of PE mainly happens on the film surface. Photocatalytic reaction first starts at the interface between PE and exposed TiO₂ photocatalyst which leads to the formation of cavities around TiO₂ particles [15]. That is after UV irradiation also cavities are observed on the surface of the film. The formation of these cavities was

induced by the escape of volatile products from the PE matrix. Examination of the films by SEM shows the formation of holes in the film which scatter light and cause whitening. This suggests that in the vicinity of the titania particles the polymer gets totally degraded to water and carbon dioxide or other volatile substances.

The SEM micrographs of the samples after UV exposure are shown in Figs. 5.21 to 5.26.

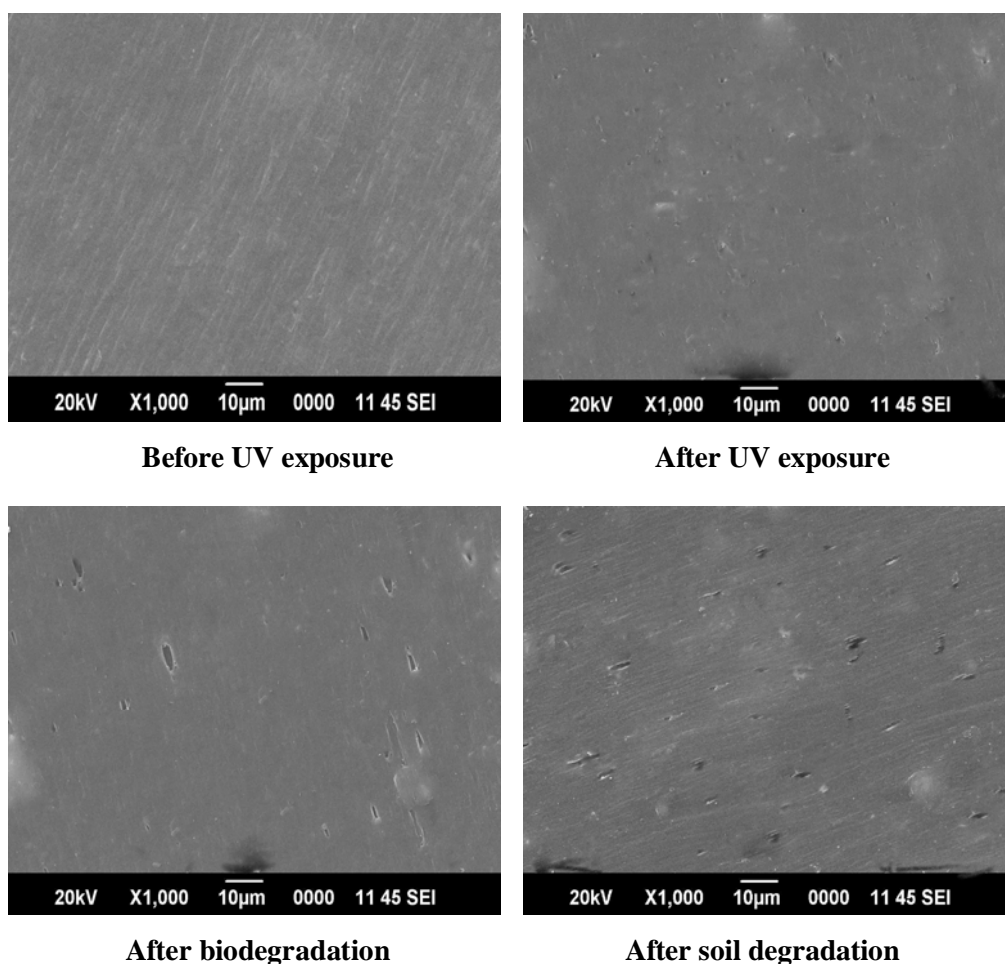


Fig.5.21 Scanning electron micrographs of LLDPE/PVA blends with rutile only

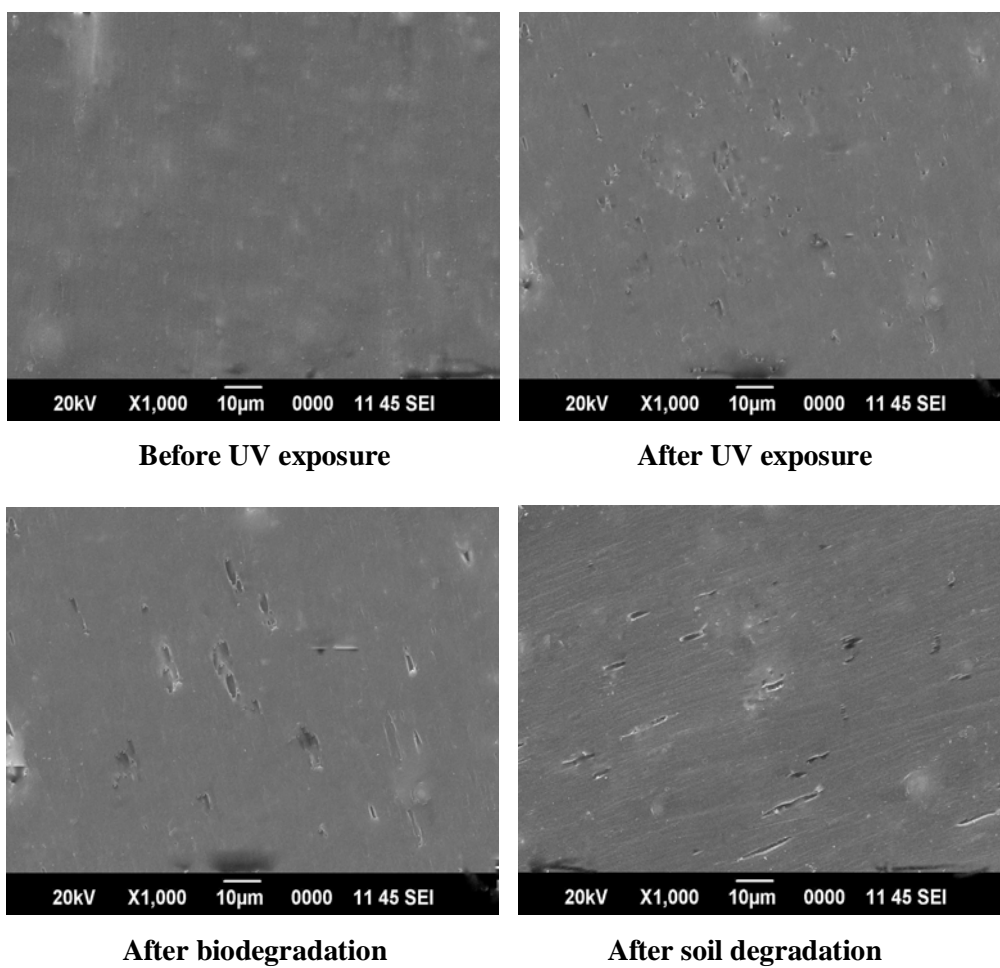


Fig.5.22 Scanning electron micrographs of LLDPE/PVA blends with rutile and vegetable oil

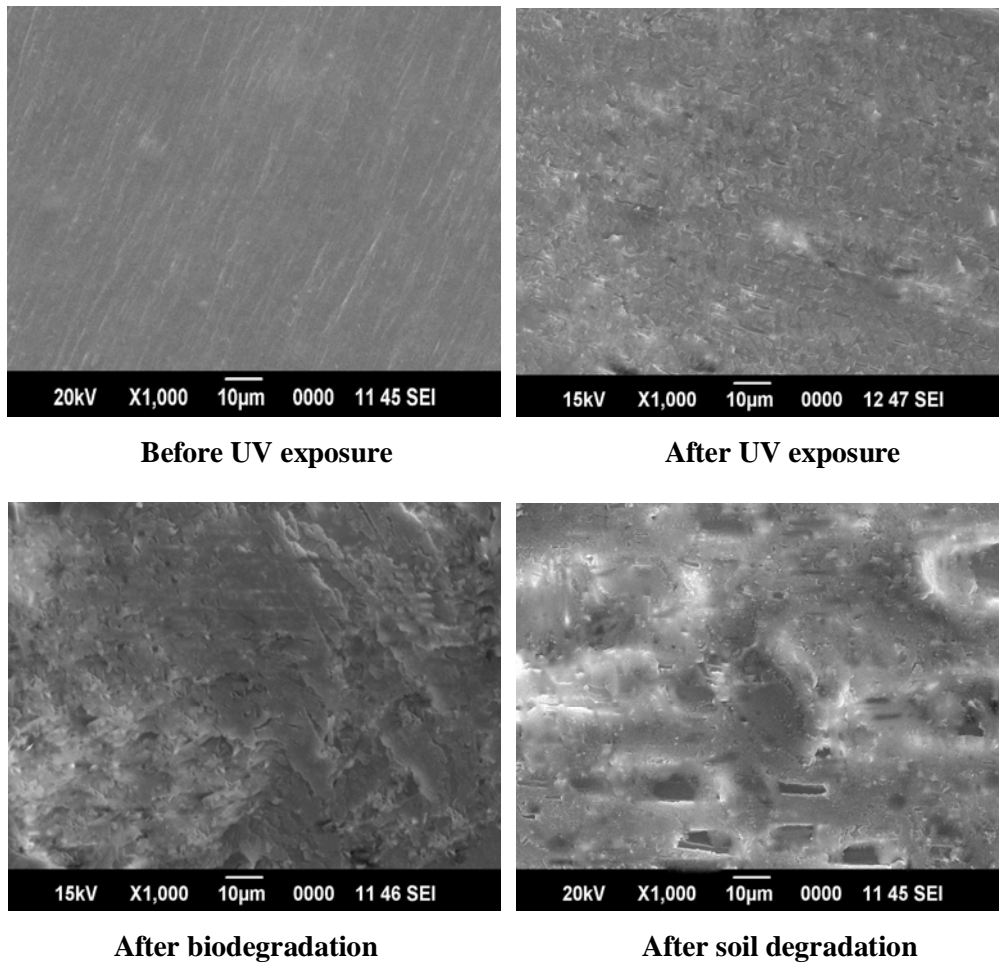


Fig.5.23 Scanning electron micrographs of LLDPE/PVA blends with anatase only

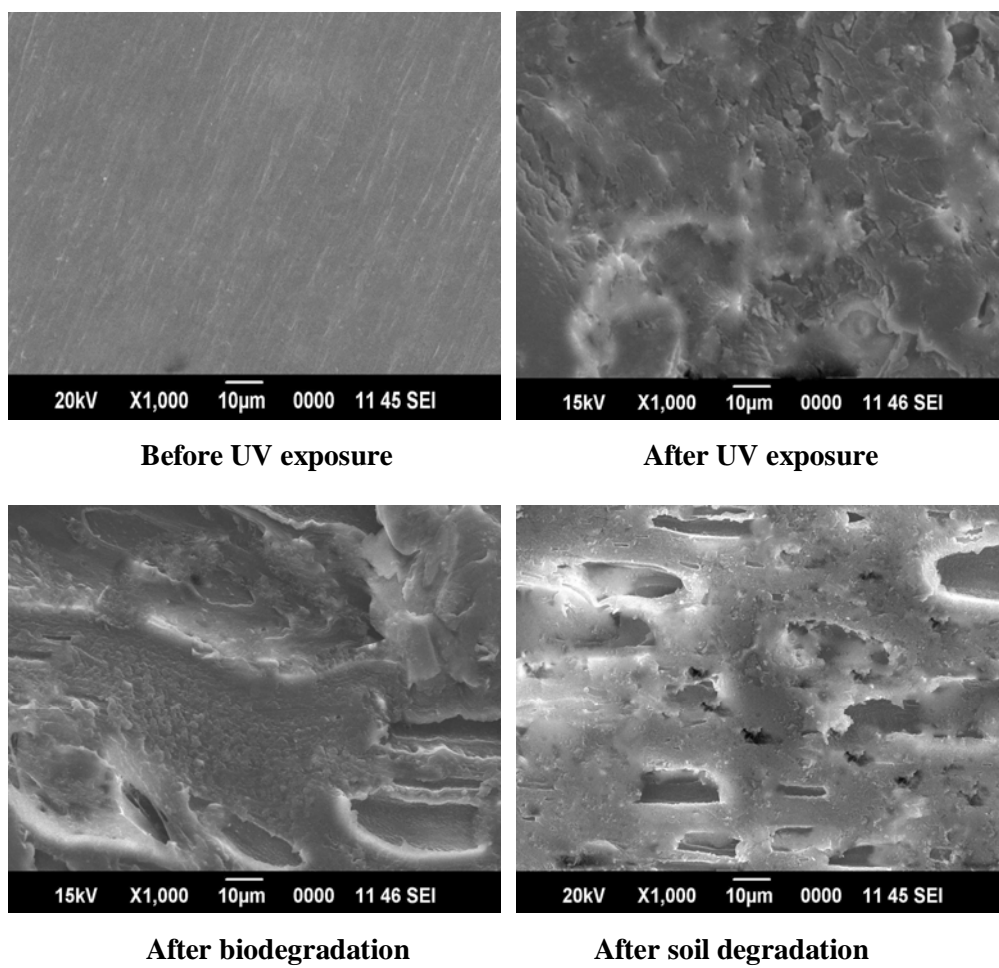


Fig.5.24 Scanning electron micrographs of LLDPE/PVA blends with anatase and vegetable oil

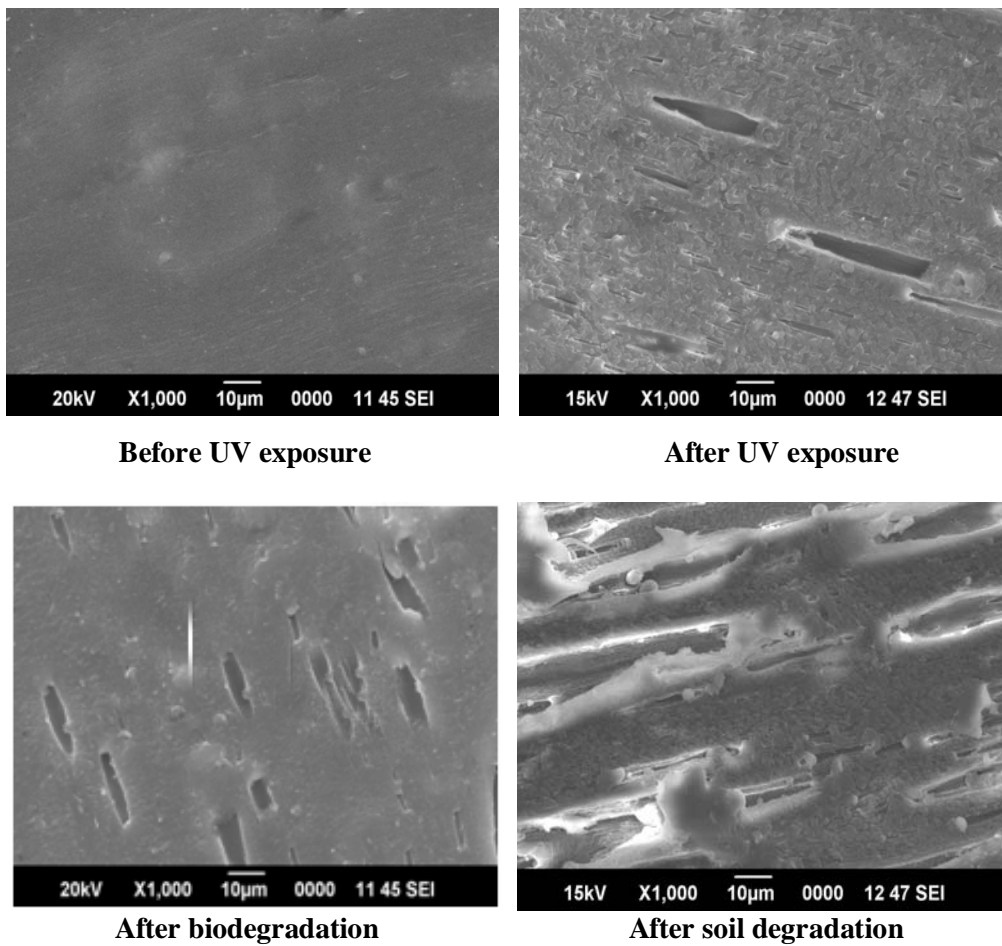


Fig.5.25 SEM of LLDPE/PVA blends with nanoanatase only

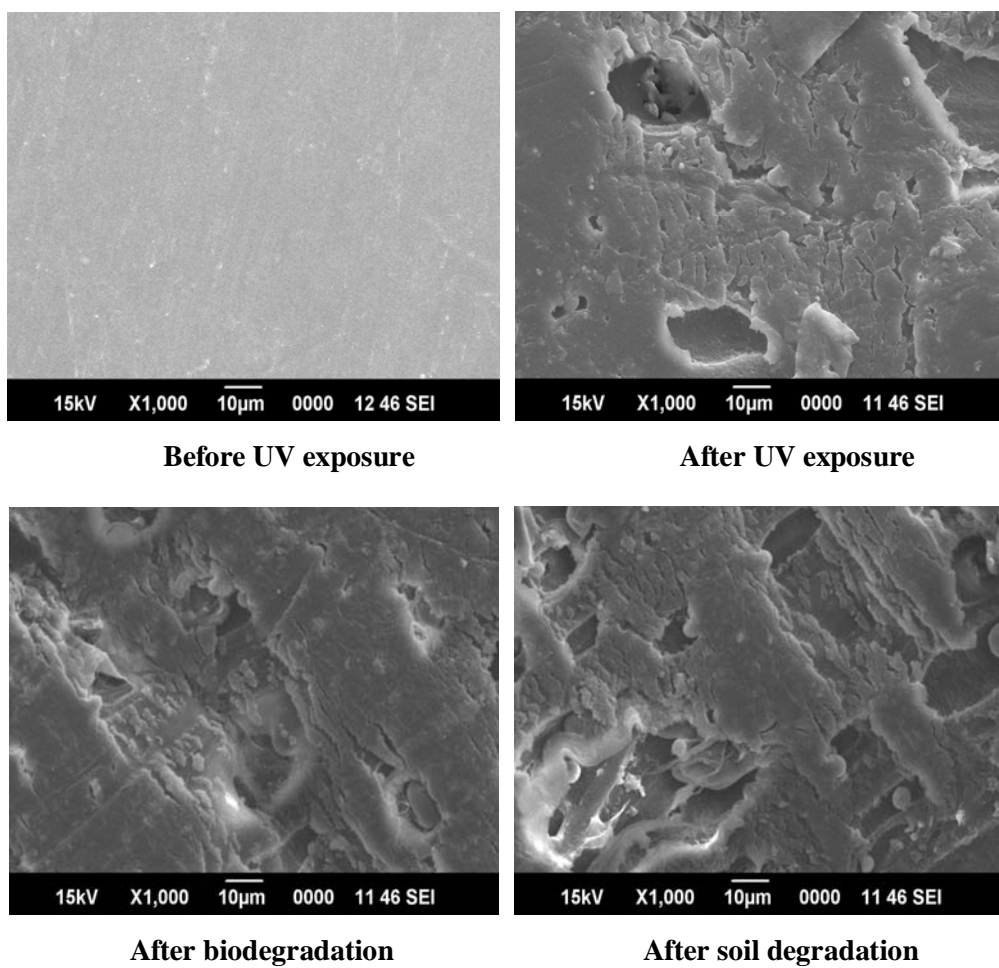


Fig.5.26 Scanning electron micrographs of LLDPE/PVA blends with nanoanatase and vegetable oil

5.4 Conclusions

- After UV exposure, the greatest reduction in tensile properties was observed in the case of samples containing the nano form of TiO₂.
- Although the three forms of TiO₂ (rutile, anatase and nanoanatase) played a significant role in promoting the photo-oxidative degradation of LLDPE films the decrease in tensile properties is more in the case of samples containing nanoanatase.
- Vegetable oil also played a significant role in the degradation of LLDPE/PVA blends.
- The elongation at break decreased for all samples containing vegetable oil as well as its combination with TiO₂, the rate being much faster in the case of samples containing the nano form of TiO₂.
- The discolouration of the samples provides an indication of the photo-oxidative degradation of the sample.
- The FTIR spectra show significant changes, especially in the carbonyl (1785-1700 cm⁻¹), amorphous (1300 cm⁻¹), and hydroxyl regions (3400 cm⁻¹) on UV degradation.
- The bands at 724 cm⁻¹ and 1469 cm⁻¹ corresponding to rocking vibrations of -CH₂ groups and bending vibrations of C-H bonds also increase in intensity.
- The increase in intensity of these peaks is a result of the fracture of the polyethylene chains in the degrading environment.

- Increase in MFI values on degradation also gives evidence for degradation.
- Broadening of the polyethylene melting endotherm and scanning electron micrographs also provide evidence for degradation.

5.5 References

- [1] S. Macro, P. Fiorella, C. Vittorio; *Coordination Chem. Rev.* **1993**, 125, 219.
- [2] J. E. Guillet; *Pure Appl. Chem.* **1980**, 52, 285.
- [3] E. Chiellini, A. Corti, G. Swift; *Polym. Degrad. Stab.* **2003**, 81, 341.
- [4] Jakubowicz; *Polym. Degrad. Stab.* **2003**, 80, 39.
- [5] Xu Zhao, Zongwei Li, Yi Chen, Liyi Shi, Yongfa Zhu; *Journal of Molecular Catalysis A: Chemical.* **2007**, 268, 101.
- [6] J. H. Braun; *Progress in Organic Coatings*, **1987**, 15, 249.
- [7] G. Kfimpf, W. Papenroth, R. Holm; *J. Paint Technol.* **1974**, 46, 56.
- [8] N. S. Allen; *Degradation and Stabilisation of Polyolefins*, Applied Science Publishers, New York, London, **1983**.
- [9] E. N. Frankel; *Pray. Lipid Res.* **1980**, 19, 1.
- [10] F. Khabbaz, A. C. Albertsson, S. Karlson; *Polym. Degrad. Stab.* **1998**, 61, 329.
- [11] R. Setnescu, S. Jipa, Z. Osawa; *Polym. Degrad. Stab.* **1998**, 60, 377.
- [12] F. Khabbaz, A. C. Albertsson, S. Karlson; *Polym. Degrad. Stab.* **1999**, 63, 127.
- [13] J. V. Gulmine, P. R. Janissek, H. M. Heise, Akcelrud; *Polym. Degrad. Stab.* **2003**, 79, 385.

- [14] P. K. Roy, P. Surekha, C. Rajagopal, V. Choudhary; J. Appl. Polym. Sci. **2008**, 108, 2726.
- [15] Z. Xu, L. Zongwei, C. Yi, S. Liyi, Z. Yongfa; Applied Surface Science, **2008**, 254, 1825.

.....❧.....

EFFECT OF COBALT STEARATE AS PRO-OXIDANT ON WEATHERING AND BIODEGRADATION OF LLDPE/PVA BLENDS

Contents	6.1	<i>Introduction</i>
	6.2	<i>Experimental</i>
	6.3	<i>Results and discussion</i>
	6.4	<i>Conclusion</i>
	6.5	<i>References</i>

6.1 Introduction

Polyethylene films with enhanced degradability have been developed by the addition of pro-oxidants basically transition metal complexes capable of inducing photo and thermal oxidation. The transition metal ion complexes, especially in the form of stearates, possess a remarkable ability to decompose the hydroperoxides formed during the oxidation of polymers [1,2] and therefore they are used as pro-oxidant additives in most of the commercial photodegradable compositions. It was recently shown that preliminary UV irradiation of polymeric materials can help subsequent biodegradation [3]. This is attributed to main chain scissions and formation of functional groups in macromolecules during photo-oxidative degradation. Such degraded polymer containing shorter chains and incorporated hydroxyl and carbonyl groups is more easily attacked by microorganisms.

In the presence of pro-oxidants, relatively fast abiotic oxidation begins after the preset period of service life. As a consequence, the material loses its

mechanical properties and disintegrates into small fragments. At the molecular level, the abiotic oxidation results in polymer chain fragmentation, dramatic reduction of molecular weight, introduction of polar groups and increase of hydrophilicity [4]. Such an oxidation process is thought to make the material much more vulnerable to microbial attack which in the longer term could reduce the accumulation of micro-fragments in the environment.

Weathering implies the action of individual or a combination of various environmental factors on polymers: heat, light, ionizing radiation, oxygen, ozone, humidity, rain, wind, dust, bacteria and chemical pollutants (SO₂ and nitric oxides). Plastics subjected to long term exposure to weather degrade to different extents depending on their structure and composition. The presence of oxygen in the atmosphere enhances the effects of degradation. As a consequence, smaller fragments of chains which do not contribute effectively to the mechanical properties are generated and the articles become brittle. Thus, weathering limits the service life of plastics used for outdoor applications [5].

In this part of the work, the effect of metallic photoinitiator cobalt stearate and different combinations of cobalt stearate and vegetable oil on the photooxidative degradation and biodegradation of LLDPE/PVA blend films has been investigated. The degradation due to weathering was monitored by various techniques as in the earlier studies.

6.2 Experimental

6.2.1 Materials

The sensitizer cobalt (II) stearate (Co 9-10%) was purchased from Alfa Aesar, Shore Road, Heysham, Lancs. Food grade sunflower oil was used for the study.

6.2.2 Materials and sample preparation

The methods adopted for the preparation of test samples were described in Chapter 4. Cobalt stearate (0.05-0.20%) and vegetable oil were added to the blends as pro-oxidants. Sample designation and formulations are shown in Table 6.1. [C = cobalt stearate, other designations are described in Chapter-4]

Table 6.1 Formulations and sample designation

Sample designation	Amount (g)				
	LLDPE	PVA	Glycerol	Vegetable oil	Cobalt stearate
F	45	4.5	0.675	–	–
FV	45	4.5	0.675	0.45	–
FVC-0.05	45	4.5	0.675	0.45	0.0225
FVC-0.10	45	4.5	0.675	0.45	0.0450
FVC-0.15	45	4.5	0.675	0.45	0.0675
FVC-0.20	45	4.5	0.675	0.45	0.090
FC-0.10	45	4.5	0.675	–	0.045

6.2.3 Degradation studies

6.2.3.1 Natural weathering

Polyethylene films were mounted on racks at an angle of 30-45° to the horizontal facing the south direction as per ASTM D 1435-99. These experiments were started in the month of May 2010 in Kochi (Kerala, India) and continued for 600 hours. Samples after weathering (outdoor exposure) were collected at regular intervals of 120, 240, 360, 480, and 600 hours, respectively to evaluate the effect of weathering time on degradation.

6.2.3.2 Biodegradation

The weathered samples were subjected to biodegradation studies according to ASTM D 5247-92 exactly following the procedure described in Chapter 2.

6.2.4 Evaluation of extent of degradation

The methods adopted for the evaluation of degradation were already described in Chapter 4.

6.3 Results and discussion

6.3.1 Degradation by natural weathering

The natural weathering of any polymeric material generally depends on various parameters like UV exposure, temperature and humidity [6]. It has been reported that the surface temperature of the plastics exposed to sunlight can be much higher than that of the surrounding air due to heat buildup [7].

Figs. 6.1 and 6.2 represent the effect of exposure time on mechanical properties after being subjected to outdoor weathering. Both tensile strength and elongation were found to be very sensitive to weathering. The films containing a mixture of cobalt stearate and vegetable oil showed rapid loss of both these mechanical properties within 120 hours of weathering.

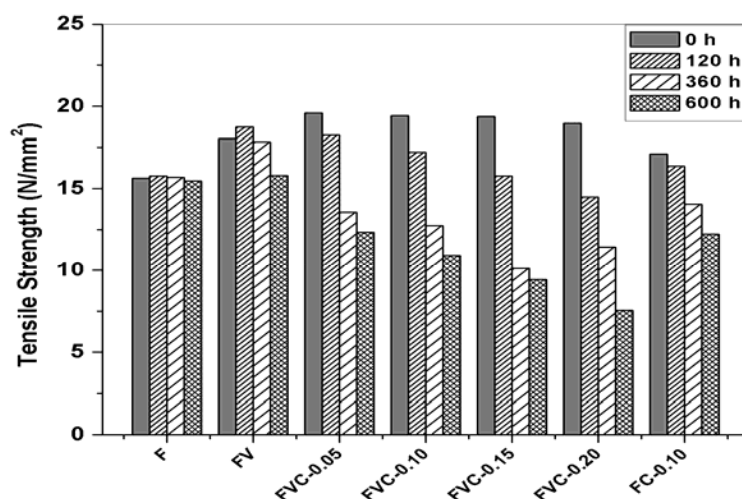


Fig. 6.1 Variation of tensile strength during outdoor weathering

The percentage decrease in tensile strength of the samples after outdoor exposure is shown in Table 6.2.

Table 6.2: Percentage decrease in tensile strength after 600hours of weathering

Sample designation	% Decrease in tensile strength after weathering
F	1.15
FV	12.42
FVC-0.05	37.11
FVC-0.10	43.84
FVC-0.15	51.34
FVC-0.20	60.25
FC-0.10	28.58

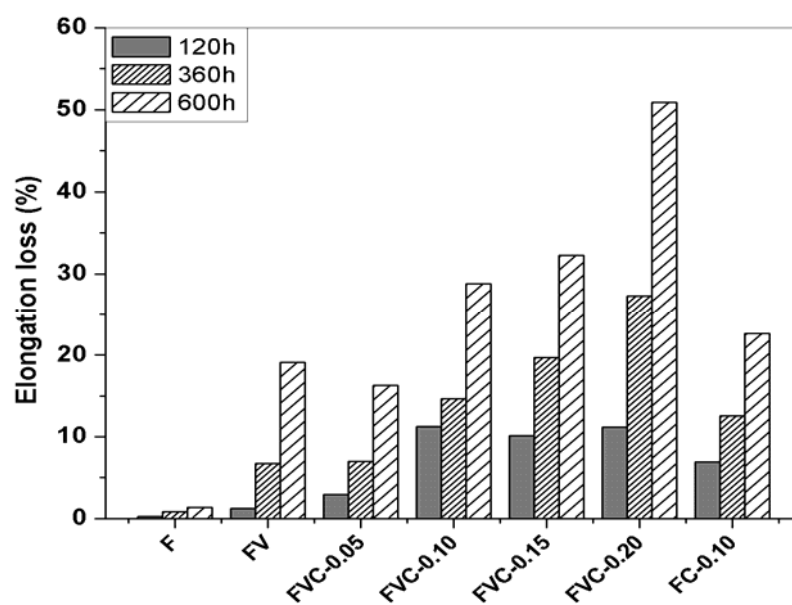


Fig. 6.2 Effect of exposure time on the percentage elongation

The materials became increasingly stiffer within a month of exposure time. The elongation at break (Fig. 6.2 and Table-6.3) decreased for all samples containing cobalt stearate as well as its mixture with vegetable oil, the rate being much faster in the case of samples containing both cobalt stearate and vegetable oil. The fall in elongation-at-break increases as the cobalt stearate content is increased.

Table 6.3 Percentage elongation loss of the samples after 600hours of weathering

Sample designation	% elongation loss after 600 h of weathering
F	1.32
FV	19.14
FVC-0.05	26.14
FVC-0.10	28.83
FVC-0.15	32.27
FVC-0.20	50.9
FC-0.10	22.62

The decrease in elongation is basically due to excessive increase in the degree of cross-linking with temperature which finally leads to embrittlement of the sample. The polymer chains take up oxygen and give rise to hydro peroxide which breaks down to give oxygenated products. The samples containing higher concentrations of cobalt stearate became too brittle and broke down to pieces after about three months of weathering. Soil degradation of the weathered samples could not be conducted as they were mechanically too weak. Further, visual effects like chalking, loss of gloss and flaking occurred for samples exposed to longer time periods.

Figs. 6.3 and 6.4 show the FTIR spectra of FC-0.10 and FVC-0.10 respectively, before and after 600 hours of weathering. The FTIR spectra, in general, show that the photo-oxidative degradation of LLDPE/PVA blends results in the formation of several functional groups; however, the extent of such functional groups is much more in the presence of cobalt stearate and vegetable oil.

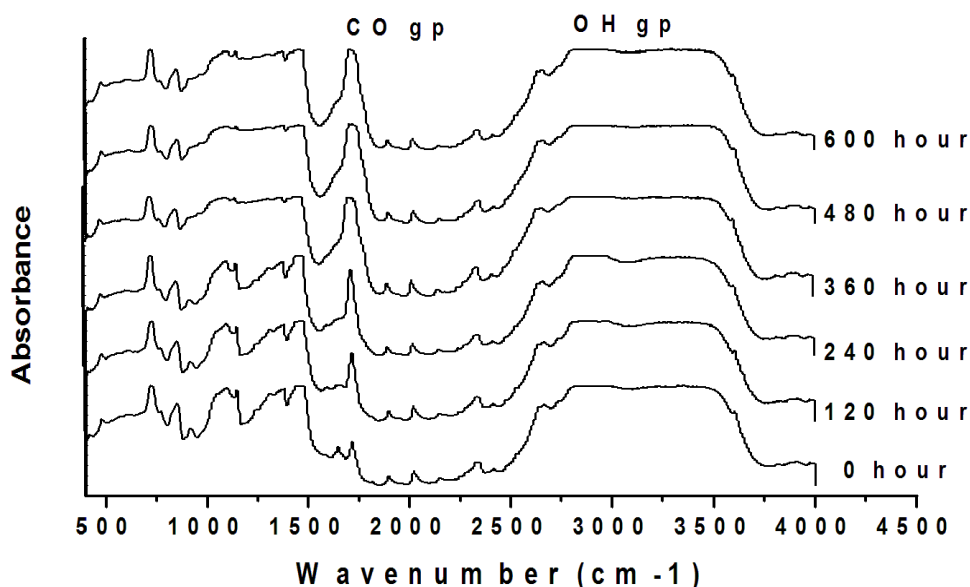


Fig. 6.3 FTIR spectra of the weathered samples containing cobalt stearate only

The most significant changes are in the carbonyl (1715-1725 cm⁻¹), amorphous (1300 cm⁻¹), and hydroxyl regions (3400 cm⁻¹). The absorption band around 1715 cm⁻¹, due to C=O stretching, increases in intensity. At the same time, a band broadening is observed which indicates the presence of multiple oxidation products overlapping in the same region. The carbonyl band can be assigned to C=O stretching vibrations in aldehydes and/or esters

(1733 cm^{-1}), carboxylic acid groups (1700 cm^{-1}), and γ lactones (1780 cm^{-1}) [8–12]. In the case of samples containing a combination of cobalt stearate and vegetable oil the absorption band around 720 cm^{-1} and 1469 cm^{-1} also increase in intensity. These bands correspond to the characteristic absorption of the crystalline and amorphous bands and bending vibrations of C-H bonds. The increase in intensity of these peaks indicates the fracture of the polyethylene chain.

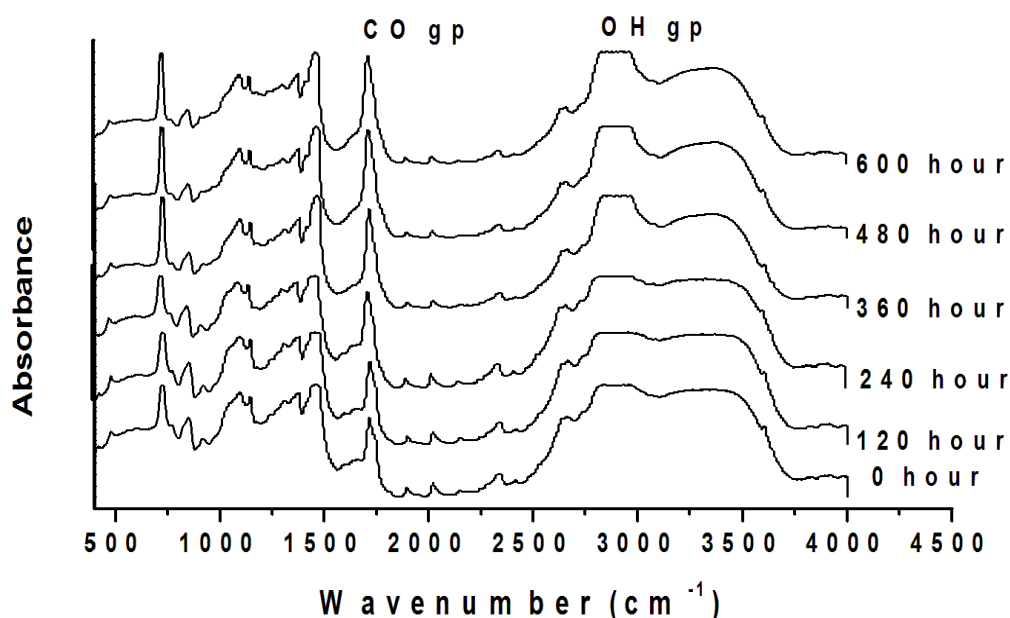


Fig. 6.4 FTIR spectra of the weathered samples containing vegetable oil and cobalt stearate

The degradation was also monitored by the increase in the carbonyl index (CI) [6]. Fig. 6.5 shows the plot of CI as a function of weathering time in LLDPE and LLDPE/PVA blends containing varying amounts of cobalt stearate and vegetable oil. CI of pure LLDPE/PVA blend increased from 1.8 to

2.4 after 600 h of UV exposure. However, incorporation of cobalt stearate and vegetable oil into the polymer led to a significant increase in the CI in a relatively short span of time. It is generally believed that polyethylene films enter into the decay stage at CI values greater than 6 [13]. This implies that LLDPE/PVA films containing a combination of cobalt stearate and vegetable oil enter the decay stage after 240 hours of exposure whereas those containing only cobalt stearate require 480 hours for entering the decay stage. Carbonyl index values obtained in this study are higher than those reported from studies employing TiO₂ (section-4.3.4).

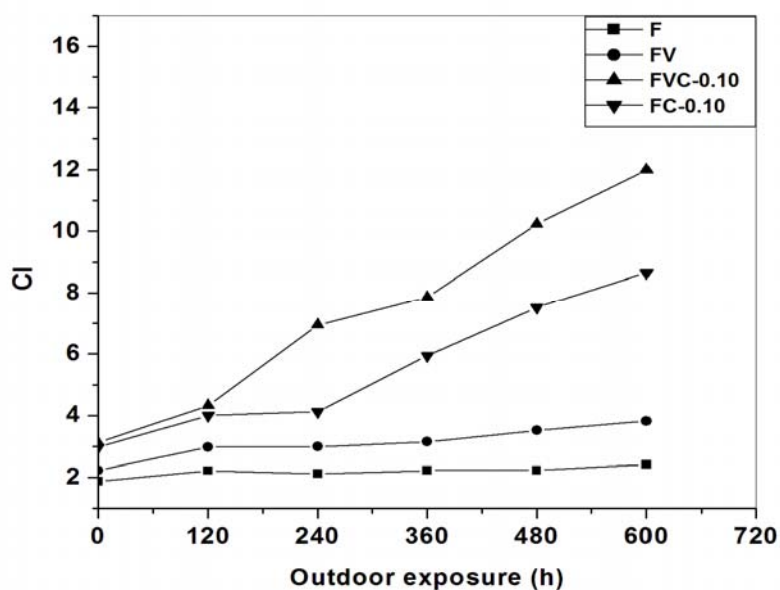
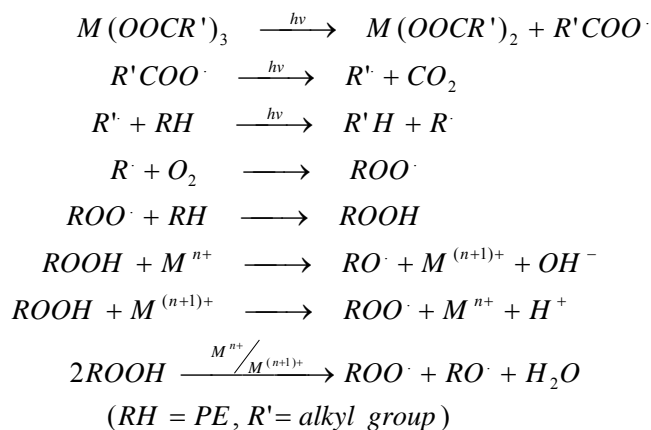


Fig. 6.5 Carbonyl index of the weathered samples

The mechanism of the transition metal catalysed degradation of polyethylene has been described in the literature as a free radical chain mechanism [14-16]. On absorption of energy in the form of light, the cobalt

carboxylates undergo decarboxylation leading to the formation of free radicals as shown in Scheme 6.1.



Scheme 6.1. Catalysis of PE degradation by transition metal carboxylates [17]

These radicals in turn give rise to free radicals on the main chain of the polymer matrix leading to chain scission. LLDPE contains butene branches which are capable of acting as weak linkages. The degradation leads to the generation of stable tertiary radicals on the surface of LLDPE. Oils are mostly triglycerides and the triglycerides containing unsaturated acids are more susceptible to oxidation. This reaction is also believed to take place via the formation of a free radical [18].

Oxidation of an inert polymer generally improves its susceptibility to biodegradation. Microorganisms attack the polymer when carbonyl groups are formed and the macromolecules decompose into shorter chains [19]. Carbonyl groups are also known to be photosensitizing species, which may accelerate further photo-degradation steps. The macro chains containing carbonyl groups are also known to undergo Norrish I and Norrish II type reactions under UV exposure. Moreover, the bio-degradation of the degradable component leads to

increased porosity and development of the film surface. Therefore, there is easier access of free oxygen, enzymes (produced by microorganisms) and free radicals formed in primary reactions to the polymer bulk. In addition, during photo and biodegradation of PE the new functional groups formed (carbonyls, hydroxyls etc) modify the polarity of the polymer. This effect may induce new molecular interactions with the OH groups of PVA. Such interactions can lead to the evolution of low molecular weight degradation products (for instance, water molecules), and weaken other neighboring chemical bonds.

The increase in MFI as a result of outdoor exposure is presented in Table 6.4. The MFI of the samples could not be determined for films containing greater than 0.10% w/w of cobalt stearate after outdoor exposure as it flowed freely under the test conditions.

Table 6.4 Effect of outdoor exposure on Melt Flow Index

Sample designation	MFI(g/10 min with a 2.16kg load)	
	Before exposure	After exposure (600h)
F	0.8	1.0
FV	1.0	2.0
FVC-0.05	0.9	3.4
FVC-0.10	0.9	10.1
FVC-0.15	1.1	*
FVC-0.20	1.3	*
FC-0.10	0.9	9.8

*The MFI could not be determined.

6.3.2 Degradation by microorganisms

The tensile strength of the weathered samples after biodegradation is shown in Fig.6.6. We can see that there is a decrease (Table 6.5) in tensile

strength of the weathered samples after biodegradation. This effect is more in the case of samples containing both cobalt stearate and vegetable oil.

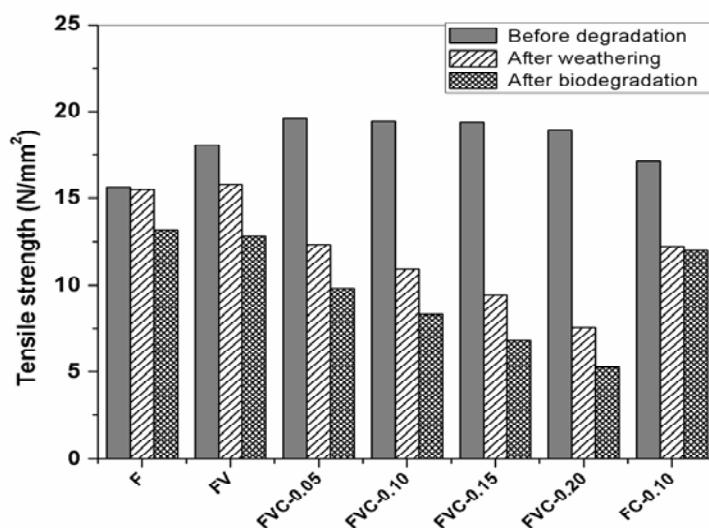


Fig. 6.6 Tensile strength of the weathered samples after biodegradation

Table 6.5: Percentage decrease in tensile strength after biodegradation

Sample Designation	% Decrease in tensile strength on biodegradation
F	14.56
FV	15.33
FVC-0.05	20.21
FVC-0.10	23.74
FVC-0.15	27.78
FVC-0.20	30.24
FC-0.10	21.28

Table 6.6 shows the percentage weight loss of the samples after weathering followed by biodegradation in culture medium. There is substantial

loss of weight for these blends after immersing in culture medium. This is, again, an indication of biodegradability.

Table 6.6 Weight loss of the samples after weathering and biodegradation in culture medium.

Sample designation	% Weight Loss	
	Weathering	Biodegradation
FVC-0.05	21.71	7.14
FVC-0.10	27.64	12.22
FVC-0.15	32.6	15.73
FVC-0.20	47.6	26.58
FC-0.10	24.22	10.92

Figs 6.7 and 6.8 show the FTIR spectra of FC-0.10 and FVC-0.10 respectively, after weathering followed by biodegradation. We can see that there is a clear decrease in intensity of the absorption spectra after biodegradation. This effect is more in the case of samples containing both cobalt stearate and vegetable oil. The intensities of the peaks at 724 cm^{-1} , 1715 cm^{-1} and $3200\text{-}3600\text{ cm}^{-1}$ which correspond to characteristic absorption of crystalline and amorphous regions, C=O stretching vibrations and absorption of hydroxyl groups respectively, show considerable reduction indicating degradation. The peak at 3371 cm^{-1} shows a remarkable reduction in peak height. This is due to the depletion of OH functionality which is often observed in microbial degradation.

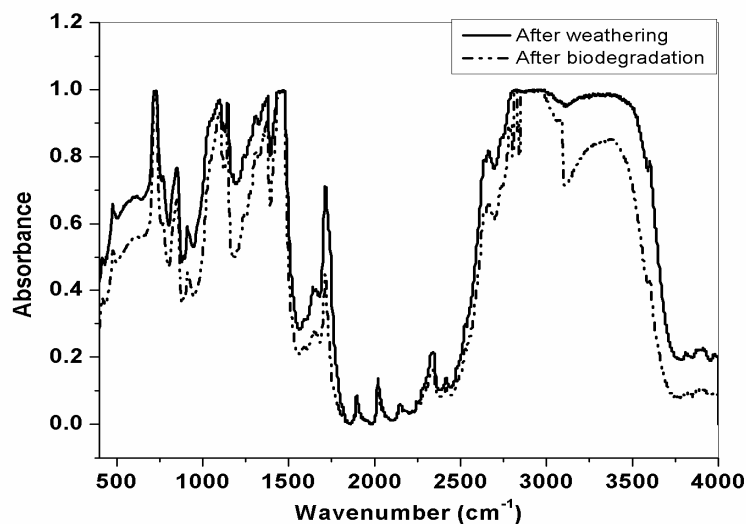


Fig. 6.7 FTIR spectra of biodegraded samples (containing cobalt stearate only) after weathering

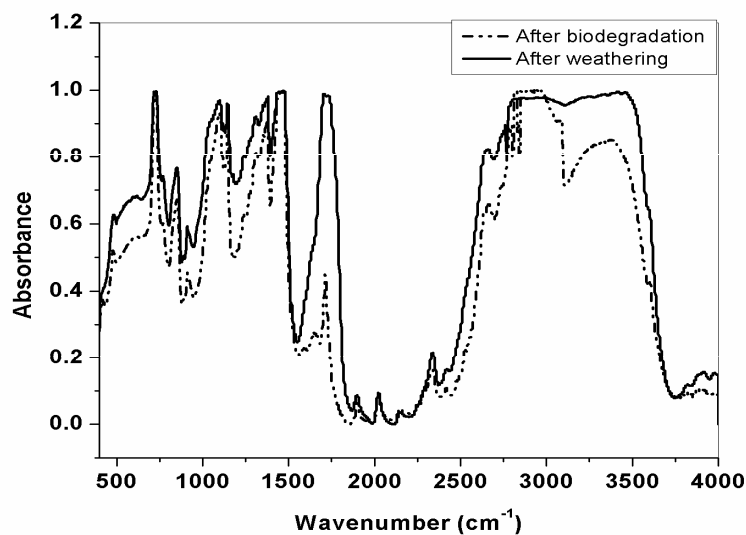


Fig. 6.8 FTIR spectra of biodegraded samples (containing both cobalt stearate and vegetable oil) after weathering

6.3.3 Differential scanning calorimetry studies

An endothermic transition due to melting at 123^oC was observed in all of the formulations. This indicates that blending with cobalt stearate did not affect the melting behavior of the base polymer. The heating and cooling scans of FC-0.10 and FVC-0.10 initially and after 600 h of outdoor exposure and subsequent biodegradation are presented in Figs. 6.9 to 6.12.

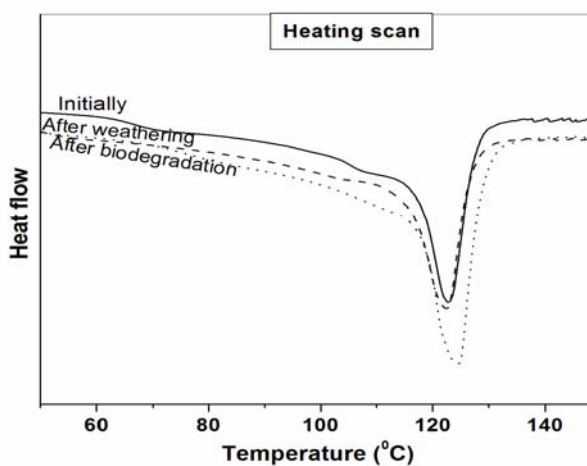


Fig. 6.9 The heating scans of samples containing cobalt stearate: before degradation, after weathering and after biodegradation

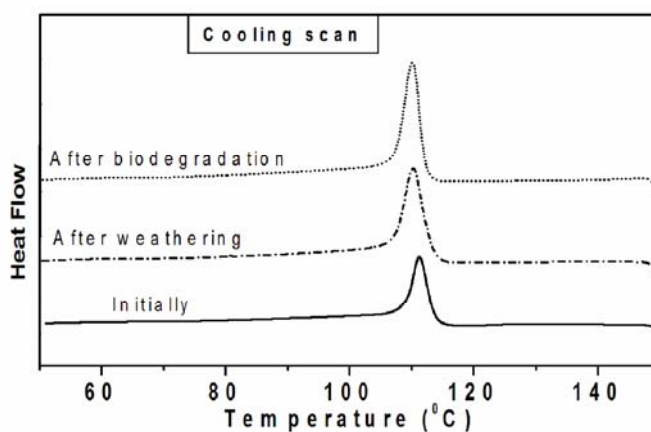


Fig. 6.10 The cooling scans of samples containing cobalt stearate: before degradation, after weathering and after biodegradation

As shown in the Figs 6.9 and 6.10, degradation did not result in any change in the melting point of the polymer. This could be explained on the basis that initial degradative changes occurred primarily in the amorphous regions of the polymer which left the crystalline regions unaffected. Hence, the melting point remained unchanged. The weathering process led to a slight broadening of the polyethylene melting endotherm and crystallization exotherm. LLDPE is a semicrystalline polymer in which both crystalline and amorphous regions coexist. Due to the gradual depletion of the amorphous phase, the crystallinity of the samples increased. This increase could also be partially attributed to the changes in the crystallite sizes, molecular weight differences that were brought about by chain breaking and secondary recrystallization [6]. The broadening of the peaks is more noticeable in the case of samples containing both cobalt stearate and vegetable oil compared to those containing cobalt stearate only.

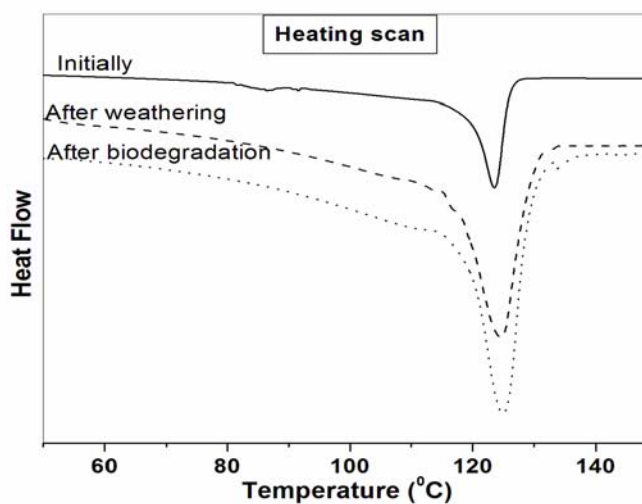


Fig. 6.11 The heating scans of samples containing both cobalt stearate and vegetable oil before degradation, after weathering and after biodegradation

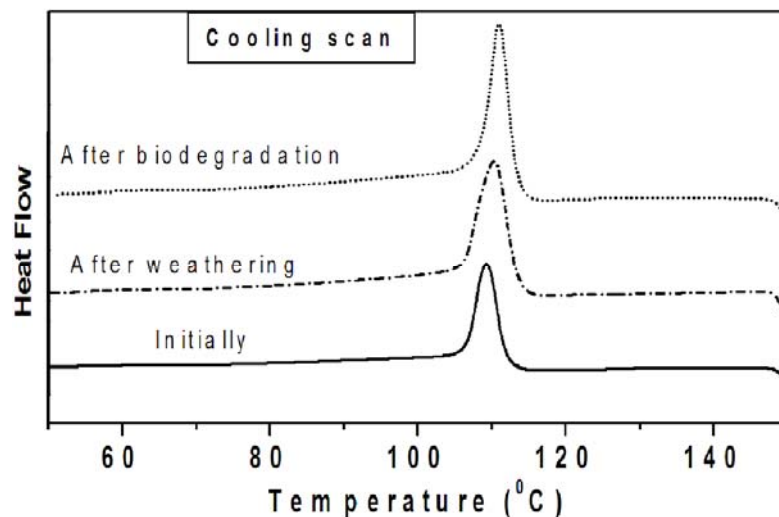


Fig.6.12 The cooling scan of samples containing both cobalt stearate and vegetable oil before degradation, after weathering and after biodegradation

6.3.4 Morphological characterization

The scanning electron micrographs of samples containing cobalt stearate with and without vegetable oil before degradation, after weathering and weathering followed by biodegradation are shown in Figs 6.13 and 6.14 respectively.

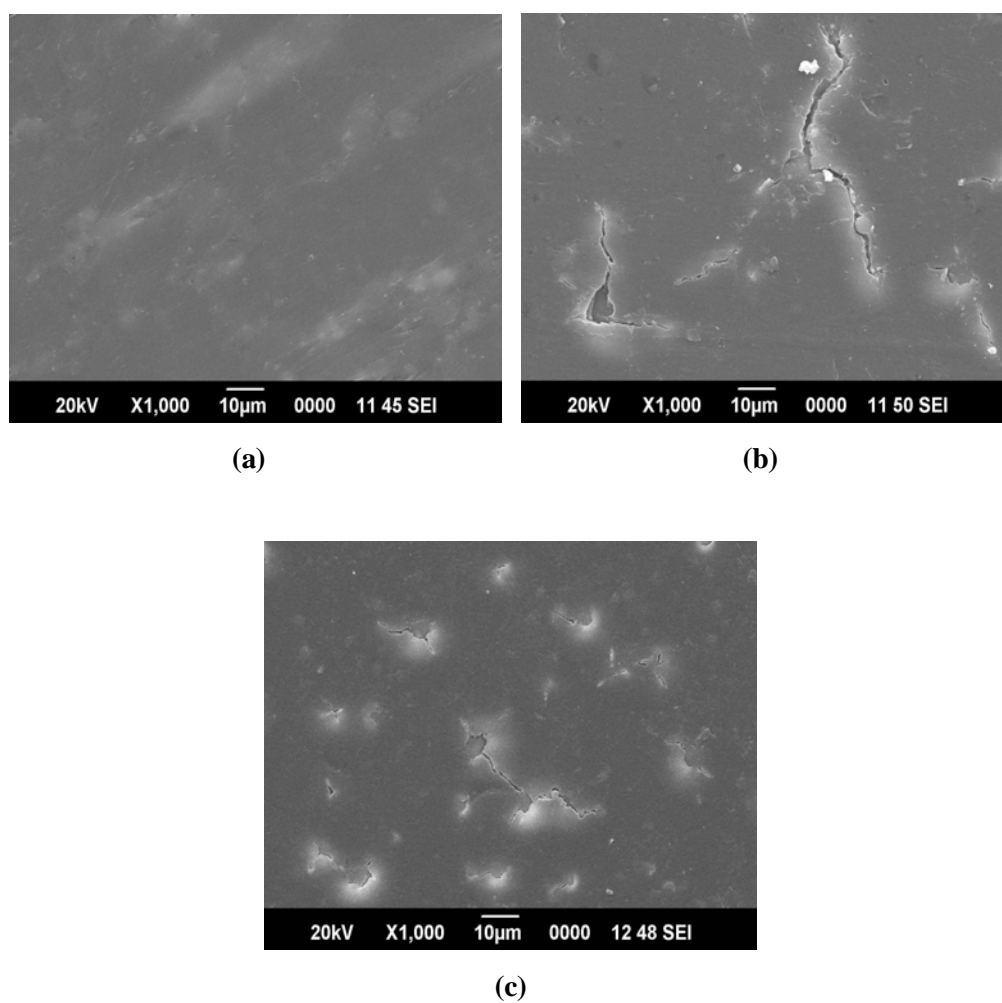


Fig. 6.13 SEM micrographs of the samples containing cobalt stearate only: (a) before weathering; (b) after 600 hours of weathering; and (c) after 15 weeks of biodegradation

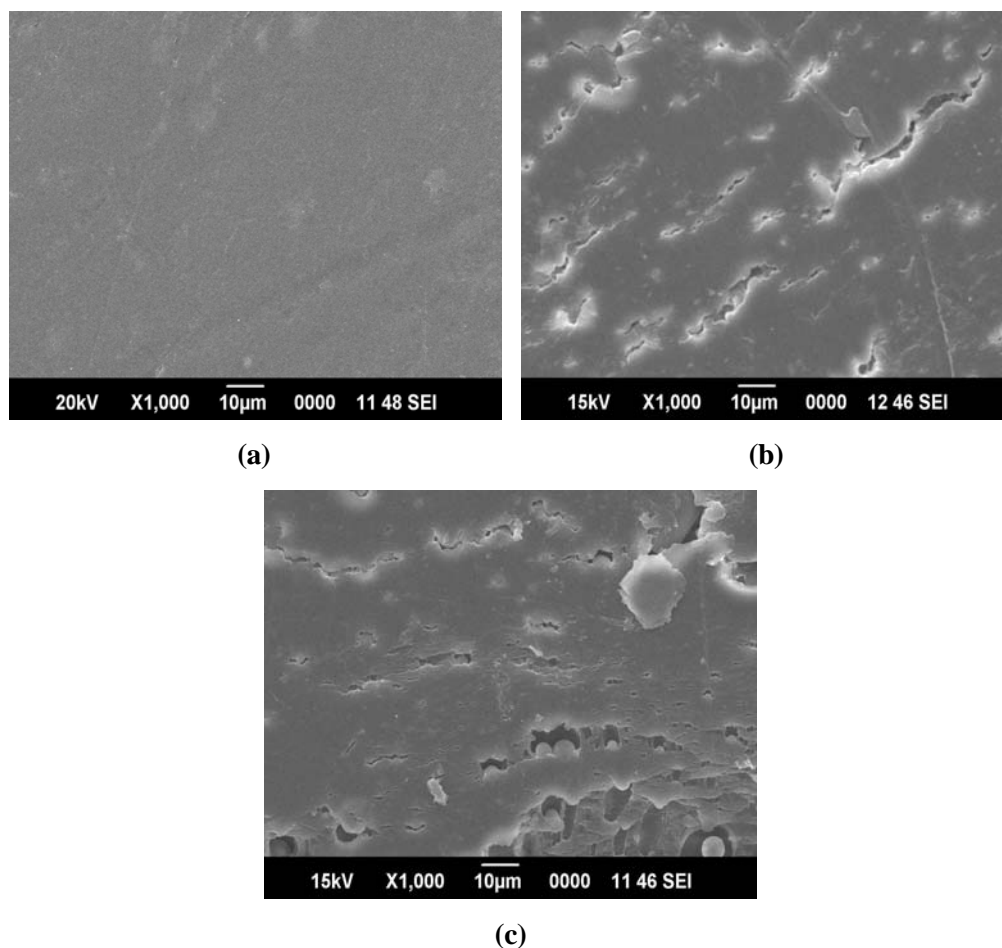


Fig. 6.14 SEM micrographs of the samples containing both cobalt stearate and vegetable oil: (a) before weathering; (b) after 600 hours of weathering; and (c) after 15 weeks of biodegradation

From these micrographs it can be seen that the surface of the samples before weathering were smooth without any cracks or grooves. However it developed numerous cracks after weathering. This suggests that oxidative chemical changes upon weathering have made the blend brittle. The number of cracks increased in the sample after subsequent biodegradation. This effect is more in the case of samples containing both vegetable oil and cobalt stearate.

6.4 Conclusions

- Both cobalt stearate and vegetable oil are capable of accelerating the oxidation of LLDPE/PVA blends during weathering.
- An accelerated rate of oxidation is observed primarily due to cobalt stearate in the case of compositions containing a combination of cobalt stearate and vegetable oil.
- The FTIR evidence indicates the presence of multiple oxidation products overlapping in the same region. Considerable reduction also occurs in the intensity of the OH absorption peak.
- The scanning electron microscopy studies also give evidence for weathering and biodegradation.
- The reduction in tensile properties of the blends after weathering and biodegradation in culture medium suggests that these blends are biodegradable to some extent.
- DSC results confirm the biodegradability and weatherability of these blends.
- Biodegradation followed by weathering is an effective means to degrade LLDPE/PVA blends for faster assimilation into the environment.
- Weight loss and melt flow index studies also indicate degradability.
- Blending with PVA is a promising step in making LLDPE biodegradable.

6.5 References

- [1] A. C. Albertsson, C. Barenstedt, S. Karlsson; *Acta. Polym.* **1994**, 45, 97.
- [2] M. Koutny, J. Lemaire, A. M. Delort; *Chemosphere.* **2006**, 64, 1243.
- [3] H. Kaczmarek, D. Oldak, P. Malanowski, H. Chaberska; *Polym. Degrad. Stab.* **2005**, 88, 189.
- [4] B. Catia. Eds.; *Handbook of Biodegradable Polymers*, Rapra Technology Limited, Shawbury, Shrewsbury, Shropshire, SY4 4NR, UK, **2005**.
- [5] S. H. Hamid, M. B. Amin, A. G. Maadhah; *Handbook of polymer degradation*. New York, Dekker, **1992**.
- [6] J. Sampers; *Polym. Degrad. Stab.* **2002**, 76, 55.
- [7] L. Andradý, S. H. Hamid, X. Hu, A. Torikai; *J. Photochem. Photobiol B: Bio*, **1998**, 46, 96.
- [8] F. Khabbaz, A. C. Albertsson, S. Karlson; *Polym. Degrad. Stab.* **1998**, 61, 329.
- [9] R. Setnescu, S. Jipa, Z. Osawa; *Polym. Degrad. Stab.* **1998**, 60, 377.
- [10] F. Khabbaz, A. C. Albertsson, S. Karlson; *Polym. Degrad. Stab.* **1999**, 63, 127.
- [11] F. Gugumus; *Polym. Degrad. Stabil.* **1996**, 52, 131.
- [12] J. V. Gulmine, P. R. Janissek, H. M. Heise, Akcelrud; *Polym. Degrad. Stab.* **2003**, 79, 385.
- [13] P. K. Roy, P. Surekha, C. Rajagopal, V. Choudhary; *J. Appl. Polym. Sci.* **2008**, 108, 2726.
- [14] Y. Lin; *J. Appl. Polym. Sci.* **1997**, 63, 811.
- [15] Z. Osawa, N. Kurisu, K. Nagashima, K. Nankano; *J. Appl. Polym. Sci.* **1979**, 23, 3583.

- [16] Z. Osawa; Polym. Degrad. Stab. **1988**, 20, 203.
- [17] P. K. Roy, P. Surekha, C. Rajagopal, S. N. Chatterjeeb, V. Choudharyc; Polym. Degrad. Stab. **2005**, 90, 577.
- [18] E. N. Frankel; Pray. Lipid Res. **1980**, 19, 1.
- [19] D. Oldak, H. Kaczmarek; Journal of Materials Science. **2005**, 40, 4189.

.....❧.....

EFFECT OF PRO-OXIDANT ACTIVITY OF COBALT STEARATE ON THE UV AND BIODEGRADATION OF LLDPE/PVA BLENDS

Contents	7.1	<i>Introduction</i>
	7.2	<i>Experimental</i>
	7.3	<i>Results and discussion</i>
	7.4	<i>Conclusion</i>
	7.5	<i>References</i>

7.1 Introduction

It was recently shown that preliminary UV irradiation of the polymeric material can induce biodegradation [1- 8]. The reason is main chain scissions and formation of functional groups during photo-oxidative degradation. Such degraded polymer, containing shorter chains and incorporated hydroxyl and carbonyl groups, as well as possible unsaturation, is further easily consumed by microorganisms [9]. It was also reported that in the case of combined action of different degrading factors, it is difficult to predict the final decomposition effect because both synergism and antagonism can occur [10, 11].

In this chapter, LLDPE/PVA films containing varying amounts of cobalt stearate were prepared in the absence as well as presence of vegetable oil and the extent of photocatalytic degradation under ultraviolet light was studied. Subsequently, partial biodegradation of the UV-degraded samples was done by microbial action of *Vibrio sp.* bacteria isolated from marine benthic environment. UV-exposure followed by biodegradation is a promising step to

make LLDPE/PVA blends assimilate faster into the environment. The photodegradation was evaluated by change in mechanical properties, FTIR spectroscopy, MFI, DSC, weight loss and SEM studies.

7.2 Experimental

7.2.1 Materials and specimen preparation

The methods adopted for the preparation of test samples were described in Chapter 4. The materials used, sample designation and formulations were described in Chapter 6.

7.2.2 Degradation studies

The photo-degradation procedure adopted for the degradation of samples was described in Chapter 5. The UV-degraded samples were then subjected to bio and soil-degradation studies as described in Chapter-4.

7.2.3 Evaluation of extent of degradation

The methods adopted for the evaluation of degradation are described in Chapter 4.

7.3 Results and discussion

7.3.1 Degradation by UV irradiation

The changes in tensile strength and percentage elongation of the film samples due to ultraviolet irradiation are shown in Figs. 7.1 and 7.2 respectively. The films containing a combination of both cobalt stearate and vegetable oil show a greater decrease in tensile strength (Table 7.1) and elongation compared to films without vegetable oil.

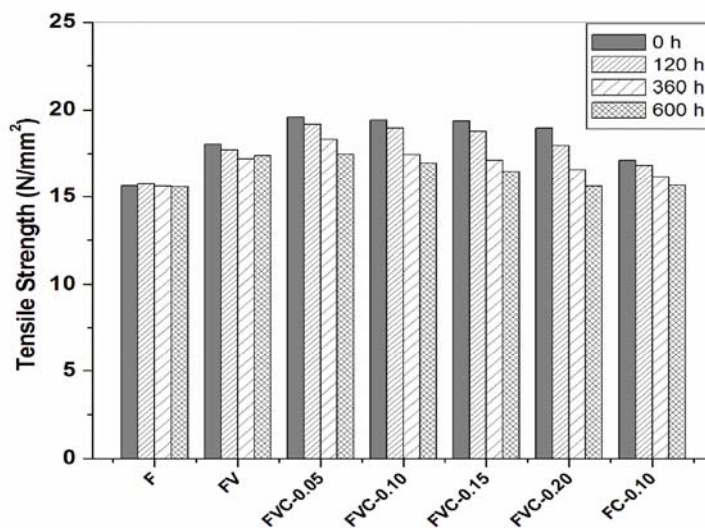


Fig. 7.1 Variation of tensile strength after UV-irradiation

Table 7.1 Percentage decrease in tensile strength after UV-irradiation

Sample designation	% Decrease in tensile strength after UV-exposure
F	0.32
FV	3.66
FVC-0.05	10.92
FVC-0.10	12.82
FVC-0.15	15.12
FVC-0.20	17.76
FC-0.10	8.42

For the sample containing cobalt stearate only (0.10%), the tensile strength decreased by 8.42% whereas, 12.82% decrease is observed for the sample containing both cobalt stearate (0.10%) and vegetable oil (Fig.7.1). As the amount of cobalt stearate increases a maximum of 17.76% decrease (for the sample containing 0.20% CS) is observed after 600 hours of exposure.

The elongation at break (Fig. 7.2 and Table-7.2) after degradation falls with cobalt stearate content, the main reason being continued cross linking and embrittlement of the sample [12].

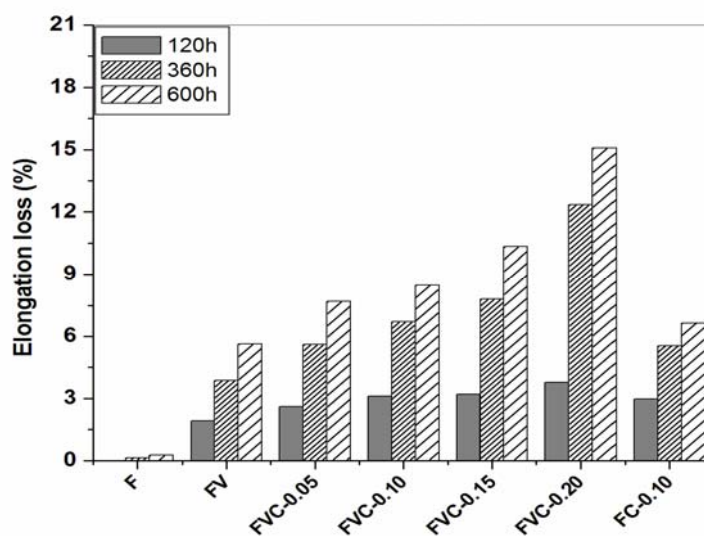


Fig. 7.2 Effect of UV exposure time on percentage elongation

Table 7.2 % elongation loss of the samples after 600hours of UV exposure

Sample designation	% elongation loss after 600 h of UV exposure
F	0.26
FV	5.64
FVC-0.05	7.69
FVC-0.10	8.48
FVC-0.15	10.33
FVC-0.20	15.08
FC-0.10	6.65

Figs. 7.3 and 7.4 show the FTIR spectra of FC-0.10 and FVC-0.10 respectively, before and after 600 hours of UV-exposure. The FTIR spectra show significant changes, especially in the carbonyl (1785-1700 cm^{-1}), amorphous (1300 cm^{-1}) and hydroxyl regions (3400 cm^{-1}). The absorption band around 1714 cm^{-1} which can be assigned to the C=O stretching ketonic functionality increases in intensity and exhibits band broadening [13-17]. The peak heights are found to be higher in the presence of vegetable oil. The absorption bands around 720 cm^{-1} and 1469 cm^{-1} also increase in intensity. These bands correspond to rocking vibrations of $-\text{CH}_2$ groups and bending vibrations of C-H bonds. The increase in the absorbance of these bands was also more pronounced for samples containing cobalt stearate and vegetable oil rather than only cobalt stearate.

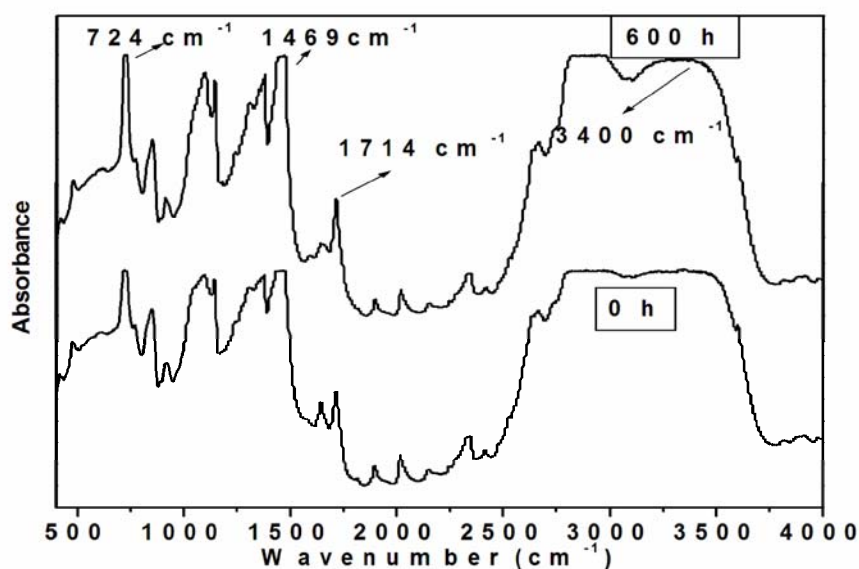


Fig. 7.3 FTIR spectra of the UV-degraded samples containing cobalt stearate only

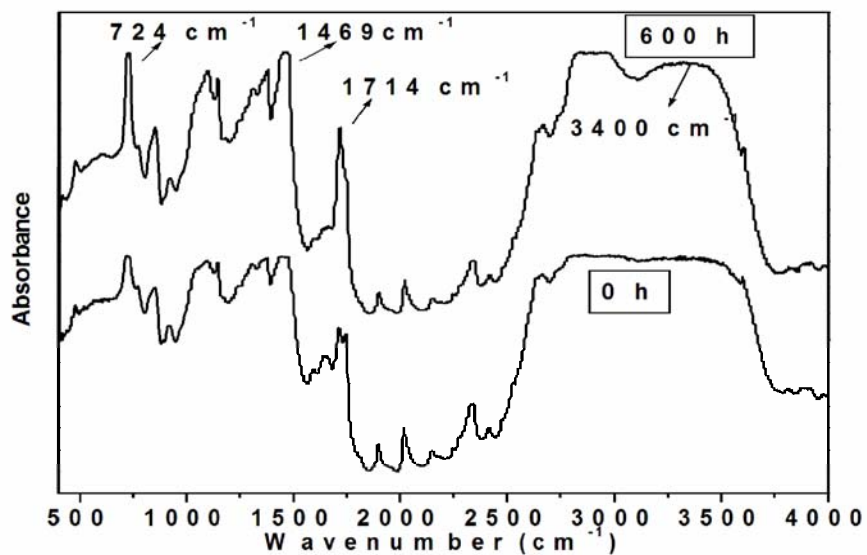


Fig. 7.4 FTIR spectra of the UV-degraded samples containing vegetable oil and cobalt stearate

Figure 7.5 shows the plot of carbonyl index as a function of UV irradiation time for LLDPE/PVA blends containing varying amounts of cobalt stearate and vegetable oil.

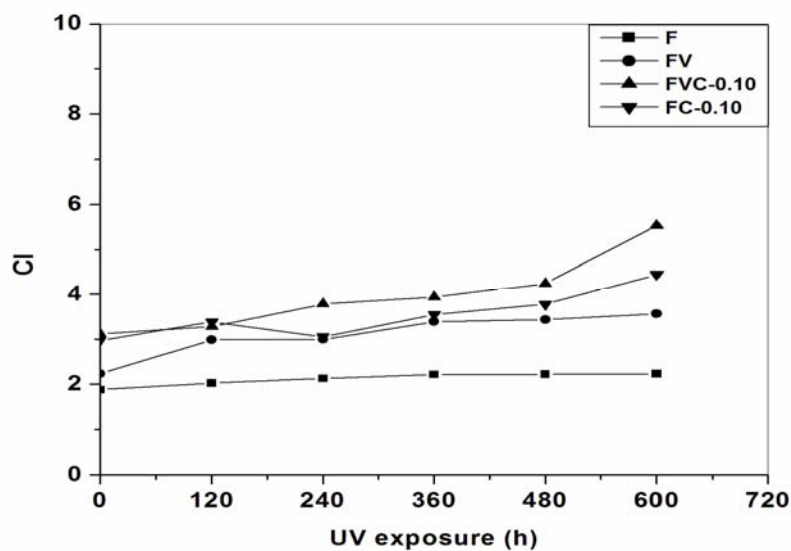


Fig. 7.5 Carbonyl index of the UV-degraded samples

The CI of LLDPE/PVA blend increased only by 18% due to UV exposure in the absence of cobalt stearate and vegetable oil. Incorporation of cobalt stearate and vegetable oil into the polymer led to 77.28% increase in the CI in a relatively short span of time. However, in the case of samples containing only cobalt stearate the increase was 49.55%.

The increase in MFI as a result of outdoor exposure is presented in Table 7.3. From the table it can be seen that the MFI of the degraded samples increases with cobalt stearate content. In the case of the sample containing 0.10% cobalt stearate alone MFI shows an increase of 2.4 units over the nondegraded sample. But the increase is 3.2 for samples containing both cobalt stearate (0.10%) and vegetable oil. As the amount of cobalt stearate increases to 0.20% the MFI increases to 4.4 over the nondegraded sample.

Table 7.3 Effect of UV exposure on Melt Flow Index

Sample designation	MFI(g/10 min with a 2.16kg load)	
	Before Exposure	After Exposure (600h)
F	0.8	0.9
FV	1.0	1.3
FVC-0.05	0.9	2.8
FVC-0.10	0.9	4.1
FVC-0.15	1.1	4.9
FVC-0.20	1.3	5.7
FC-0.10	0.9	3.3

7.3.2 Degradation by microorganisms

The tensile strength of the UV-degraded samples after biodegradation is shown in Fig. 7.6. We can see that there is a further decrease in tensile strength after biodegradation. This effect is greater in the case of samples containing both cobalt stearate and vegetable oil.

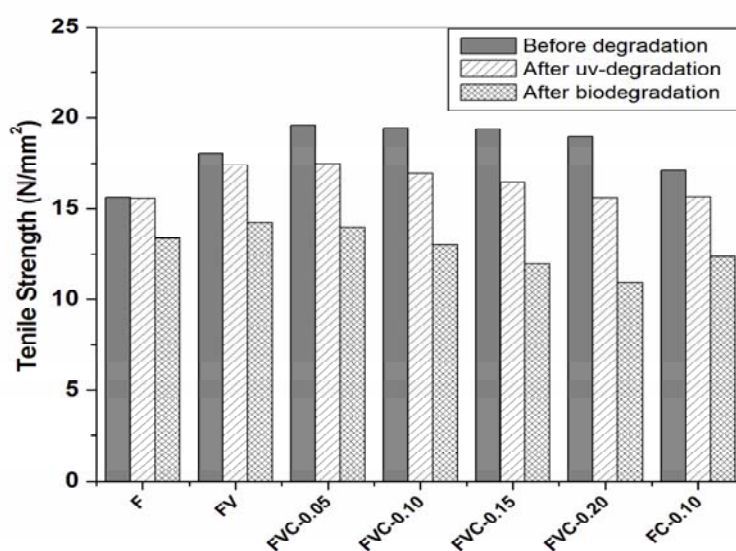


Fig. 7.6 Tensile strength of the biodegraded samples after UV-exposure

Table 7.4 shows the percentage weight loss of the samples after UV exposure followed by biodegradation in culture medium. In the case of sample containing 0.10% cobalt stearate alone, a weight loss of 21.37% was observed after UV exposure and a further 8.03% was observed after biodegradation. A weight loss of 23.21% was observed after UV exposure and 9.83% after biodegradation for samples containing both cobalt stearate (0.10%) and vegetable oil. As the amount of cobalt stearate is increased to 0.20% a weight loss of 41.53% was observed after UV exposure and a further 22.24% after biodegradation for samples containing the same

amount of vegetable oil. There is a massive loss of weight for these blends after UV exposure and biodegradation. This is a clear indication of biodegradability.

Table 7.4 Weight loss of the samples after UV exposure and biodegradation in culture medium

Sample designation	%Weight Loss	
	UV exposure	Biodegradation
FVC-0.05	17.62	5.18
FVC-0.10	23.21	9.83
FVC-0.15	27.84	11.17
FVC-0.20	41.53	22.24
FC-0.10	21.37	8.03

Figs. 7.7 and 7.8 show the FTIR spectra of FC-0.10 and FVC-0.10 respectively, after biodegradation subsequent to UV-irradiation. Here also considerable reduction in peak height is observed in the case of intensities, 724 cm^{-1} , 1715 cm^{-1} and $3200\text{-}3600\text{ cm}^{-1}$. The significance of this has already been discussed in earlier sections. The reduction in peak height at $1600\text{-}1800\text{ cm}^{-1}$ corresponding to carbonyl groups can be attributed to preferential attack of microorganisms at sites of oxidation resulting from UV degradation [10].

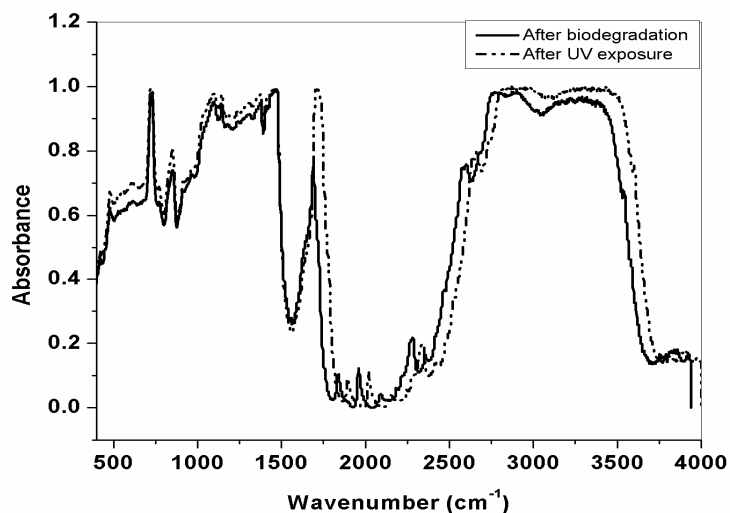


Fig. 7.7 FTIR spectra of the biodegraded samples after UV-exposure; containing cobalt stearate only

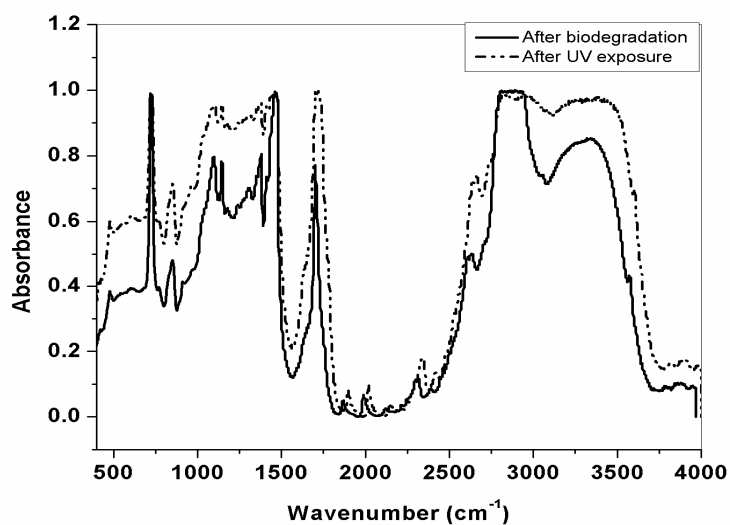


Fig. 7.8 FTIR spectra of the biodegraded samples after UV-exposure; containing both cobalt stearate and vegetable oil

7.3.3 Thermal studies

The heating and cooling scans of FC-0.10 and FVC-0.10 initially and after 600 hours of UV exposure and subsequent biodegradation are presented

in Figs. 7.9 and 7.10 respectively. The UV exposure led to a slight broadening of the polyethylene melting endotherm. The broadening of the peaks is more noticeable in the case of samples containing both cobalt stearate and vegetable oil compared to that containing cobalt stearate only which is an indication of the increased degradation.

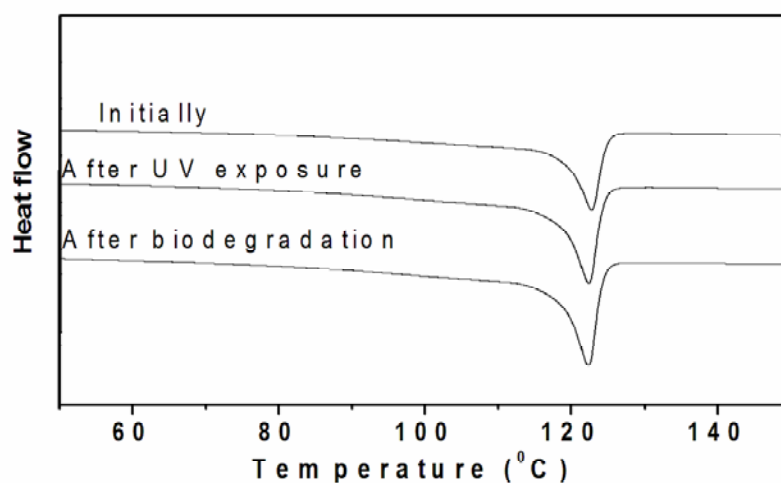


Fig. 7.9 The heating scans of samples containing cobalt stearate only; before degradation, after UV exposure and after biodegradation

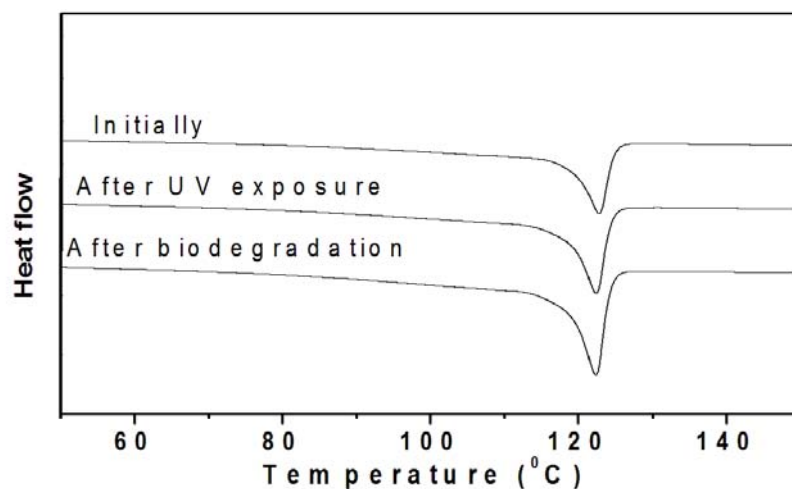


Fig. 7.10 The heating scans of samples containing both cobalt stearate and vegetable oil before degradation, after UV exposure and after biodegradation

7.3.4 Morphological characterization

Figs. 7.11 and 7.12 show the scanning electron micrographs of samples containing (1) cobalt stearate alone and (2) both cobalt stearate and vegetable oil respectively: (a) refers to sample before any degradation, (b) after UV-exposure and (c) UV-exposure followed by biodegradation. It can be seen that the surface of the samples before UV-degradation were smooth without any cracks or grooves. However it developed cracks after UV-exposure. The extent of damage was much more pronounced in samples containing both cobalt stearate and vegetable oil. The oxidative chemical changes upon UV-exposure have made the blends brittle. The number of cracks/grooves increased in the sample after subsequent biodegradation.

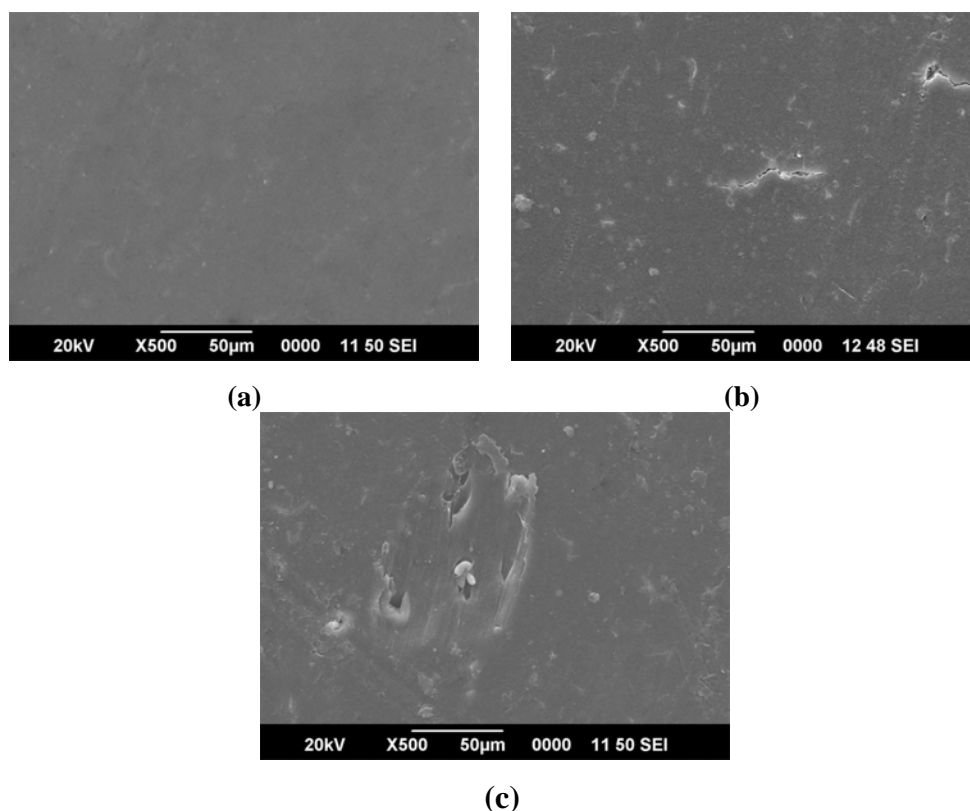


Fig.7.11 SEM micrographs of the samples containing cobalt stearate only: (a) before UV-exposure; (b) after 600 hours of UV-exposure; and (c) after 15weeks of biodegradation following UV irradiation

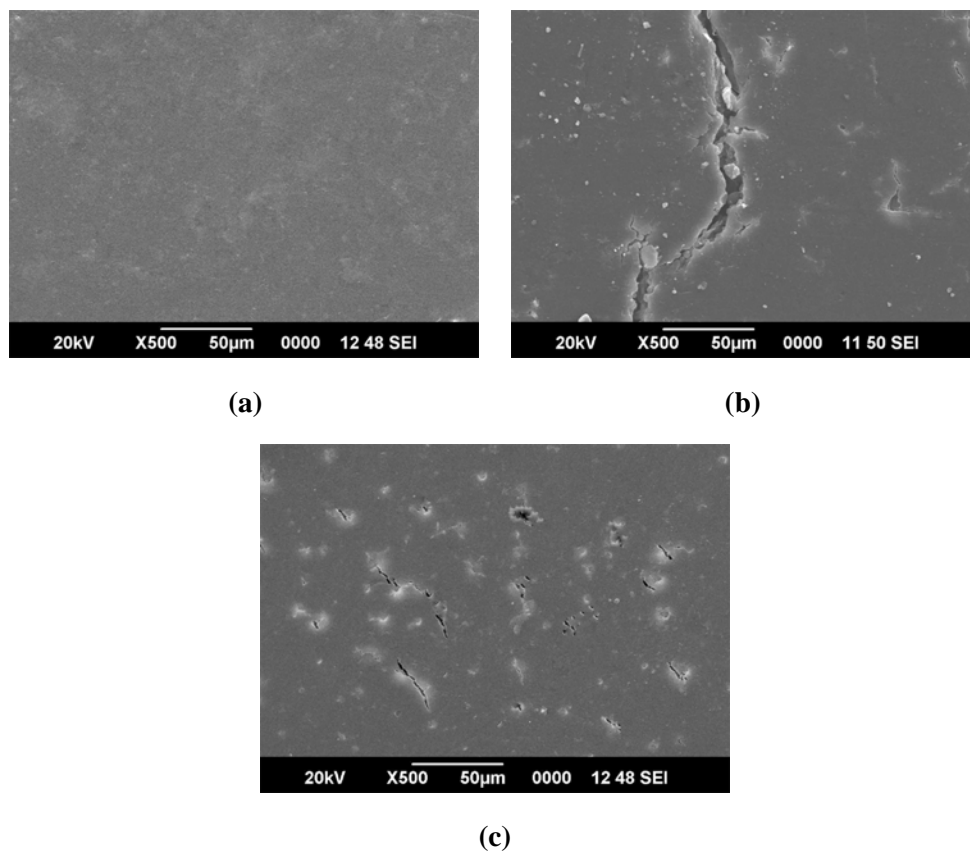


Fig.7.12 SEM micrographs of the samples containing both cobalt stearate and vegetable oil: (a) before UV-exposure; (b) after 600 hours of UV-exposure; and (c) after 15weeks of biodegradation following UV irradiation

It is noticed that striking changes appear on the blend surfaces and in internal structure upon either UV degradation, or biodegradation following UV degradation after a somewhat lengthy induction period. This induction period is dependent not only on the chemical nature of the blend components but also on the sample morphologies which control the penetration of any active low molecular weight product.

7.4 Conclusions

- A combination of cobalt stearate and vegetable oil is capable of accelerating the degradation of LLDPE/PVA blends during UV exposure.
- The reduction in tensile properties of the blends after UV exposure and biodegradation in culture medium indicates partial biodegradability.
- Accelerated rate of oxidation is primarily due to cobalt stearate in the case of compositions containing a combination of cobalt stearate and vegetable oil.
- There is an increase in carbonyl index values with progressive degradation.
- FTIR data give ample evidence of degradation during both photo and biodegradation steps.
- Increase in MFI values after UV exposure point to degradation.
- There is substantial loss of weight for these blends both after UV exposure and biodegradation which indicates degradation.
- The combination of cobalt stearate and vegetable oil is very effective for UV irradiation.
- The presence of cracks and cavities in the scanning electron microgram proves UV and biodegradation.
- Biodegradation followed by UV exposure is an effective means to degrade LLDPE/PVA blends for faster assimilation into the environment.

- In the two-step degradation process UV exposure is responsible for the bulk of the degradation when weight loss and tensile strength are considered

7.5 References

- [1] J. Sipinen, D.R. Rutheford; Proc. Am. Chem. Soc. **1992**, 67,185.
- [2] F. Khabbaz, A. C. Albertsson, S. Karlsson; Polym. Degrad. Stab. **1998**, 61, 329.
- [3] F.Khabbaz, A. C. Albertsson, S. Karlsson; Polym. Degrad. Stab. **1999**, 63,127.
- [4] F. Khabbaz, A. C. Albertsson; J. Appl. Polym. Sci. **2001**, 79, 2309.
- [5] F. Khabbaz, A. C. Albertsson; Biomacromolecules, **2002**, 1, 665.
- [6] Scott G; Trends Polym. Sci. **1997**, 5, 361.
- [7] G. Scott, D. Gilead, Eds. Degradable Polymers, Chapman & Hall: London, **1995**.
- [8] H. Kaczmarek, D. Ołdak, P. Malanowski, H. Chaberska; Polym. Degrad. Stab. **2005**, 88, 189.
- [9] K. Bajer, H. Kaczmarek, J. Dzwonkowski, A. Stasiak, D. Ołdak; J. Appl. Polym. Sci. **2007**, 103, 2197.
- [10] N.S Allen; Degradation and stabilization of polyolefins. Applied Science Publishers, New York, **1983**, 204.
- [11] J. F Rabek; Mechanisms of Photophysical Processes and Photochemical Reactions in Polymers. Theory and Applications; Wiley: Chichester, **1987**.
- [12] F. Khabbaz; Photo and thermo-oxidation of polyethylene with enhanced degradability, Royal Institute of Technology, Sweden, **1998**.

- [13] F. Khabbaz, A. C. Albertsson, S. Karlson; Polym. Degrad. Stab. **1998**, 61, 329.
- [14] R. Setnescu, S. Jipa, Z. Osawa; Polym. Degrad. Stab. **1998**, 60, 377.
- [15] F. Khabbaz, A. C. Albertsson, S. Karlson; Polym. Degrad. Stab. **1999**, 63, 127.
- [16] F. Gugumus; Polym. Degrad. Stab. **1996**, 52, 131.
- [17] J. V. Gulmine, P. R. Janissek, H. M. Heise, Akcelrud; Polym. Degrad. Stab. **2003**, 79, 385.

.....❧.....

SUMMARY AND CONCLUSIONS

The focus of this study is on developing linear low density polyethylene (LLDPE) with higher levels of bio and photo degradability. For this it was blended with a biodegradable polymer, namely polyvinyl alcohol (PVA). After characterizing these blends by various analytical techniques they were subjected to weathering and UV irradiation studies in the presence of different pro-oxidants, viz. titanium dioxide (rutile and anatase), cobalt stearate and vegetable oil individually and in combinations. These partially degraded samples were subjected to various analytical and property evaluation tests to estimate the extent of degradation. Subsequently, these samples were subjected to biodegradation studies, one employing a culture medium containing a consortium of *Vibrio sp.* bacteria and the other, soil degradation involving burial of the samples in garden soil. After due passage of time the samples were again subjected to various analytical and property evaluation tests to determine the extent of biodegradation. In addition, experimental techniques were developed for preparing nano-TiO₂ in the laboratory. These samples were characterized and their pro-oxidant activity compared with that of commercial rutile and anatase.

The blending of PVA with LLDPE has led to a marginal loss of mechanical properties such as tensile strength and elongation at break. But the modulus of the

blends increased as the PVA content increased. Thermogravimetric analysis and differential scanning calorimetry established that the thermal properties of the blends are not much different from those of LLDPE. Water absorption studies on the blends proved that they absorbed somewhat more water than pure LLDPE. This is a factor favourable to biodegradation.

These samples were first subjected to weathering and UV irradiation each for 600 hours as the first step of the degradation process. These studies were done in the presence of three pro-oxidants namely titanium dioxide, cobalt stearate and vegetable oil. Judicious combinations of these pro-oxidants were employed for the studies. The extent of degradation of the samples was estimated by tensile property measurements, FTIR, MFI, weight loss, DSC and SEM. It was concluded that a combination of cobalt stearate and vegetable oil is the best choice for giving maximum degradation of these blends by both degradation techniques.

Partially degraded samples from the above studies were subjected to biodegradation by two methods namely (i) culture medium containing a bacterial consortium of *Vibrio sp.* and (ii) burial in garden soil for 15 weeks each. As in the earlier case, property evaluation and analytical studies were done on the samples. It was observed that the degraded samples containing cobalt stearate showed maximum degradability during the biodegradation step also.

Experimental studies done in the laboratory to develop nanoanatase (TiO_2) produced anatase of approximately 6nm crystallite size. Calcination time was optimized for the preparation of these samples.

The overall results prove that blending LLDPE with PVA is a promising method for making LLDPE more degradable. Blending with PVA does not cause

any deterioration of the properties of LLDPE. Among the pro-oxidants studied, cobalt stearate and vegetable oil combination gives the best performance as far as photo degradation and subsequent biodegradation are concerned. Nano-TiO₂ developed in the laboratory has also considerable pro-oxidant activity.

Photo degradation followed by biodegradation holds great promise for making LLDPE degradable by the combined technique of blending with PVA and addition of pro-oxidants. By this procedure, LLDPE can be broken down to fragments in a reasonable amount of time and assimilated into the environment.

The future outlook

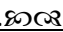
- In this study these *Vibrio sp.* were selected because they are native to the Cochin backwater area. But there are other well known species which are known to attack PVA. Studies in that direction can be taken up in the case of LLDPE/PVA blend.
- LLDPE can be blended with a combination of biodegradable substances rather than PVA alone. Thus substances like starch, chitosan, polycaprolactone, polyhydroxybuterate, PVA etc can be used in combinations for blending with LLDPE to study biodegradability.
- Photo and UV degradation studies have been done in this study in the presence of either TiO₂ or cobalt stearate in combination with vegetable oil. It is worth studying how far a combination of TiO₂ and cobalt stearate in the presence of vegetable oil will function as far as degradability is concerned.

.....✍.....

Abbreviations

ASTM	American society for testing and materials
CdS	Cadmium sulphide
CI	Carbonyl index
DSC	Differential scanning calorimetry
FDIS	Final draft international standard
FTIR	Fourier transform infra red
GPC	Gel permeation chromatography
HCl	Hydrochloric acid
HDPE	High density polyethylene
H _f	Heat of fusion
IR	Infra red Spectroscopy
J/g	Joule per gram
ISO	International organization for standardisation
kJ/mol	Kilo Joule per Mol
LDPE	Low density polyethylene
LLDPE	Linear low density polyethylene
MFI	Melt flow index
mg	milligram
min	minutes
ml	millilitre
mm	millimetre
MPa	Mega Pascal
M _w	Weight average molecular weight
M _z	z-average molecular weight
nm	nanometre
OD	Optical density
PB	Polybut-1-ene
PIB	Polyisobutylene
PCL	Poly-ε-caprolactone
PE	Polyethylene
PEEK	Polyether ether ketone
PET	Polyethylene terephthalate

PHA	Polyhydroxyalkanoates
PHBV	Poly- β -hydroxybutyrate-co- β -hydroxyvalerate
PIB	Polyisobutylene
PLA	Poly(lactic acid)
PMMA	Poly(methylmethacrylate)
PNA	Polynuclear aromatics
PP	Polypropylene
PS	Polystyrene
PTFE	Polytetrafluoroethylene
PVA	Poly (vinyl alcohol)
PVC	Poly (vinyl chloride)
rpm	revolutions per minute
SEM	Scanning electron microscope
SiO ₂	Silicon Dioxide
<i>sp</i>	Species
T _c	Crystallization temperature
TGA	Thermogravimetric analysis
T _m	Melting temperature
TiO ₂	Titanium dioxide
T _{max}	Maximum temperature
T _{onset}	Onset temperature
UHMWPE	Ultra high molecular weight polyethylene
UTM	Universal testing machine
UV	Ultraviolet
V _m	Molar volume
W _f	Final weight
W _w	Wet weight
W _c	Conditioned weight
XRD	X-ray diffraction
ZnO	Zinc oxide

..........

Publications

- [1] **Vidya Francis**, S. Raghul Subin, Sarita G. Bhat, Eby Thomas Thachil; Characterisation of Linear Low-density Polyethylene/Poly(vinyl alcohol) blends and its extent of biodegradability by *Vibrio sp.* isolated from marine benthic environment; *Journal of Applied Polymer Science*, 2012, 124, 1, 257-265.
- [2] **Vidya Francis**, S. Raghul Subin, Sarita G. Bhat, Eby Thomas Thachil; Effect of cobalt stearate and vegetable oil on the UV and biodegradation of linear low-density poly(ethylene)-poly(vinyl alcohol) blends; *Polymers from renewable resources*, 2011, 2, 4, 131-148.
- [3] Ayswarya E.P, **Vidya Francis**, Renju V. S, Eby Thomas Thachil; Rice Husk Ash- A valuable reinforcement for High Density Polyethylene; *Journal of Materials and Design*, 2012, 41, 1-7.
- [4] **Vidya Francis**, S. Raghul Subin, Sarita G. Bhat, Eby Thomas Thachil; Study on the Degradation of Linear Low-Density Poly(ethylene)-Poly(vinyl alcohol) Blends in the Presence of Cobalt Stearate and Vegetable oil; *Accepted in Journal of Chemistry and Chemical Engineering*.
- [5] Raghul Subin S, Sarita G Bhat, **Vidya Francis**, Eby Thomas Thachil; Biodegradation of a polyvinyl alcohol -LLDPE blended plastic film by a consortium of *Vibrio sp.* from marine benthic environments and their characterization; *Under review in International Journal of Environmental Science and Technology*.
- [6] **Vidya Francis**, Ayswarya E. P, Eby Thomas Thachil; Weathering Studies of Degradable Polyethylene-Polyvinylalcohol Plastics Containing Nano-anatase Photocatalyst Synthesized by Hydrothermal Method; *To be communicated*.
- [7] **Vidya Francis**, Beena T Abraham, Eby Thomas Thachil; Effect of TiO₂ photocatalyst in ultraviolet degradation of LLDPE/PVA blends; *To be communicated*.

Conference Papers

- [1] **Vidya Francis**, S. Raghul Subin, Sarita G. Bhat, Eby Thomas Thachil; Weathering and biodegradation studies on LLDPE/PVA blends; International Conference on Advancements in Polymeric Materials (APM-2011), CIPET, Chennai-2011.
- [2] **Vidya Francis**, Eby Thomas Thachil; Photo-oxidation of Polyethylene/ Polyvinyl alcohol Blends in the Presence of TiO₂ and Vegetable oil; International Conference on Functional Polymers, NIT, Calicut-2011.
- [3] **Vidya Francis**, Raghul Subin S, Sarita G Bhat and Eby Thomas Thachil; Biodegradation of Linear Low-Density Poly(ethylene)/Poly(vinyl alcohol) Blends Aided by Pro-oxidant Additives; International Conference on Materials for the Future, Government Engineering College, Trissur-2011.
- [4] **Vidya Francis**, Raghul Subin S, Sarita G Bhat and Eby Thomas Thachil; Microbial Degradation Studies on Linear Low-Density Poly (ethylene)/ Poly(vinyl alcohol) Blends Using *Vibrios*; International Conference on Advances in Polymer Technology, Cusat, Kochi-2010.
- [5] **Vidya Francis**, Raghul Subin S, Sarita G Bhat and Eby Thomas Thachil; Study on the Degradation of Linear Low-Density Poly(ethylene)/Poly(vinyl alcohol) Blends in the Presence of Cobalt Stearate and Vegetable oil; International Conference on Polymer Science and Engineering, Chandigarh, Punjab-2010.
- [6] **Vidya Francis**, Ajalesh B Nair, Aswathy N. S, Eby Thomas Thachil; Modification of LDPE with Casein; National Conference on Advances in Chemical Sciences, Sacred Heart College, Thevara-2008.